

國立交通大學

電子工程學系電子研究所

博士論文

以離子場效電晶體為基礎之微型酵素型生物感測器及
其參考系統開發

**Development of an Ion Sensitive Field Effect Transistor
Based Urea Biosensor with Solid State Reference Systems**



研究生：張知天

Chih-Tien Chang

指導教授：張國明 博士

Dr. Kow-Ming Chang

中華民國九十九年七月

以離子場效電晶體為基礎之微型酵素型生物感測器及其參
考系統開發

**Development of an Ion Sensitive Field Effect Transistor Based Urea
Biosensor with Solid State Reference Systems**

研 究 生：張知天

Student: Chih-Tien Chang

指 導 教 授：張國明 博士

Advisor: Dr. Kow-Ming Chang



A Dissertation

Submitted to Department of Electronics Engineering & Institute of
Electronics

College of Electrical and Computer Engineering

National Chiao Tung University

in Partial Fulfillment of the Requirements

for the Degree of Doctor Philosophy

in

Electronics Engineering

July 2010

Hsinchu, Taiwan, Republic of China

中華民國九十九年七月

以離子場效電晶體為基礎之微型酵素型生物感測器及其參 考系統開發

研究生:張知天

指導教授:張國明 博士

國立交通大學

電子工程學系電子研究所

摘要

本論文旨在開發一種以電化學感測原理結合半導體製程製作的場效電晶體，成為具有對生物訊號有感測能力的微型生物感測器。係利用酸鹼值離子感測場效電晶體(pH-Ion Selective Field Effect Transistor, pH-ISFET)為基礎，在其感測層表面固定化生物材料，例如酵素，來達到生物感測器的功能。此外，為達到微小化之目的，其參考電位系統也一併加入設計考量，以期與後段訊號讀出電路設計能有良好匹配。

pH-ISFET 係以金氧半場效電晶體(MOSFET)為基礎發展出之感測器，其金屬閘以離子感應層(Ion Sensing Layer)、酸鹼緩衝溶液(pH Buffer Solution) 和一參考電極取代。場效電晶體的臨界電壓(Threshold voltage)隨著感應層和待測溶液的表面接觸電位變化而改變，而感應層和待測溶液的表面接觸電位變化和溶液中的氫離子濃度有直接的關係。可藉此將電化學反應中離子濃度變化轉換成電子訊號，達到感測的目的。利用此元件特性，改變其感測層特性，將可開發出特定目的之感測器，例如可感測生物訊號的生物感測器。

本論文發現某些質子交換膜，例如 NafionTM，結合一些高分子材料可以應

用在微型固態電極(Solid-state Reference Electrode, SRE)以及場效電晶體型參考電極(Reference Electrode Field Effect Transistor, REFET)上，此類的固態電極有降低干擾達到穩定電位的能力，同時使得整個感測元件結構簡單。另外，利用 Nafion™ 及包埋法 (entrapment) 可製作生物分子的包埋層，例如酵素場效電晶體(Enzyme Field-Effect Transistor, EnFET)。

為實現微型生物感測器的開發，此研究為分為三個進程。首先，我們研究並尋找出最佳化製程條件之 ZrO_2 作為離子感應層的 ISFET。這樣的元件擁有約 58mV/pH 高靈敏以及小於 1mV/hr 的低電壓飄移值，極具作為生物型感測器基礎的優勢，同時也針對其對其它離子(例如鉀離子和鈉離子)的干擾特性作一分析。其次，利用 Nafion™ 等質子交換膜結合高分子材料，例如：polyimide、PR、P3HT 等，在不同的材料比例、不同的加熱溫度和不同的結構下來製作微型化固態參考電極(SRE)以及場效電晶體型參考電極(REFET)，這樣的參考電極擁有極低的氫離子感測靈敏度，可與高氫離子感測靈敏度的 ISFET 結合成差動對來完成一個完整的微型離子感測場效電晶體。如此完成的元件具備轉換成生物感測器的基礎。第三部份根據已完成的微型離子感測場效電晶體為平台，再次利用 Nafion™ 來包埋或混合生物感測材料以形成感測層，探討其生物訊號感測能力、飽和點、重現性以及操作範圍。

在此論文中，我們將詳述酸鹼離子感測器、微小化參考電極以及尿素生物感測器的製作流程及量測條件，並且分析各種感應特性。並針對後段補償電路和差動電路對元件之需求條件作電性匹配調整。

Development of an Ion Sensitive Field Effect Transistor Based Urea Biosensor with Solid State Reference Systems

Student: Chih-Tien Chang

Advisor: Dr. Kow-Ming Chang

Department of Electronics Engineering &
Institute of Electronics
National Chiao-Tung University
Hsinchu, Taiwan, R.O.C

Abstract

In this dissertation, a miniaturized urease biosensor constructed with an enzymy field-effect transistor (EnFET) and solid state reference systems were designed and developed. The EnFETs and the reference systems were developed based on the ion-sensitive FET (ISFET) technology. The ISFETs based biosensors have the advantages of rapid response, small size, high input-impedance and low output-impedance as well as the applicability of semiconductor and integrated-circuit technologies.

The ISFET, which is a MOSFET with the gate connection separated in the form of a reference gate immersed in aqueous solution which is contact with the sensing layer above gate oxide. It is working based on the approach of electrochemical measurement of pH. With incorporating the entrapment immobilization technology, the biological or ion-insensitive materials can be attached on the ISFETs and transform the functionalities to be EnFETs or reference FETs (REFETs). Entrapment

was a popular method to immobilize the various biological materials, such as urease, glucose and protein, with ISFETs. This method needs supporting matrixes provided by polymers with resistant to chemical attack and low interference to the materials entrapped. In our study, the NafionTM was found to be suitable candidate as supporting material.

To develop a miniaturized ISFET based biosensor, three programs were executed. Firstly, the ZrO₂-gated ISFET was fabricated and characterized. The optimal post annealing process was determined to be 600 °C, 30 mins. with N₂ gas. The fabricated ISFET demonstrated good performances of high sensitivity, linearity, low drift and hysteresis. Secondly, the immobilization method was developed. The Nafion was utilized as supporting matrix, which entrapped ion-insensitive polymers, to produce REFET. Meanwhile, the EnFET was fabricated with similar approach of immobilizing urease in Nafion. Finally, for the miniaturization purpose, the reference systems, such as solid-state reference electrode (SRE) and reference FET (REFET) with quasi-reference electrode (QRE), were integrated with the sensors in the on-chip level. With differential measurements, the biosensors demonstrated comparable detecting performances.

Acknowledgement

There are many thanks to those who have supported me during my research life at NCTU. First I am heartily thankful to my supervisor, Professor Kow-Ming Chang, whose encouragement, guidance and support from the initial to the final level enabled me to accomplish the development of the subject. Without his guidance and persistent help this dissertation would not have been possible.

I would like to appreciate the members of my oral examination committee, Prof. Shui-Jinn, Prof. Tseung-Yuen Tseng, Prof. Chin-Long Wey, Prof. Chao-Ming Fu, Prof. Horng-Chih Lin, Prof. Yuh-Shyong Yang and Prof. I-Chung Deng. Their suggestions, corrections and research directions truly inspire me. I am appreciative of the cooperation and assistance from the members of Nano OME Devices Lab. Helpful discussion with Dr. Kuo-Yi Chao, are gratefully acknowledged. I would also like to appreciate Jin-Li Chen, Chia-Hung Lin, Kun-Mou Chan, Cho-Ching Lin and Bin-Yu Chan for their help in my experiments. In addition, I am thankful to NDL for the largely support.

Finally, to my parents and family, I would like to thank them for their understanding and support during the long period. Especially for my dear wife, words can not express my gratefulness. Because of her, the difficult challenge of completion of this dissertation was made possible.

Contents

Abstract (in Chinese).....	i
Abstract (in English).....	iii
Acknowledgements	v
Contents.....	vi
Table captions.....	x
Figure captions.....	xi

Chapter 1 Introduction

1.1 Background and motivation	1
1.2 Thesis organization.....	3
References.....	5

Chapter 2 Principles of ISFET-based biosensors: pH-ISFETs, reference systems and readout circuits

2.1 pH-ISFETs	6
2.2 Reference systems for pH-ISFETs	11
2.2.1 Reference electrodes.....	11
2.2.1.1 Aqueous reference electrode.....	11
2.2.1.2 Solid-state reference electrode.....	12
2.2.1.3 Pseudo reference electrode	13
2.2.2 Reference electrodes for ISFETs	14
2.3 Readout circuits	15
2.4 Biosensors.....	16
2.4.1 Overview.....	16

2.4.2 ISFET based biosensors	18
References.....	19

Chapter 3 Optimization of the post deposition annealing process and characterization of ion interferences for ZrO₂ gated ISFETs

3.1 Introduction.....	27
3.2 Experiment.....	28
3.2.1 Device fabrication	29
3.2.2 Packaging and measurement setup	30
3.2.3 Hysteresis and drift measurement	30
3.2.4 Preparation of Na ⁺ and K ⁺ ion solutions	30
3.3 Results and discussions.....	31
3.3.1 Optimization of post deposition annealing process.....	31
3.3.2 Characterization of ion selectivity	33
3.4 Summary	34
References	36

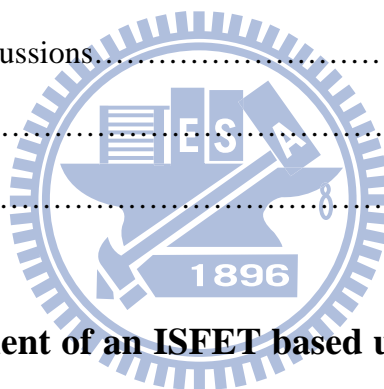
Chapter 4 A novel pH-dependent drift improvement method for ZrO₂ gated pH-ISFETs

4.1 Introduction.....	49
4.2 Experiment.....	51
4.2.1 Device fabrication	51
4.2.2 Packaging and measurement	52
4.3 Results and discussions.....	52
4.3.1 pH sensitivity of n-channel and p-channel ZrO ₂ gate ISFETs	52

4.3.2 Drift rate of n-type and p-type ZrO ₂ gate ISFETs	53
4.3.3 Drift rate and pH sensitivity of combined n-channel and p-channel ZrO ₂ gate ISFETs	55
4.4 Summary	56
References	58

Chapter 5 Development of a novel FET type reference electrodes for pH-ISFET applications

5.1 Introduction.....	69
5.2 Experiment.....	71
5.3 Results and discussions.....	72
5.4 Summary	76
References	77



Chapter 6 Development of an ISFET based urea biosensor with solid state reference systems

6.1 Introduction.....	90
6.2 Experiment.....	93
6.2.1 Reagents preparation	93
6.2.2 ISFET fabrication and membranes preparation	94
6.2.3 Packaging and measurement	95
6.3 Results and discussions.....	95
6.4 Summary.....	100
References	101

Chapter 7 Conclusions and future prospects

7.1 Conclusions117

7.2 Future prospects118

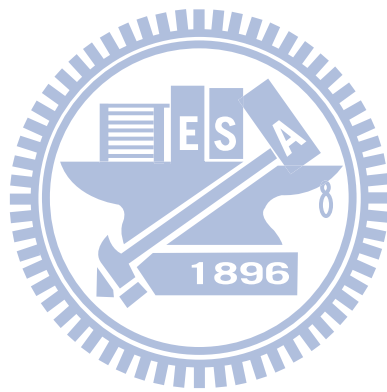


Table captions

Chapter 3

Table 5-1. The overall performances for samples with different post annealing temperature

Chapter 5

Table 5-1. Responses of hydrogen ions and sodium ions for tested structures.

Chapter 6

Table 6-1. The urea responses and performance of urease biosensors with different ratio of urease entrapped.

Table 6-2. The storage and repeatability performances of GRE/EnFET

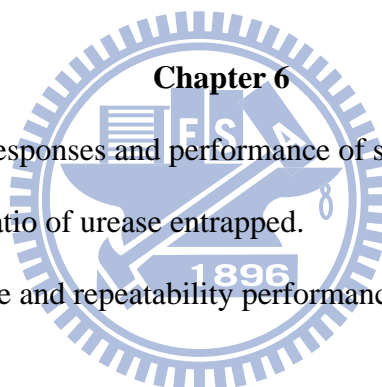


Figure captions

Chapter 2

- Figure 2-1. Properties of the electrode/electrolyte interface.
- Figure 2-2. The site-binding model for the electrode/electrolyte interface.
- Figure 2-3. Different approaches for ISFET reference systems. (a) ISFET with pH buffer compartment (b) miniaturized Ag/AgCl reference electrode (c) ISFET with ion insensitive membrane. 1. pH buffer solution or KCl solution 2. glass capillary or hole 3. cover layer 4. measuring electrode with metallic lead 5. chemically modified sensing layer.
- Figure 2-4. Different measuring circuits for ISFETs. (a) One-ended measuring circuit (b) ISFET/REFET differential measuring circuit.
- Figure 2-5. Schematic diagram of biosensor elements.

Chapter 3

- Figure 3-1. Schematic diagram of ZrO_2 gate ISFET fabricated by the MOSFET technology.
- Figure 3-2. Setup of measurement using HP4156A semiconductor parameter analyzer and temperature controller.
- Figure 3-3. The pH sensitivity and linearity of ZrO_2 membrane annealed at 600 - 900°C and no annealing.
- Figure 3-4. The SEM images of the ZrO_2 films which annealed at 600 (a), 700 (b), 800(c), 900 °C (d) and not annealed (e), respectively.
- Figure 3-5. The hysteresis curves obtained in pH loop 7→3→7→11→7 for the

ZrO₂ films which annealed at 600 (a), 700 (b), 800(c), 900°C (d) and not annealed (e), respectively.

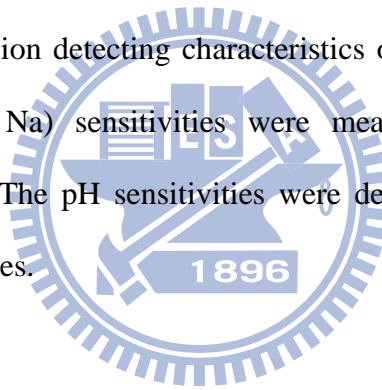
Figure 3-6. The hysteresis curves obtained in pH loop 7→11→7→3→7 for the ZrO₂ films which annealed at 600 (a), 700 (b), 800(c), 900°C (d) and not annealed (e), respectively.

Figure 3-7. The drift performances of the ZrO₂ films which annealed at 600 (a), 700 (b), 800(c), 900°C (d) and not annealed (e), respectively.

Figure 3-8. The pK (a) and pNa (b) responses of the ZrO₂ ISFET at pH=9.

Figure 3-9. Detection limits and sensitivities of K⁺ (a) and Na⁺ (b) at the buffers of pH=3 to pH=11.

Figure 3-10. The multi-ion detecting characteristics of ZrO₂ gated ISFET. The pX (X=K or Na) sensitivities were measured at various pH buffer solutions. The pH sensitivities were degraded due to the K⁺ or Na⁺ interferences.



Chapter 4

Figure 4-1. Schematic diagram of ZrO₂ gate ISFET, which was fabricated by the Metal Oxide Semiconductor Field Effect Transistor (MOSFET) technique.

Figure 4-2. The measurement setup and a HP4156A semiconductor parameter analyzer, which was used for measuring the I_{DS}-V_{GS} characteristics for the ZrO₂ gate ISFETs.

Figure 4-3. The sensitivity of (a) n-channel and (b) p-channel ZrO₂ gate ISFETs.

Figure 4-4. The drift of the n-channel ISFET over the first seven hours at (a) pH=3 (b) pH=5 (c) pH=7 (d) pH=9 (e) pH=11. The drift over the first seven

hours was (a) -58.55mV (b) -51.54mV (c) -41.61mV (d) -34.64mV and (e) -32.52mV, respectively.

Figure 4-5. The drift of the p-channel ISFET over the first seven hours at (a) pH=3 (b) pH=5 (c) pH=7 (d) pH=9 (e) pH=11. The drift over the first seven hours were (a) 13.33mV (b) 6.04mV (c) -4.91mV (d) -25.92mV and (e) -30.82mV, respectively.

Figure 4-6. The drift rate of (a) n-channel ISFET and (b) p-channel ISFET for the first seven hours.

Figure 4-7. The schematic diagram of the proposed system and measurement method.

Figure 4-8. (a) The pH-dependent drift of n-channel, p-channel and corrective ISFETs measured at the seventh hour. (b) The pH sensitivities with the proposed compensation method.

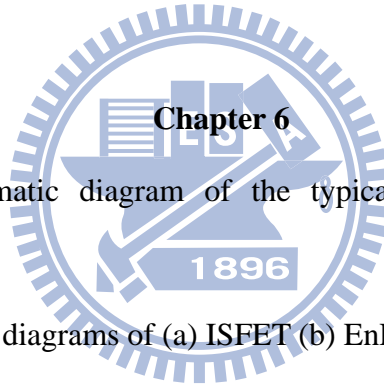
Figure 4-9. The variations of the drift measured at different pH values from the second hour to seventh hour for n-channel, p-channel ISFETs and the proposed compensation method.

Chapter 5

Figure 5-1. Tested membranes prepared with two methods: (a) Encapsulation and (b) entrapment.

Figure 5-2. Hydrogen and sodium sensitivities of (a) ZrO_2 and (b) ZrO_2 with Nafion coating gated ISFETs. The pH and pNa sensitivities are (a) 57.89 and (b) 58.92 mV/pH and (a) 15.88 and (b) 16.34 mV/pNa, respectively. (c) The $I_{DS}-V_{GS}$ curves of ZrO_2 with and without Nafion coating.

- Figure 5-3. Measurement results of pH and pNa sensitivity for tested structures.
- Figure 5-4. I_{DS} - V_{GS} curves of HMDS coated ZrO_2 membrane.
- Figure 5-5. The pH and pNa response of Nafion-PR composite/HMDS/ ZrO_2 ISFET.
- Figure 5-6. Measurement results of pH and pNa response with ISFET/REFET differential arrangement.
- Figure 5-7. Transconductance ($g_m = dI_{DS}/dV_{GS}$) of the ZrO_2 gated ISFET, the proposed REFET (ion-unblocking) and REFET with epoxy coating on ZrO_2 gate (ion-blocking).
- Figure 5-8. Drift performance of the proposed REFET.



- Figure 6-1. The schematic diagram of the typical common-mode differential circuit.
- Figure 6-2. Schematic diagrams of (a) ISFET (b) EnFET and REFET.
- Figure 6-3. Test structures: (a) single-ended (b) two-ended differential pairs.
- Figure 6-4. The I_{DS} - V_{GS} and transconductance (g_m) curves of ZrO_2 gate ISFETs with and without NafionTM coating.
- Figure 6-5. Equivalent circuit of (a) ideally polarizable interface and (b) ideally nonpolarizable interface.
- Figure 6-6. The urea responses of urease biosensors with different ratio of urease entrapped.
- Figure 6-7. (a) Urea response of the GRE/EnFET (b) Storage and repeatability performances of the GRE/EnFET dL in axis label.
- Figure 6-8. The I_{DS} - V_{GS} and g_m curves of ISFET, EnFET and REFETs.

Figure 6-9. Urea response of test structures of the GRE/EnFET, SRE/EnFET, GRE/EnFET/REFET , QRE/EnFET/REFET and SRE/REFET.



Chapter 1

Introduction

1.1 Background and motivation

The Metal-Oxide-Semiconductor Field-Effect Transistor (MOSFET) technology dominates modern electronic industry for decades, due to the advantages of vast fabrication experience, optimized reliability and yield, on-chip electronics, existence of many circuit design libraries and offers a low cost of processes. It provides the basis for the development of numerous applications, such as the sensors for the measurements of physical and chemical parameters. The equations of the MOSFET drain current exhibit a number of parameters that can be directly affected by external signals, and the stability of the original MOSFET configuration also support the sensing properties.

Integration of ISFET in a standard CMOS technology contains the following advantages: (1) Minimization of ISFET sensors provides an ability of embedding into medical tools for continuous in-vivo measurements. Additional applications were presented for needles containing pH sensors, etc. (2) On-chip integration of ISFETs with CMOS electronics allows system-on-chip implementation of complex measuring devices with multiple types of sensors and data-processing circuitry. (3) Fabrication under standard process technologies, with minimal additional process steps and post-processing will significantly reduce the cost of ISFETs, while improving the quality, fabrication yield and uniformity of the produced sensors.

A series of MOSFET-based sensors, such as the GASFET, OGFET, ADFET, SAFET, CFT, PRESSFET, CHEMFET, ISFET, REFET, ENFET, BIOFET, and others were widely discussed [1.1-1.3]. Among the numerous sensors, the ISFET, REFET, ENFET and

BIOFET were the most popular devices as the basis of biosensors development. The ion-sensitive FET (ISFET) has similar structure with the MOSFET except the gate was replaced by the sensing component, a reference electrode and the tested electrolyte. The sensing characteristics were mainly determined by the properties of sensing layers. The reference FET (REFET) was identical to the ISFET but insensitive to the ion activities, it was usually utilized to replace the complicated miniaturized solid-state reference electrodes. The enzyme FET (ENFET) was a kind of the biological FET (BIOFET) which based on the ISFET platform with enzyme or other biological materials immobilized on the surface of the sensing layer. Through developing proper immobilization methods many kinds of miniaturized biosensors can be achieved.

There are four principal methods available for immobilizing enzymes: adsorption, covalent binding, entrapment and membrane confinement. Adsorption of enzymes onto insoluble supports is a very simple method by simply mixing the enzyme with a suitable adsorbent, under appropriate conditions of pH and ionic strength and followed by washing off loosely bound and unbound enzyme. The driving force causing this binding is usually due to the physical links between the enzyme molecules and the support. Examples of suitable adsorbents are ion-exchange matrices, porous carbon, clays, hydrous metal oxides, glasses and polymeric aromatic resins. Immobilization of enzymes by covalent binding is an extensively researched technique. The covalent link formation depends upon the availability and reactivity of enzymes. The strength of binding is very strong and very little leakage of enzyme from the support occurs. However, only small amounts of enzymes may be immobilized by this method, which limits the detection ability. Entrapment of enzymes within gels or fibers is a convenient method for use in processes involving low molecular weight substrates and products. The entrapment process may be a purely physical caging or involve covalent binding. Entrapment is the method of choice for the immobilization of

microbial, animal and plant cells, where calcium alginate is widely used. Membrane confinement of enzymes depends on the semipermeable nature of the membrane. The simplest of these methods is achieved by placing the enzyme on one side of the semipermeable membrane whilst the reactant and product stream is present on the other side.

A miniaturized biosensor can deliver many novel benefits, such as the continuous monitoring for biological tissues while incorporating the micro-fluidic channel fabricated with MEMS technology [1.4], the pain-free body sensor [1.5] and the in-vivo measurement [1.6, 1.7], etc. However, the development of the technologies of miniaturization and immobilization for the biosensors are still challenging. The aim of this thesis is to develop the platform of miniaturized MOSFET based biosensors.

1.2 Thesis organization

In this thesis, the development processes of FET based biosensor were described. In chapter 2, the operation principles of the pH-ISFET, reference systems, readout circuits and biosensors will be introduced. Those are the fundamentals of developing a miniaturized biosensor. In chapter 3, the optimization for the developed ZrO_2 gated pH-ISFET was performed. The optimal post-annealing process conditions were determined. Based on the optimized pH-ISFET, the ion-interference was also characterized. A novel method was proposed to improve the drift behavior in chapter 4. Through the measurement method, the pH-dependent drift can be improved significantly.

Chapter 5 will describe the development of a polymer based REFET. The ISFET/REFET pair with differential arrangement demonstrated good sensitivity of hydrogen ions and achieved the mini feature of sensors. In chapter 6, the urease biosensor

with the integration of the solid-state reference system was developed. The considerations of electrical match for the ENFET/ISFET differential pair were also addressed. The last chapter concludes the whole work.



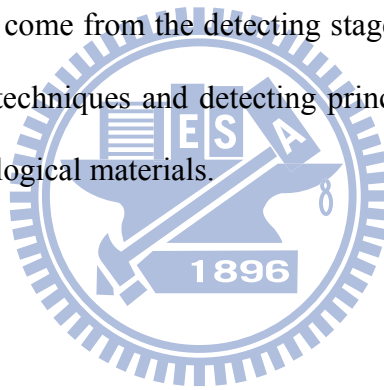
References

- [1.1] Bergveld, P. The impact of MOSFET-based sensors. *Sens. Actuat. B* **1985**, 109-127.
- [1.2] Madou, M. J.; Morrison, S. R. Chemical sensing with solid state devices, New York: *Academic Press* **1989**.
- [1.3] Sze, S.M. Semiconductor sensors, New York: *John Wiley & Sons* **1994**.
- [1.4] Kim, Dong-Sun; Park, Jee-Eun; Shin, Jang-Kyoo; Kim, Pan Kyeom; Lim Geunbae; Shoji, Shuichi. An extended gate FET-based biosensor integrated with a Si microfluidic channel for detection of protein complexes. *Sens. Actuat. B* **2006**, 117, 2, 488-494.
- [1.5] Newman, J. D.; Turner, A.P.F. Home blood glucose biosensors: a commercial perspective. *Biosens. Bioelectron.* **2005**, 20, 12, 2435-2453.
- [1.6] Wilson, G. S.; Hu, Yibai. Enzyme-based biosensors for in vivo measurements. *Chem. Rev.* **2000**, 100, 7, 2693-2704.
- [1.7] Wilson, G. S.; Gifford, R. Biosensors for real-time in vivo measurements. *Biosens. Bioelectron.* **2005**, 20, 12, 2388-2403.

Chapter 2

Principles of ISFET-based biosensors: pH-ISFETs, reference systems and readout circuits

In this chapter, the composition and working principles of pH-ISFET based biosensors are introduced. The biosensors composed of pH-ISFETs, reference systems and readout circuits incorporate the immobilization technology transforming the detecting capability of chemical signals to biological ones. The pH-ISFETs perform the detecting function. The reference systems provide stable potential as measurement basis. The readout circuits deal with the signals and noises come from the detecting stage and send them to post treatment tools. The immobilization techniques and detecting principles are different depend on the characteristics of tested biological materials.



2.1 pH-ISFETs

In its most common interpretation, pH is used to specify the degree of acidity or basicity of an aqueous solution. In formal, the definition of pH is expressed as

$$pH = -\log a_{H^+} = -\log \gamma[H^+] \quad (2-1)$$

where a_{H^+} is the hydrogen ion activity, γ is the activity coefficient which equals to 1 for diluted solution, and $[H^+]$ is the molar concentration of solvated protons in units of moles per liter. In practice, the measurement of pH is not accomplished by the direct determination of the hydrogen ion activity but relative to standard solution of known pH.

The ISFET, which is a MOSFET with the gate connection separated in the form of a reference gate immersed in aqueous solution which is contact with the sensing layer above gate oxide. It is working based on the approach of electrochemical measurement of pH.

The general expression for the drain current of the MOSFET and thus also of the ISFET in the non-saturated mode is

$$I_d = C_{ox}\mu \frac{W}{L} \left[(V_{gs} - V_t)V_{ds} - \frac{1}{2}V_{ds}^2 \right] \quad (2-2)$$

with C_{ox} is the oxide capacity per unit area, W and L is the width and the length of the channel, respectively, and μ is the electron mobility in the channel.

Another important MOSFET equation describes the physical properties in nature is that of the threshold voltage

$$V_t = \frac{\Phi_M}{q} - \frac{\Phi_{Si}}{q} - \frac{Q_{ox} + Q_{ss} + Q_B}{C_{ox}} + 2\phi_f \quad (2-3)$$

Where the first two terms describe the work function difference between the gate metal (Φ_M) and the silicon (Φ_{Si}), the second term is describes the effect of accumulated charge in the oxide (Q_{ox}), at the oxide-silicon interface (Q_{ss}) and the depletion charge in the silicon bulk (Q_B), the last term determines the onset of inversion depending on the doping level of the silicon.

The measurement of pH with the ISFET was that it immersed in a liquid and the electrical circuits are connected to the reference electrode and source/drain contacts. When the device operating in linear mode, the constant drain-source voltage V_{ds} was applied. The hydrogen activity influences the gate voltage was described in terms of V_t , hence the expression for the ISFET threshold voltage becomes

$$V_t = E_{ref} - \Psi_0 + \chi^{sol} - \frac{\Phi_{Si}}{q} - \frac{Q_{ox} + Q_{ss} + Q_B}{C_{ox}} + 2\phi_f \quad (2-4)$$

where E_{ref} is the constant potential of the reference electrode, Ψ_0 is the chemical input parameter and χ^{sol} is the surface dipole potential of the solvent and thus having a constant

value [2.1]. As a result, the term Ψ_0 dominates the pH sensitivity of the ISFET since all the other terms are constant.

Prior to determine the term Ψ_0 , the properties of the electrode/electrolyte interface, as shown in Figure 2-1, should be studied. There are four possible properties of the interface: first, the local concentration of both cation and anion changes at the interface; second, the ion-electron exchange, i.e., redox reaction; third, the ion-electron interaction, no redox reaction; and last, the ion-molecular interaction. Yates *et al.* [2.2] firstly introduced the site-binding model, as illustrated in Figure 2-2, for the electrode/electrolyte interface. This model describes the equilibrium between the amphoteric SiOH surface sites and the H^+ -ions in the solution. The reactions are



and



where H_B^+ denotes the protons in the bulk of the solution. An originally neutral surface hydroxyl site can bind a proton from the bulk solution, becoming a positive site and leaving a negative site on the oxide surface. It is called amphoteric site.

It is known that the background electrolyte has a large influence on the surface charge [2.3]. This dependence is ascribed to variations in the double layer capacitance. The Gouy-Chapman-Stern model is most widely used to describe the double layer structure in ISFET literature [2.4]. Gouy and Chapman proposed independently the idea of a diffuse layer to interpret the capacitive behavior of an electrode/electrolyte solution interface. The excess charge in the solution side of the interface is equal in value to that on the solid state surface, but is of opposite sign. The ions in the solution are therefore electrostatically attracted to the solid-state surface but the attraction is counteracted by the random thermal motion which acts to equalize the concentration throughout the solution. Stern modified the

model with proposing a diffuse layer of charge in the solution starting at a distance X from the surface.

A new model was introduced by van Hal and Eijkel [2.5, 2.6] and is in fact nothing else than the well-known equation for capacitors $Q = CV$, where Q is surface charge in the form of protonized (OH_2^+) or deprotonized (O^-) OH groups of the oxide surface, C is the double-layer capacitance at the interface and V is the resulting surface potential. The potential between the gate insulator surface and the electrolyte solution causes a proton concentration difference between bulk and surface. According to Boltzmann equation:

$$a_{H_s^+} = a_{H_B^+} \exp \frac{-q\Psi_0}{KT} \quad (2-7)$$

or

$$pH_S = pH_B + \frac{q\Psi_0}{2.3KT} \quad (2-8)$$

where $a_{H_i^+}$ is the activity of H^+ ; q is the elementary charge, K is the Boltzmann constant and T is the absolute temperature. The subscripts B and S refer to the bulk and the surface, respectively.

Here define two parameters: β_s and C_{diff} . The intrinsic buffer capacity β_s represents the ability of the oxide surface to deliver or take up protons, it is the capability to buffer small changes in the surface pH (pH_s) but not in the bulk pH (pH_B); the C_{diff} is the differential double-layer capacitance, of which the value is mainly determined by the ion concentration of the bulk solution via the corresponding Debye length. We have

$$\frac{\Delta\sigma_0}{\Delta pH_s} = -q \frac{\Delta(\nu^- - \nu^+)}{\Delta pH_s} = -q\beta_s \quad (2-9)$$

where σ_0 is the surface charge per unit area, ν^- and ν^+ are the fixed number of negative and positive surface sites per unit area, and $\beta_s \equiv \frac{\Delta(\nu^- - \nu^+)}{\Delta pH_s}$.

An equal but opposite charge is built up in the electrolyte solution side of the double layer σ_{DL} because of the charge neutrality. The σ_{DL} can be described as a function of the integral double layer capacitance, C_i , and the electrostatic potential

$$\sigma_{DL} = -C_i \Psi_0 = -\sigma_0 \quad (2-10)$$

The integral capacitance will be used later to calculate the total response of the ISFET on the change in pH. The ability of the electrolyte solution to adjust the amount the of stored charge as result of a small change in the electrostatic potential is the differential capacitance, C_{diff}

$$\frac{\Delta \sigma_{DL}}{\Delta \Psi_0} = -\frac{\Delta \sigma_0}{\Delta \Psi_0} = -C_{diff} \quad (2-11)$$

From the Equations 2-7 ~ 2-11, we obtain that

$$\frac{\Delta \Psi_0}{\Delta pH_s} = \frac{\Delta \Psi_0}{\Delta \sigma_0} \frac{\Delta \sigma_0}{\Delta pH_s} = -\frac{q\beta_s}{C_{diff}} = \frac{\Delta \Psi_0}{\Delta(pH_B + \frac{q\Psi_0}{2.3KT})} \quad (2-12)$$

Rearrange Equation 2-12 gives a general expression for the sensitivity of the electrostatic potential to changes in the bulk pH

$$\Delta \Psi_0 = -2.3\alpha \frac{kT}{q} \Delta pH_B \quad (2-16)$$

with

$$\alpha = \frac{1}{\frac{2.3kTC_{diff}}{q^2\beta_s} + 1} \quad (2-17)$$

Note that α is a dimensionless sensitivity parameter which determined by the intrinsic buffer capacity and the differential capacitance, and the value of α varies between 0 and 1. Only in the case α approach 1, the maximum Nernstian response of 58.2 mV /pH at 298K can be achieved. In other word, the high pH sensitivity requires a large value of the surface buffer capacity β_s and a low value of the double layer capacity C_{diff} . Meanwhile, the high β_s reduces the importance of the C_{diff} ; as a result, a Nernstian sensitivity can be

achieved over wide pH range due to the independency of the electrolyte concentration. In conclusion, the selectivity and chemical sensitivity concerning the surface potential of the ISFET are dominated by the conditions of the electrode/electrolyte interface.

2.2 Reference systems for pH-ISFETs

According to the operational principle of the ISFET, the reference system with providing stable reference potential is essential. The stability of the reference electrode is an important factor in any electroanalytical procedure since any variation can affect the response of the working electrode. Ideal reference electrodes are required to meet the following characteristics: (1) Stable and reproducible potential (2) Low temperature dependence of potential (3) Low electrical resistance (4) Application in variety of media (5) Reproducible and small liquid junction potentials.

To fabricate the miniaturized ISFET, there are two types of on-chip reference systems were proposed: the reference electrode and the reference FET (REFET).

2.2.1 Reference electrode

A Reference electrode is an electrode which has a stable and well-known electrode potential. The high stability of the electrode potential is usually reached by employing a redox system with constant concentrations of each participants of the redox reaction. The reference electrodes can be divided into 3 categories: aqueous, solid-state and pseudo reference electrodes.

2.2.1.1 Aqueous reference electrode

The first type is aqueous reference electrode. A typical aqueous reference electrode is

the glass electrode. It is a type of ion-selective electrode made of a doped glass membrane that is sensitive to a specific ion. The electric potential of the electrode system in solution is sensitive to changes in the content of a certain type of ions, which is reflected in the dependence of the electromotive force (EMF) of galvanic element concentrations of these ions. Another popular aqueous reference electrode is the silver chloride electrode. The electrode functions as a redox electrode and the reaction is between the silver metal (Ag) and its salt — silver chloride (AgCl).

The corresponding equations can be presented as follows:



This reaction characterized by fast electrode kinetics, meaning that a sufficiently high current can be passed through the electrode with the 100% efficiency of the redox reaction (dissolution of the metal or cathodic deposition of the silver-ions). The Nernst equation below shows the dependence of the potential of the Ag/AgCl electrode on the activity or effective concentration of chloride-ions:

$$E = E^0 - \frac{RT}{F} \ln a_{Cl^-} \quad (2-19)$$

The standard electrode potential E^0 against standard hydrogen electrode is $0.230V \pm 0.01V$. Based on the principles, some miniaturized Ag/AgCl reference electrodes with encapsulated liquid reference solutions were developed [2.7–2.9]. However, the activity of potential determining ions can vary due to an outflow of inner electrolyte via the liquid–liquid connection. Meanwhile, the leakage of the reference solutions limits the device lifetime and affects the measurement accuracy.

2.2.1.2 Solid-state reference electrode

Traditional reference electrodes used for electrochemical measurements, such as the calomel and silver/silver chloride electrodes, have a limited range of applicability. The

liquid junction is problematic with these electrodes, and they cannot be used either with wholly solid-state electrochemical cells or for very high-temperature reactions such as those in molten electrolytes. As an alternative to standard commercial reference electrodes, a solid state reference electrode is fabricated for in situ voltammetric analysis in solutions containing little or no added supporting electrolyte. It can be used under specific conditions in which traditional reference electrodes cannot be used.

The activities in the improvement of solid-state reference electrodes are divided into four main groups: (1) To improve the classical rod-shaped reference electrode (2) To realize the planar conventional reference electrode (3) To implement the reference systems for ISFETs (4) To establish an all-solid-state reference. Different approaches for ISFET reference systems are shown in Figure 2-3.

Many approaches to fabricate solid state reference electrode were investigated. Daniel Rehm *et. al.* fabricated an all solid-state macro electrode in which a Ag/AgCl wire is embedded directly in the salt-doped resin [2.10]. I-Yu Huang *et. al.* introduced a novel agarose-stabilized KCl-gel membrane to serve both as a polymer-supported solid reference electrolyte and an ionic bridge for Ti/Pd/Ag/AgCl electrode [2.11, 2.12]. A nanoporous platinum oxide electrodes work as a noble solid-state reference electrode was also reported [2.13]. Two different strategies for the use of sensors have been pursued. On the one hand, low-cost disposables with simple designs and cheap component parts have been produced—especially in the field of medical sensors. On the other hand, sensor systems have been developed with sophisticated technologies to increase the lifetime of the devices without reduction of the sensor performances.

2.2.1.3 Pseudo reference electrode

A pseudo-reference electrode is a class of electrodes, they do not maintain a constant

potential but vary predictably with conditions. The potential of such electrodes is not established in accordance with the Nernst Equation but rather by some other interaction with its environment. As long as its environment remains constant, its reference potential will likely remain constant.

2.2.2 Reference electrodes for ISFETs

Like all other potentiometric electrochemical sensors, the ISFET pH indicator electrode must be complemented by a reference electrode, the potential of which should be completely independent of the pH value and the presence of other ions in the measuring solution. Three main approaches for ISFET reference systems development: (1) ISFET with pH buffer compartment (2) miniaturised Ag/AgCl, Cl⁻ reference electrode (3) ISFET with modified pH-insensitive membrane.

The earliest ISFET on-chip reference system, Figure 2-3 (a), was described by Comte and Janata [2.14]. At this Janata-type configuration, a small closed epoxy compartment EC containing a pH-buffered gel is placed on one of a matched pair of pH ISFETs. The electrolytic connection to the solution is made via a glass capillary. However, since it has only restricted lifetime and cannot be produced completely by using IC technology, it did not obtain noticeable acceptance. Figure 2-3 (b) shows the second type of reference electrodes. It is more like a miniaturized planar version of a conventional Ag/AgCl, Cl⁻ reference electrode. It is called Prohaska-type microelectrode, which was prepared in thin film technology using IC-compatible techniques. The general aim is to eliminate the need of a separate reference electrode and to facilitate the use of ISFET. Many researches based on this type were reported [2.11, 2.12, 2.15].

The most popular version of reference electrodes is reference FET (REFET). As shown schematically in Figure 2-3 (c), where the ion-sensitive membrane of an ISFET is

covered with a pH-insensitive membrane or is itself modified to become pH insensitive. This version was initiated by Matsuo *et al.* [2.16, 2.17], who deposited an ion-blocking parylene film on the Si_3N_4 layer on the gate of an ISFET. Errachid *et al.* [2.18] described a simple REFET for pH detection in differential mode measurements. The device is based on a pH-insensitive polymeric PVC membrane cast on the gate insulator of an ISFET device that has been previously silylated by chemical grafting of a silane compound. The REFET shows low pH sensitivity (1.8 mV/pH) and is only slightly affected by the concentration of Na^+ and K^+ .

Two types of REFET structures can be distinguished with respect to the penetration of ions into the polymeric layer, resulting in two different mechanisms of the REFET operation. In an ion-unblocking REFET structure, ion exchange occurs between the solution and the polymer, whereas in an ion-blocking REFET structure ion exchange is negligible. In the first case, the electrical potential is a membrane potential; in the second, however, it is a surface potential resulting from reversible ion-complexation reactions at the surface of the polymer.

2.3 Readout circuits

Depending on the kind of the reference electrode, different measuring circuits for ISFETs are recommended. If any really potential-stable reference electrode is available, a simple one-ended circuit is suitable, as shown in Figure 2-4 (a). This structure can be considered as an optimal among the interfaces without feedback. In order to achieve stable signal detection under noisy and unstable environmental conditions and to maintain the response linearity, sophisticated sensor interfaces are used. However, since the development of miniaturized reference electrode with thermodynamically defined interface

potential is still challenging, the ISFET/REFET differential measuring circuit as shown in Figure 2-4 (b) is widely accepted. In contrast to a real reference electrode, this electrode must not exhibit a stable potential because its potential fluctuations are eliminated by the common mode rejection of the differential amplifier. An electrode from any chemically resistant material, such as a platinum wire or a Pt layer deposited on the ISFET sensor chip, can be applied for this purpose. This arrangement seems to be particularly favorable with regard to the compensation of influences of temperature, light and other disturbance variables. However, the compensating effect must not be overestimated because it is only noticeable if the ISFET and the REFET have identical operating parameters. Chodavarapu *et al.* designed a differential circuit without any post-fabrication processing or material deposition [2.19]. This system has two identical ISFETs as the inputs to a pair of ISFET operational transconductance amplifiers (IOTAs) arranged in a novel differential architecture. The IOTAs have different sized p-MOSFET load transistors with different amplification factors. The CMOS ISFET chip is fabricated in an unmodified 1.5 mm commercial process. However, the sensitivity is only 20 mV/pH, which is insufficient for biological applications. Another Fully CMOS-integrated pH-ISFET interface circuit design was reported [2.20], the sensor chip is fabricated in a standard 0.35,um 4-metal and 2-poly layer CMOS process to which extra post processing steps are added for depositing membranes. The ISFET/REFET pair was fabricated with Ta₂O₅ ion sensitive layer and the other with PVC insensitive layer. The differential measurement result achieved 40.76 mV/pH, demonstrated the necessary and importance of REFET development.

2.4 Biosensors

2.4.1 Overview

Since the biosensor was first described by Clark and Lyons in 1962 [2.21], the development of biosensors were vigorous. Many biological materials provide a broad platform of functional units for their integration with electronic elements. For example, the biomolecules of optimal recognition and binding capabilities lead to high selectivity and specific biopolymer complexes (antigen-antibody, hormone-receptor, or duplex DNA complexes). Biosensors are small analytical bioelectronic devices that combine a transducer with a sensing biological component.

The transducer transforms the weight, electrical charge, potential, current, temperature or optical activity measured with the biologically sensitive material to electrical signals. The schematic diagram was shown in Figure 2-5. The biological sensing element was in close proximity or integrated with a signal transducer, it produces a reagentless sensing system specific for the target analyte. The immobilization of the biosensing material represents a critical step in the production of biosensors, especially in dealing with enzyme and antibodies.

A biosensor can be specified by the following characteristics:

- (1) Selectivity and sensitivity. This is the capability to select and to measure the specific biochemical species with minimal interference from others.
- (2) Detection Limit. This defines the minimum concentration of the analyte to be measured.
- (3) Lifetime. This parameter in concerning how long the biosensor can be used with limited loss of the original biological function.
- (4) Response Time. The enzymatic or immunological reactions are characterized by fast kinetics; thus the response time of the biosensor is often not reaction-limited, but is rather diffusion-limited.

The biosensor applications are classifying according to the field in which the devices are deployed. (1) Clinical diagnosis (2) Agriculture development and monitoring (3) Food

quality (4) Environmental monitoring (5) New drug development (6) Point-of-care-testing (POCT) system.

2.4.2 ISFET-based biosensors

In recent years there has been great progress in applying FET-type biosensors for highly sensitive biological detection. Among them, the ISFET is one of the most popular approaches in electrical biosensing technology. One distinct merit of the ISFETs is the feasibility of miniaturization, thereby allowing its easy integration into the required electronics. Therefore an ISFET device of small size and low weight might be use in a portable monitoring system, i.e., a hand-held drug monitoring system.

Currently, various kinds of biological recognition materials for biological analysis such as DNA, proteins, enzymes, and cells are being applied to ISFET measurements owing to the unique electrical and biological properties, thereby elevating the sensitivity and specificity of detection [2.22, 2.23]. In the ISFET system based on different bio-contents for biological analysis, assorted concepts of biosensors like enzyme FETs, Immuno FETs, and DNA FETs that contain layers of immobilized enzymes, antibodies, and DNA strands respectively, have been reported in a large number of documents [2.23–2.28]. Nevertheless, although various types of ISFET-based biosensors have been developed, they still suffer from a variety of fundamental and technological problems such as rigid immobilization for biological materials, electrical properties and instability of functional groups in the sensing layer. To overcome these problems, interdisciplinary cooperation from various research fields such as chemistry, biology, electrics, and physics are essential.

References

- [2.1] Bergveld, P. Thirty years of ISFETOLOGY: What happened in the past 30 years and what may happen in the next 30 years. *Sens. Actuat. B* **2003**, 88, 1-20.
- [2.2] Yates, D. E.; Levine, S.; Healy, T. W. Site-binding model of the electrical double layer at the oxide/water interface. *J. Chem. Soc., Faraday Trans. 1* **1974**, 70, 1807-1818.
- [2.3] Siu, W.M.; Cobbold, R.S.C. Basic properties of the electrolyte-SiO₂-Si system: Physical and theoretical aspects. *IEEE Trans. Electron devices ED-26* **1979**, 1805-1815.
- [2.4] Hiemstra, T.; Van Riemsdijk, W.H.; Bolt, G.H. Multisite proton adsorption modeling at the solid/solution interface of (hydr) oxides: A new approach. *J. Colloid Interface Sci.* **1989**, 133, 91-104.
- [2.5] Van Hal, R.E.G.; Eijkel, J.C.T.; Bergveld, P. A novel description of ISFET sensitivity with the buffer capacity and double layer capacitance as key parameters. *Sens. Actuat. B* **1995**, 24/25, 201-205.
- [2.6] Van Hal, R.E.G.; Eijkel, J.C.T.; Bergveld, P. A general model to describe the electrostatic potential at electrolyte oxide interfaces. *Adv. Colloid and Interface Sci.* **1996**, 31-62.
- [2.7] Shimada, K.; Yano, M.; Shibatani, K.; Komoto, Y.; Esashi, M.; Matsuo, T. Application of catheter-tip isfet. for continuous in-vivo measurement. *Med. Biol. Eng. Comput.* **1980**, 18, 741-745.
- [2.8] Smith, R.L.; Scott, D.C. A solid state miniature reference electrode, in: Proceedings of the IEEE/VSF Symposium on Biosensors. Los Angeles, CA, **1984**, 15-17, 61-62.
- [2.9] Suzuki, H.; Hirakawa, T.; Sasaki, S.; Karube, I. Micromachined liquid-junction

- Ag/AgCl reference electrode. *Sens. Actuat. B* **1998**, 46, 146-154.
- [2.10] Rehm, Daniel; McEnroe, Eamonn; Diamond, Dermot. An all solid-state reference electrode based on a potassium chloride doped vinyl ester resin. *Anal. Proc.* **1995**, 32, 319-322.
- [2.11] Huang, I. Y.; Huang, R. S.; Lo, L. H. Improvement of integrated Ag/AgCl thin-film electrodes by KCl-gel coating for ISFET applications. *Sens. Actuat. B* **2003**, 94, 53-64.
- [2.12] Huang, I. Y.; Huang, R. S.; Lo, L. H. A new structured ISFET with integrated Ti/Pd/Ag/AgCl electrode and micromachined back-side P⁺ contacts. *J. Chinese Institute of Engineers* **2002**, 25, 3, 327-334.
- [2.13] Nolan, M. A.; Tan, S. H.; Kounaves, S. P. Fabrication and characterization of a solid state reference electrode for electroanalysis of natural waters with ultramicroelectrodes. *Anal. Chem.* **1997**, 69, 1244-1247.
- [2.14] Comte, P. A.; Janata, J. A field effect transistor as a solid state reference electrode. *Anal. Chim. Acta.* **1978**, 101, 247.
- [2.15] Prohaska O. Patent US 4682602, 1987.
- [2.16] Nakajima, H.; Esashi, M.; Matsuo, T.; The cation concentration response of polymer gate ISFET. *J. Electrochem. Soc.* **1978**, 129, 141.
- [2.17] Matsuo, T.; Nakajima, H. Characteristics of reference electrodes using a polymer gate ISFET. *Sens. Actuat.* **1984**, 5, 293-305.
- [2.18] Errachid, A.; Bausells, J.; Jaffrezic-Renault, N. A simple REFET for pH detection in differential mode. *Sens Actuat. B* **1999**, 60, 43-48
- [2.19] Chodavarapu, V.P.; Titus, A.H.; Cartwright, A.N. Differential read-out architecture for CMOS ISFET microsystems. *Electron. Lett.* **2005**, 41, 12.
- [2.20] Yang, H.; Sun, H.; Han, J.; Wei, J.; Lin, Z.; Xia, S.; Zhong, H. A pH-ISFET based

- micro sensor system on chip using standard CMOS technology. *Fifth International Workshop on System-on-Chip for Real-Time Applications (IWSOC'05)* **2005**, 180-183.
- [2.21] Clark Jr., L.C.; Lyons, C. Electrode systems for continuous monitoring in cardiovascular surgery. *Ann. N.Y. Acad. Sci.* **1962**, 102, 29-45.
- [2.22] Caras, S.; Janata, J. Field effect transistor sensitive to penicillin. *Anal. Chem.* **1980**, 52, 1935-1937.
- [2.23] Janata, J.; Moss, S. Chemically sensitive field effect transistors. *Biomed. Eng.* **1976**, 6, 241-245.
- [2.24] Zayats, M.; Kharitonov, A.; Katz, E.; Bückmann, A.; Willner, I. An integrated NAD⁺-dependent enzyme-functionalized field-effect transistor (ENFET) system: development of a lactate biosensor. *Biosens. Bioelectron.* **2000**, 15, 671-680.
- [2.25] Schasfoort, R.; Kooyman, R.; Bergveld, P.; Greve, J. A new approach to immunofET operation. *Biosens. Bioelectron.* **1990**, 5, 103-124.
- [2.26] Zayats, M.; Raitman, O.; Chegel, V.; Kharitonov, A.; Willner, I. Probing antigen-antibody binding processes by impedance measurements on ion-sensitive field-effect transistor devices and complementary surface plasmon resonance analyses: development of cholera toxin sensors. *Anal. Chem.* **2002**, 74, 4763-4773.
- [2.27] Fromherz, P.; Offenhausser, A.; Vetter, T.; Weis, J. A neuron-silicon junction: a Retzius cell of the leech on an insulated-gate field-effect transistor. *Science* **1991**, 252, 1290-1293.
- [2.28] Wolf, B.; Brischwein, M.; Baumann, W.; Ehret, R.; Kraus, M. Monitoring of cellular signalling and metabolism with modular sensor-technique The Physio Control-Microsystem (PCM[®]). *Biosens. Bioelectron* **1998**, 13, 501-509.

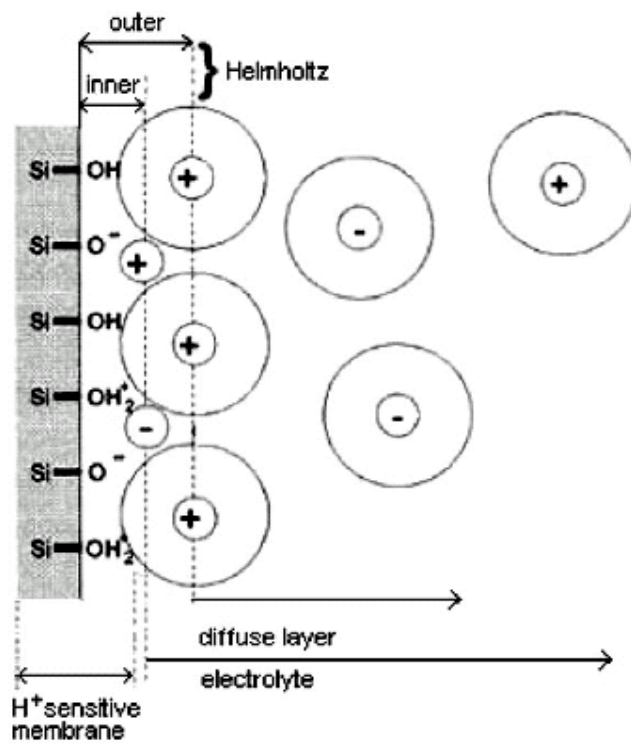


Figure 2-1 Properties of the electrode/electrolyte interface.

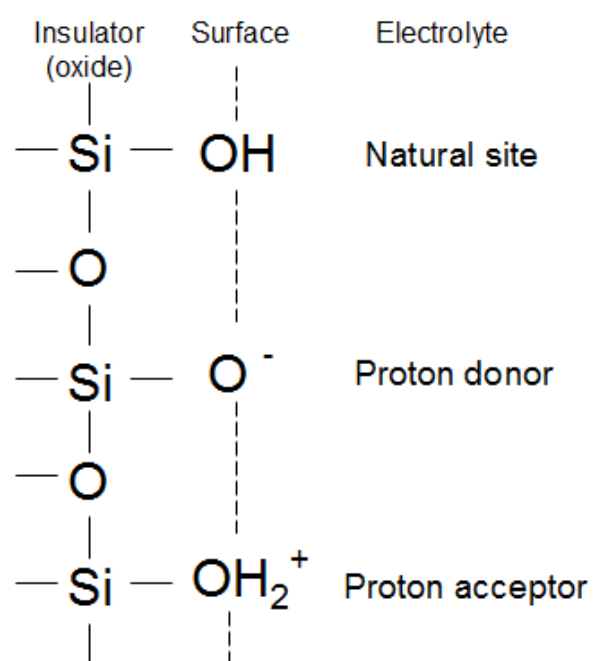
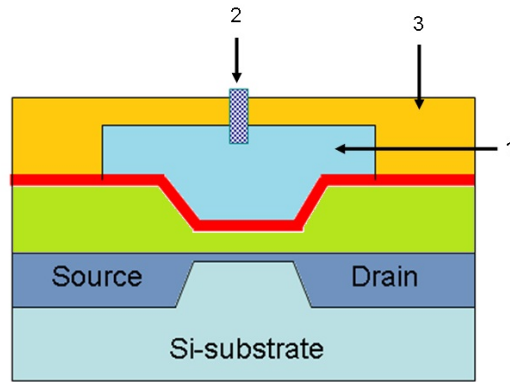
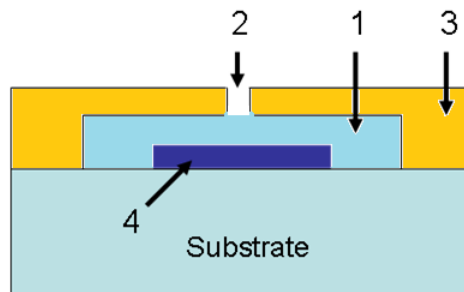


Figure 2-2 The site-binding model for the electrode/electrolyte interface.



(a)



(c)

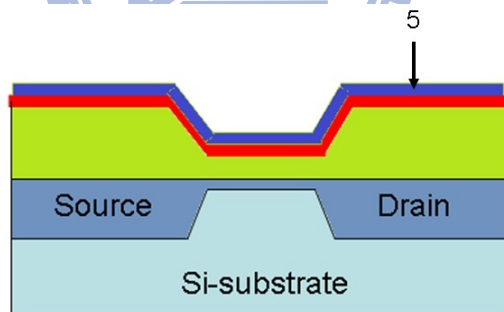
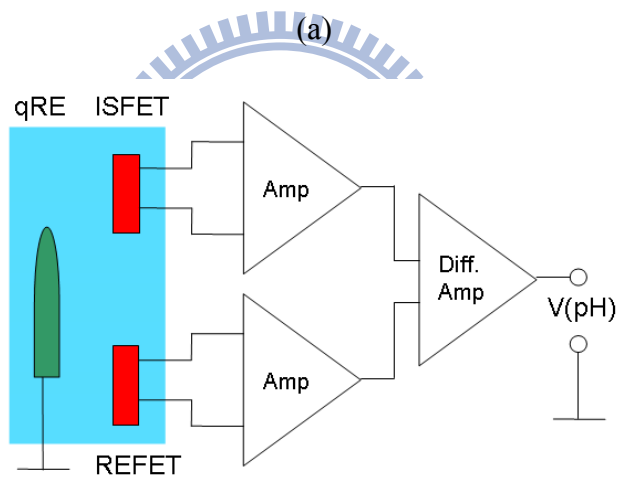
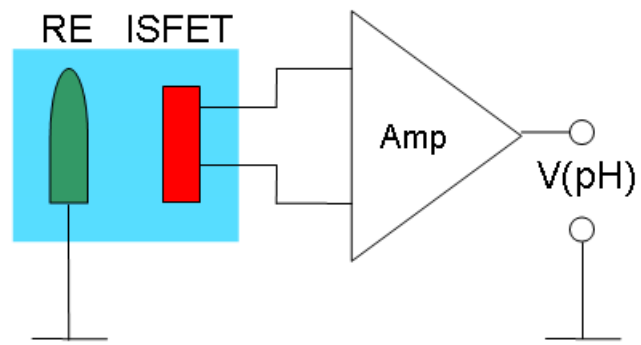


Figure 2-3 Different approaches for ISFET reference systems. (a) ISFET with pH buffer compartment (b) miniaturized Ag/AgCl reference electrode (c) ISFET with ion insensitive membrane. 1. pH buffer solution or KCl solution 2. glass capillary or hole 3. cover layer 4. measuring electrode with metallic lead 5. chemically modified sensing layer



(b)

Fig. 2-4 Different measuring circuits for ISFETs. (a) One-ended measuring circuit (b) ISFET/REFET differential measuring circuit.

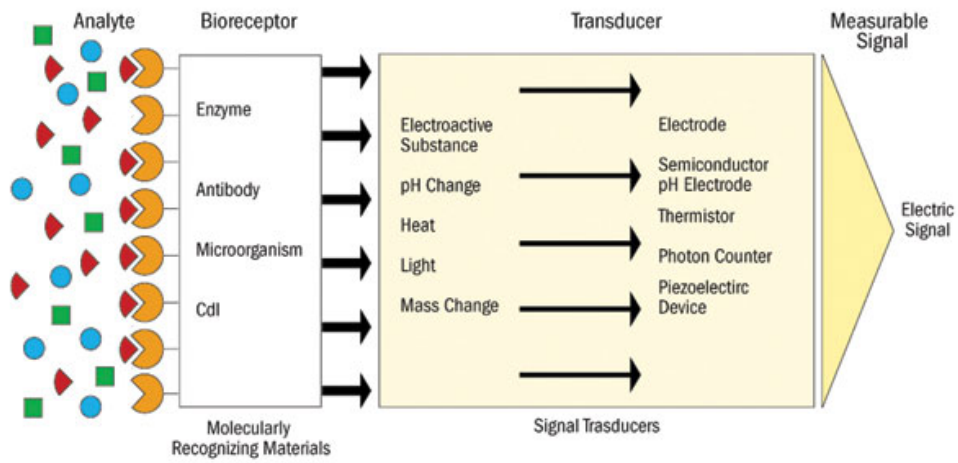


Fig. 2-5 Schematic diagram of biosensor elements.

Chapter 3

Optimization of post-annealing process and characterization of ion selectivity for ZrO₂ gated ISFETs

3.1 Introduction

The ISFETs fabricated with ZrO₂ gate as sensing membrane was reported [3.1]. To obtain the best performances, such as pH sensitivity, drift and hysteresis, the optimization of processes and characterization of ion interference are essential.

According to Equations (2-16) and (2-17), the pH sensitivity has been extensively described in terms of the intrinsic buffer capacity and the differential capacitance. It is determined by the reactions in solid/electrolyte interface. On the other hand, the drift and hysteresis are effects of surface slow effect. The phenomenon and algorithms have been widely discussed by many research groups [3.2-3.8]. The reports indicated that the material and surface condition of sensing layer dominated the drift and hysteresis.

Eisenman's theory of ion selectivity has shown that the selectivity is determined by the electrostatic field strength at the ion exchange sites [3.9]. Surface sites of ZrO₂ are considered to have strong field strength and therefore should have pH sensitivity. Meanwhile, due to the intrinsic mechanical stability of metal oxide, easy miniaturization and compatibility with CMOS processing, ZrO₂ is a good candidate for ISFET development.

Annealing is a heat treatment wherein a material is altered, causing changes in its properties such as surface morphology and atom density. It is a process that produces conditions by heating to above the re-crystallization temperature and maintaining a suitable

temperature, and then cooling. Annealing occurs by the diffusion of atoms within a solid material, so that the material progresses towards its equilibrium state. Heat is needed to increase the rate of diffusion by providing the energy needed to break bonds. The movement of atoms has the effect of redistributing and destroying the dislocations.

Recently, Pan *et al.* investigated the influence of thermal annealing on the structural characteristics of the Tm_2O_3 sensing membrane for pH detection [3.10]. The results revealed that the sensitivity, drift, and hysteresis are annealing temperature dependent. They were attributed to the formation of a well-crystallized Tm_2O_3 structure, a thinner low- k interfacial layer at the oxide/Si interface, and the higher surface roughness at optimal thermal annealing conditions. Lai *et al.* also reported that the pH sensitivity of 8 nm thick HfO_2 without underlying SiO_2 was increases from 46.2 to 58.3 mV/pH by 900°C post deposition annealing treatment [3.11].

Another important characteristic of pH-ISFETs is the membrane selectivity. The potentiometric selectivity coefficients are expressed according to the Nicolsky – Eisenman equation [3.12] as

$$\Delta V_T = \frac{RT}{z_i F} \ln \left[a_i + \sum_{j \neq i} k_{ij}(T) \cdot a_j^{\frac{z_i}{z_j}} \right] \quad (3-1)$$

where F is the Faraday constant, R is the gas constant, T is the absolute temperature, a is the ion activity, i, j are the main and interfering ion indices respectively, z is the ion electrovalence and k_{ij} is the selectivity coefficient. While performing the detection for the main ions, e.g. hydrogen ions, other so-called interference ions, K^+ , Na^+ , for example, are also join to determine the potential change. As a result, the exact concentration of main ions can not be measured. Since it is unavoidable, the impact of the interference ions on a sensing membrane should be evaluated.

3.2 Experiment

3.2.1. Device Fabrication

The detailed fabrication procedures and fundamental characteristics of ZrO₂ gate ISFETs has been reported [3.1]. Figure 3-1 shows the schematic diagram of fabricated ZrO₂ gate ISFET. The SiO₂ dielectric FETs were fabricated on p-type silicon wafers with (100) orientation accordingly, and their source/drain areas were fabricated with phosphorus/boron ion implantation respectively. A 30-nm-thickness sensing layer of the ZrO₂ membrane was deposited onto the SiO₂ gate FET by DC sputtering with 4-inch diameter and 99.99% purity of Zirconium target in oxygen atmosphere. The total sputtering pressure was 20 mTorr in the mixed gases Ar and O₂ for 200 mins while the base pressure was 3×10^{-6} Torr, and the RF power was 200 W and the operating frequency 13.56 MHz. Brief manufacturing process steps are addressed as follows:

- (1) Standard RCA clean for 4-inch p-type silicon wafers
- (2) Wet oxidation growth for silicon dioxide (600 nm)
- (3) Defining of Source/Drain areas and wet etching of silicon dioxide by Buffered Oxide Etching (BOE)
- (4) Thermal growth of silicon dioxide as screen oxide (30 nm)
- (5) Phosphorus or boron ions implantation and post annealing at 950 °C
- (6) Plasma Enhanced Chemical Vapor Deposition (PECVD) deposition of silicon dioxide as passivation layer
- (7) Defining of contact hole and gate region and wet etching of silicon dioxide by BOE
- (8) Dry oxidation of gate oxide (30 nm)
- (9) DC sputtering of ZrO₂ (30 nm) and post annealing in N₂ at 600, 700, 800 and 900 °C for 30 minutes, respectively
- (10) Defining of gate region and wet etching of oxide by BOE

(11) Aluminum sputtering with hard contact mask (500 nm)

3.2.2. Packaging and Measurement setup

Figure 3-2 shows the measurement setup. A HP4156A semiconductor parameter analyzer was used for measuring the I_{DS} - V_{GS} characteristics for the ZrO_2 gate ISFETs soaked in pH buffer solutions (purchased from R.D.H., Seelze, Germany). The source-drain voltage was kept constant at $V_{DS} = 2V$. A container was bonded to the gate region of ISFET by using epoxy resin. All the measurements were performed based on a commercial Ag/AgCl glass reference electrode, which was connected to the gate of the device and the power supplier to provide stable bias potential for device operation. The measurements were performed at room temperature of 25 °C, which was kept constant by a temperature control system, and all the setup was placed in a dark box.

3.2.3 Hysteresis and drift measurement

Prior to perform the measurement, the pH-ISFETs were immersed in the pH=7 buffer solution for 2 hours to keep the devices stable. The hysteresis curve was obtained by measuring in the first sequence of pH = 7→3→7→11→7 and then the second sequence of pH = 7→11→7→3→7, with loop time of 15 minutes. Three measuring points were obtained for each pH value in the duration of one minute.

The ISFET's sensing layer was soaked in the buffer solution (pH=7) for 13 hours before drift measurement. 36 points were obtained during 10 minutes in the same pH value of aqueous solution.

3.2.4 Preparation of Na⁺ and K⁺ ion solutions

The K⁺ and Na⁺ test solutions were prepared as follows:

- (1) The 0.1M Na⁺ or K⁺ ion solutions were prepared by diluting 1ml 3M NaCl and KCl solution with 30ml of each pH buffer solution.
- (2) The 0.1M Na⁺ and K⁺ ion solutions were prepared by diluting 1ml 0.1M Na⁺ or K⁺ ion solutions with 100ml of pH buffer solution.
- (3) Repeating step (2) to obtain the ion solutions of pNa and pK equal to 10.

3.3 Results and discussions

3.3.1 Optimization of post-annealing process

Figure 3-3 shows the pH sensitivity and linearity of ZrO₂ membrane annealed at different temperatures. For the sample without any post annealing, the pH sensitivity was only 39.54 mV/pH, which is lower than others. On the contrary, the pH sensitivity of 900 °C annealed sample was 48.17 mV/pH, which is higher than 700 °C and 800 °C annealed samples, which few defects were found. Meanwhile, the results show that the ZrO₂ layer annealed at 600 °C presents the best sensitivity (54.5 mV/pH) and linearity (0.9996) performances.

To explain the post deposition annealing effects on sensitivity, the site-binding model was applied again as Equation 3-2.

$$\varphi_0 = 2.303 \frac{kT}{q} \frac{\beta}{\beta+1} (pH_{PZC} - pH) \quad (3-2)$$

where $pH_{PZC} = -\log(k_a + k_b)^{1/2}$ is the point of zero surface charge. The pH_{pzc} is where the surface charge switches from negative through zero to positive. k_a is the acidic equilibrium constant, k_b is the basic equilibrium constant, k is the Boltzmann constant, T is the measuring temperature, and β is a parameter, given by $\beta = \frac{2q^2 N_s (k_a k_b)^{1/2}}{kTC_{diff}}$ where N_s is

the surface site density and C_{diff} is the differential double-layer capacitance. According to Equation 3-2, the k_a , k_b , C_{diff} and N_s , which determined by the electrolyte/solid interface condition, dominate the pH sensitivity.

Figures 3-4 (a)-(e) show the scanning electron microscope (SEM) images of the ZrO_2 films which annealed at 600, 700, 800, 900 °C and not annealed, respectively. The sputter-deposit ZrO_2 film without post deposition annealing seems to be amorphous. As a result, it demonstrated low sensitivity and low linearity performances, which represents the k_a , k_b , and N_s are smaller than others. For the films with post deposition annealing at 700 to 900 °C, the grain sizes as well as surface roughness of films are proportional to the annealing temperatures, it is inferred that the N_s should be larger accordingly. As a result, the pH sensitivities were proportional to the annealing temperature. However, for the case of 600 °C annealing, the pH sensitivity was higher than other conditions. It could be explained that though the size of surface grains are smaller than others, but due to the tight arrangement, the effective N_s could be larger than others.

The hysteresis effect may induce the inaccurate measurement of pH-ISFET devices. The hysteresis is caused by the slow response of the pH-ISFET [3.13], the ions diffuse from the surface of the sensing film into the buried site are very slow, and results in slow response. In addition, due to the different sizes of H^+ and OH^- ions, the diffusion speed of H^+ ions into the buried site are faster than that of OH^- ions, as described by Bousse et al. [3.14]. This causes the asymmetric hysteresis behavior of the pH-ISFET devices. Figures 3-5 (a)-(e) show hysteresis curves in pH loop 7→3→7→11→7 and Figures 3-6 (a)-(e) show hysteresis curves in another pH loop 7→11→7→3→7 for samples. The asymmetric hysteresis behavior can be observed in all samples. Table 3-1 summarized the overall performances for all samples with different annealing temperature. It is observed that the 600 °C sample demonstrates the smallest hysteresis, which can be attributed to the surface quality with dense atoms arrangement. The

similar results also happened in drift behaviors as shown in Figures 3-7 (a)-(e). According to Yule et al. [3.15] and Jamasb et al. [3.16], the drift is due to the hydration. The thickness of the hydrated layer is increased with time. Thus, the overall insulator capacitance would be decreased, results in the threshold voltage increases with time. Again, the film annealed at 600 °C demonstrates the best drift performance than other. For the application of pH-ISFETs, the ZrO₂ films with optimal post deposition annealing process at 600 °C demonstrated the best performance in pH sensitivity, linearity, hysteresis and drift.

3.3.2 Characterization of ion selectivity

The ISFET with ZrO₂ sensing film which fabricated in 600 °C post deposition annealing process demonstrated the high sensitivity property for hydrogen ions. However, since the ISFETs are possible use in complex electrolyte environment, the selectivity to other ions, such as K⁺ and Na⁺, becomes important and requires further study.

Ions are charged so they interact in the solution attracting and repelling each other with coulomb forces. These interactions influence ions behavior and does not allow to treat every ion in the solution independently. Figures 3-8 (a) and (b) show the pK and pNa responses of the ZrO₂ ISFET at pH=9, respectively. While the K⁺ concentration lower than pK=5 or the Na⁺ concentration lower than pNa=3 at pH=9, the potential differences caused by K⁺ or Na⁺ are very small which can be ignored. On the contrary, while the K⁺ or the Na⁺ concentration larger than the same values above, the sensitivities are estimated as 8.67 mV/pK and 7.5 mV/pNa, respectively. The ranges and sensitivities are influenced by the ionic strength of the buffer solutions. In chapter 2 we described the relationship between ion concentration, activity and activity coefficient as Equation 2-1. To obtain the precise ion activities, the most popular method used to calculate ions activities proposed by Debye and Hückel [3.17] in 1923 is incorporated. First step in calculations is calculation of so

called ionic strength, using following formula:

$$I = \frac{1}{2} \sum C_i z_i^2 \quad (3-3)$$

where C_i is a molar concentration of i^{th} ion present in the solution and z_i is its charge. Summation is done for all charged molecules present in the solution. Second step is calculation of activity coefficients given by formula:

$$\log \gamma_z = \frac{-0.51 z^2 \sqrt{I}}{1 + \sqrt{I}} \quad (3-4)$$

Activity coefficient for all ions bearing the same charge is identical.

Activity of any ion (with charge z) is

$$a_i = \gamma_z C_i \quad (3-5)$$

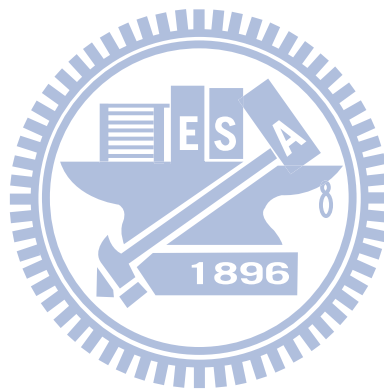
where γ_z denotes activity coefficient for z -charged ions.

Figures 3-9 (a) and (b) describe the detection limits and sensitivities of K^+ and Na^+ at the buffers of pH=3 to pH=11. As the hydrogen ion concentration increased, where the ionic strength of H^+ is also increased, the detection limits and sensitivities of K^+ and Na^+ are decreased due to the interference from the H^+ . In contrast, the activity of H^+ is also interfered by that of K^+ and Na^+ . The pH sensitivity is decreased significantly while the pK or pNa less than 5. Meanwhile, the maximal pH sensitivities of ZrO_2 film are around 45 mV/pH and 39 mV/pH with K^+ and Na^+ adding in pH buffer solutions. It revealed that the selectivity coefficient $\gamma_{(H^+, K^+)}$ and $\gamma_{(H^+, Na^+)}$ are different for ZrO_2 sensing film.

Figure 3-10 summarizes the multi-ion detecting characteristics of ZrO_2 gated ISFET. With the K^+ and Na^+ interference, the pH sensitivity was degraded. On the other hand, with the interference from different ionic strength of hydrogen ions, both the pK and pNa sensitivity curves are linear and lower than 10 mV/pX ($X = K$ or Na).

3.4 Summary

The optimal post-annealing process of fabricating ZrO_2 gated ISFETs are developed. The results reveal that the post deposition annealing temperature of 600°C for 30 minutes is essential, it improves the surface condition of the ZrO_2 film. As a result, the high pH sensitivity and linearity, low hysteresis and drift characteristics are obtained. Based on the ISFETs with optimal annealing process, the characterization of ion selectivity and interference are investigated. Through the characterization of multi-ion detection, the ion sensitivity under different ionic strength conditions can be more precisely described. It is important for ISFET used in the biological applications.



References

- [3.1] Chang, K.M.; Chao, K.Y.; Chou, T.W.; Chang, C.T. Characteristics of zirconium oxide gate ion-sensitive field-effect transistors. *Jpn. J. Appl. Phys.* **2007**, *46*, 4333-4337.
- [3.2] Bousse, L.; Bergveld, P. The role of buried OH sites in the response mechanism of inorganic-gate pH-sensitive ISFETs. *Sens. Actuat.* **1984**, *6*, 65-78.
- [3.3] Jamasb, S.; Collins, S. D.; Smith, R. L. A physical model for threshold voltage instability in Si₃N₄-gate H⁺-sensitive FET's (pH-ISFET's). *IEEE Trans. Electron Devices* **1998**, *45*, 1239-1245.
- [3.4] Abe, H.; Esashi, M.; Matsuo, T. ISFET's using inorganic gate thin films. *IEEE Trans. Electron Devices* **1979**, *26*, 1939-1944.
- [3.5] Topkar, A.; Lal, R. Effect of electrolyte exposure on silicon dioxide in electrolyte-oxide-semiconductor structures. *Thin Solid Films* **1993**, *232*, 265-270.
- [3.6] Buck, R. P. Kinetics and drift of gate voltages for electrolyte-bathed chemically sensitive semiconductor devices. *IEEE Trans. Electron Devices* **1982**, *29*, 108-115.
- [3.7] Dun, Y.; Wei, Y. D.; Wang, G. H. Time-dependent response characteristics of pH-sensitive ISFET. *Sens. Actuat. B* **1991**, *3*, 279-285.
- [3.8] Esashi, M.; Matsuo, T. Integrated micro multi ion sensor using field effect of semiconductor. *IEEE Trans. Biomed Eng.* **1978**, *BME 25*, 84-92.
- [3.9] Abe, H.; Esashi, M.; Matsuo, T. ISFET's using inorganic gate thin films. *IEEE Trans. Electron Devices* **1979**, *26*, 1939-1944.

- [3.10] Pan, T. M.; Lee, C. D.; Wu, M. H. High-k Tm_2O_3 sensing membrane-based electrolyte-insulator-semiconductor for pH detection. *J. Phys. Chem. C* **2009**, 113, 21937-1940
- [3.11] Lai, C. S.; Yang, C. M.; Lu, T. F. pH sensitivity improvement on 8 nm thick hafnium oxide by post deposition annealing. *Electrochem. Solid-State Lett.* **2006**, 9, 3, 90-92.
- [3.12] Janicki, M. Napieralski, A. Department of microelectronics and computer science, technical university of Lodz, Al. Politechniki 11, 93-590 Lodz, *Poland*.
- [3.13] Bousse, L.; Mostarshed, S.; van der schoot, B.; de Rooij, N.F. Comparison of the hysteresis of Ta_2O_5 and Si_3N_4 pH-sensing insulators. *Sens. Actuat. B* **1994**, 17, 157-164.
- [3.14] Bousse, L.; Bergveld, P. The role of buried OH^- sites in the response mechanism of inorganic-gate pH-sensitive ISFETs. *Sens. Actuat. B* **1984**, 6, 65-8.
- [3.15] Yule, Z.; Shouan, Z.; Tao, L. Drift characteristic of pH-ISFET output. *Chin. J. Semicond.* **1994**, 12, 15, 838-843.
- [3.16] Jamasb, S.; Collins, S.; Smith, R. L. A physical model for drift in pH ISFETs. *Sens. Actuat. B* **1998**, 49, 146-155.
- [3.17] Debye, P.; Hückel, E. The theory of electrolytes. I. Lowering of freezing point and related phenomena. *Physikalische Zeitschrift* **1923**, 24, 185-06.

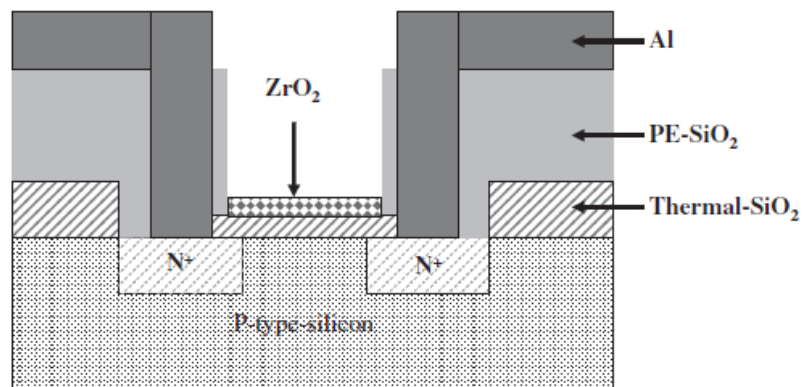


Figure 3-1 Schematic diagram of ZrO₂ gate ISFET fabricated by the MOSFET technology.

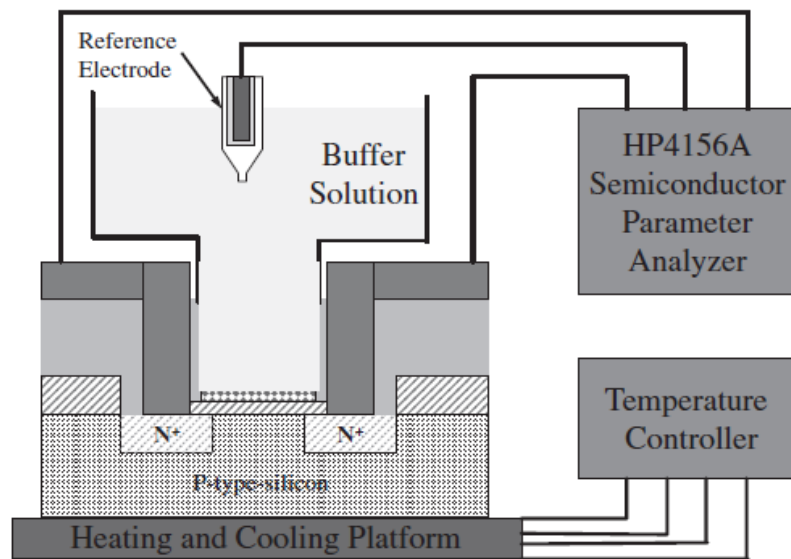


Figure 3-2 Setup of measurement using HP4156A semiconductor parameter analyzer and temperature controller.

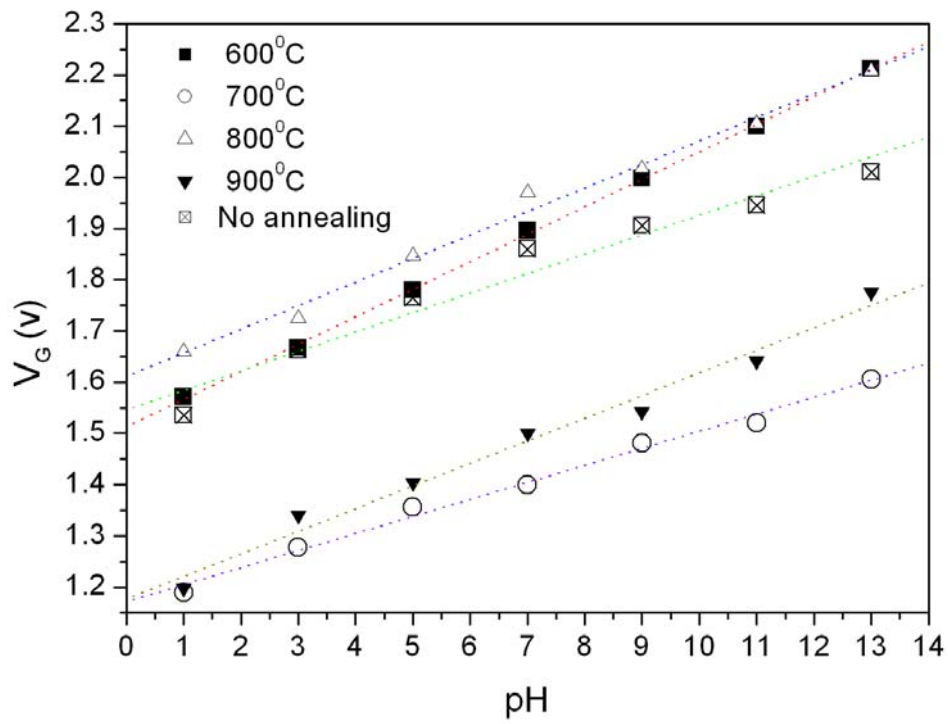
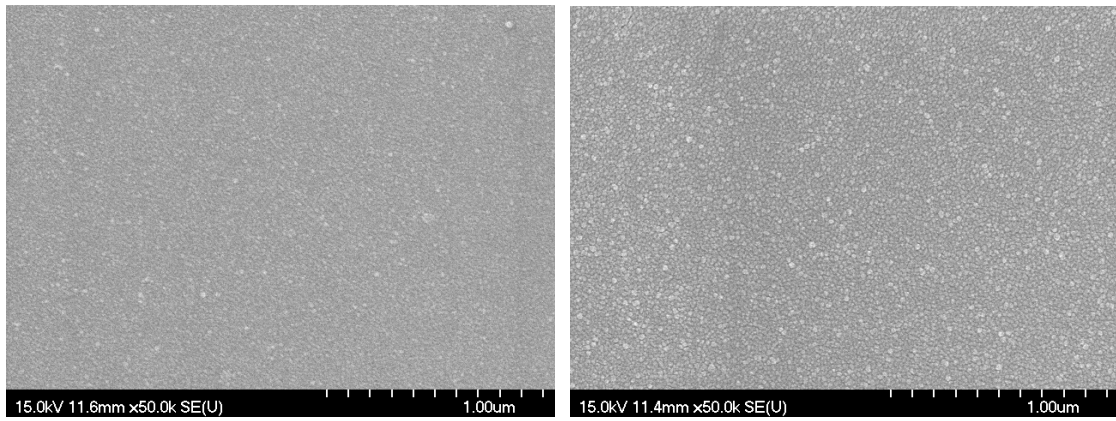
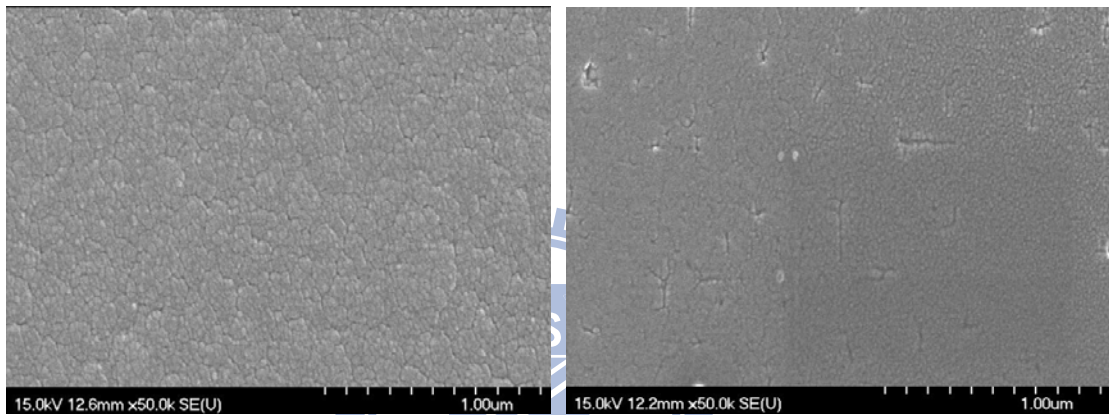


Figure 3-3 The pH sensitivity and linearity of ZrO₂ membrane annealed at 600 - 900°C and no annealing.



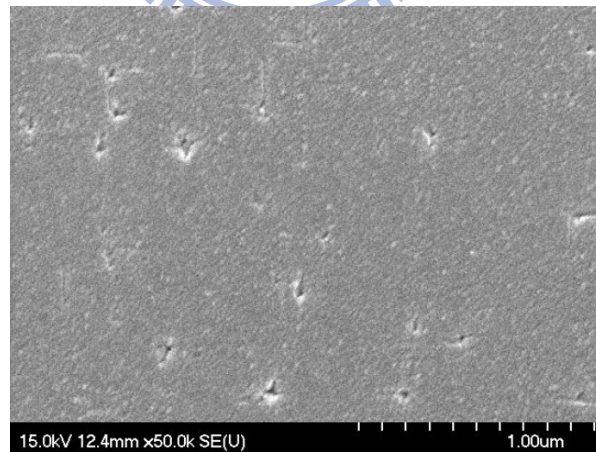
(a)

(b)



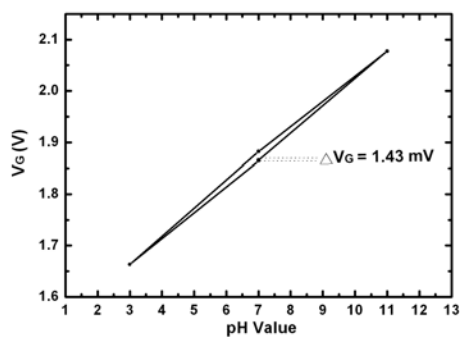
(c)

(d)

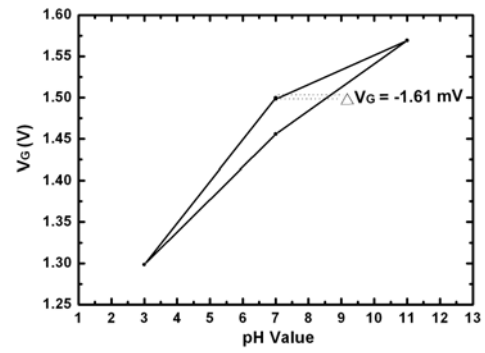


(e)

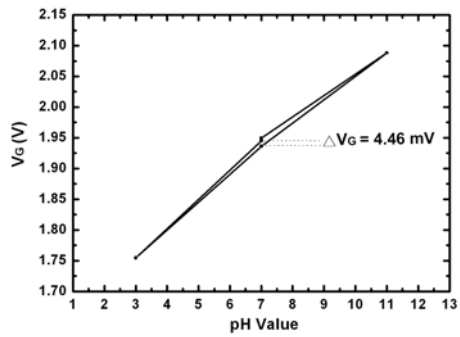
Figure 3-4 The SEM images of the ZrO₂ films which annealed at (a) 600, (b) 700, (c) 800, (d) 900°C and (e) not annealed, respectively.



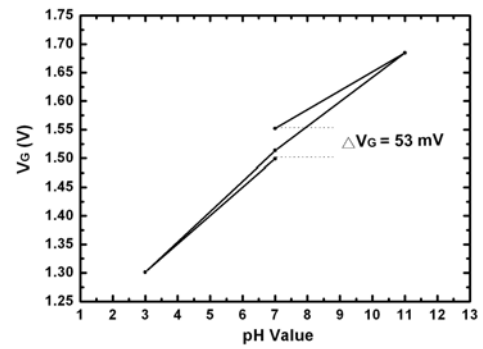
(a)



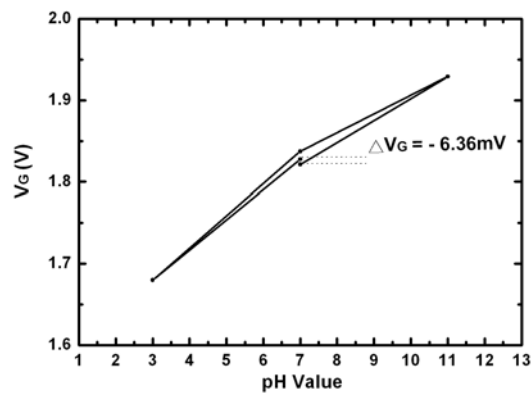
(b)



(c)

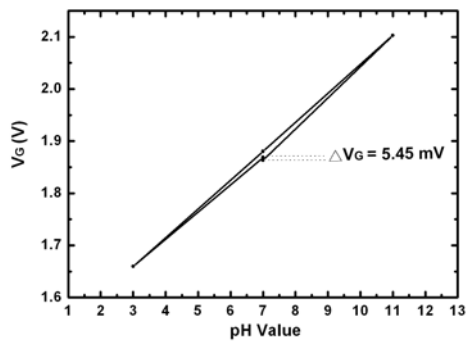


(d)

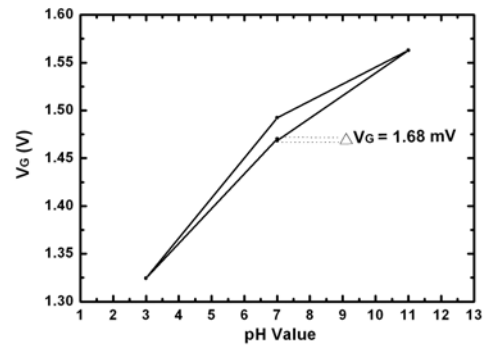


(e)

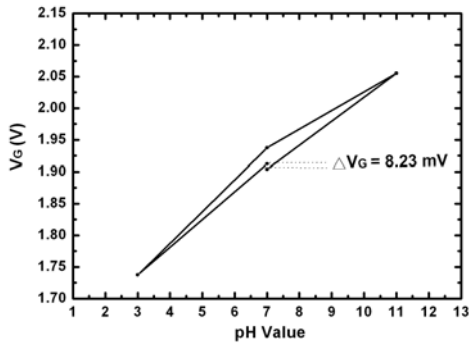
Figure 3-5 The hysteresis curves obtained in pH loop 7→3→7→11→7 for the ZrO_2 films which annealed at (a) 600, (b) 700, (c) 800, (d) 900°C and (e) not annealed, respectively.



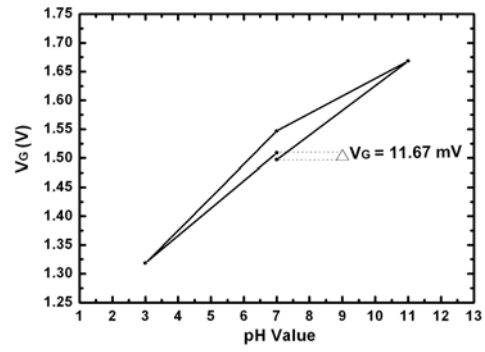
(a)



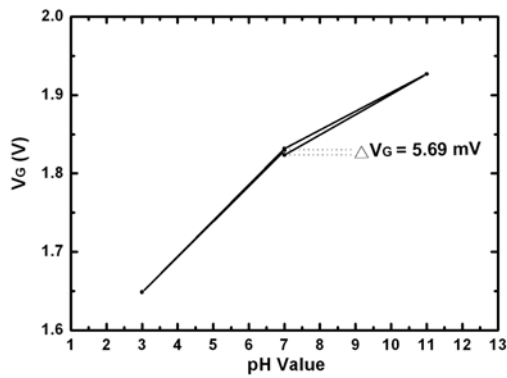
(b)



(c)

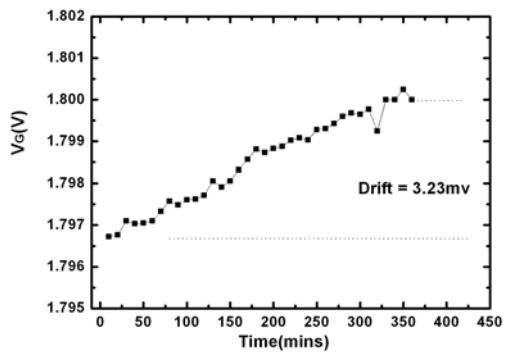


(d)

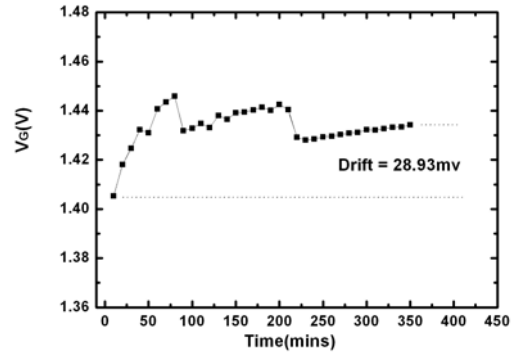


(e)

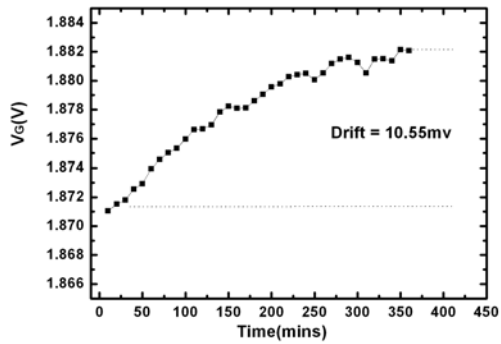
Figure 3-6 The hysteresis curves obtained in pH loop 7→11→7→3→7 for the ZrO₂ films which annealed at (a) 600, (b) 700, (c) 800, (d) 900°C and (e) not annealed, respectively.



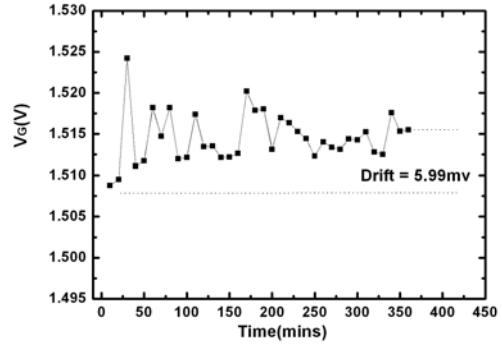
(a)



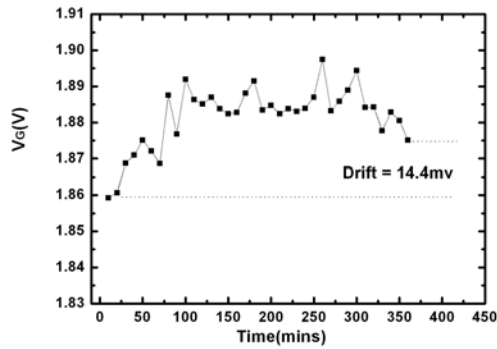
(b)



(c)

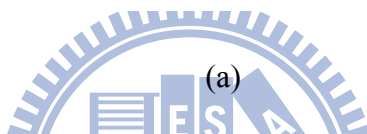
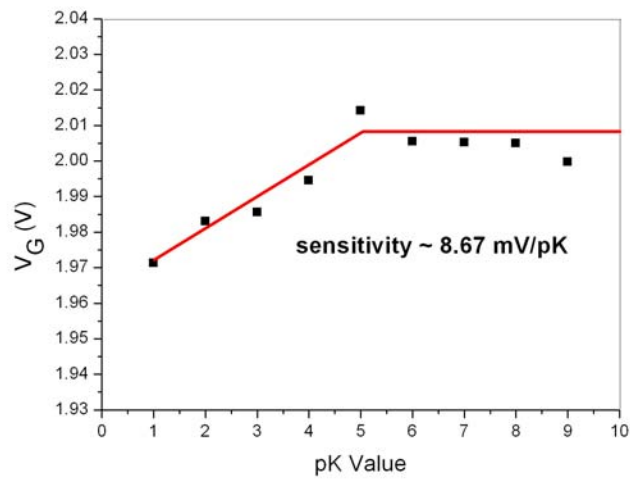


(d)

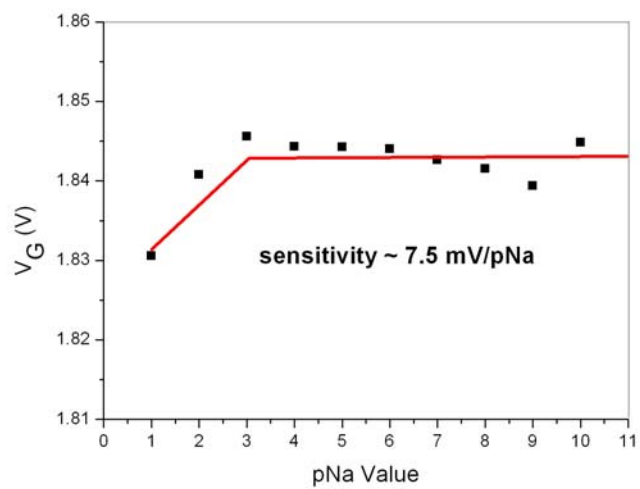


(e)

Figure 3-7 The drift performances of the ZrO_2 films which annealed at (a) 600, (b) 700, (c) 800, (d) 900°C and (e) not annealed, respectively.

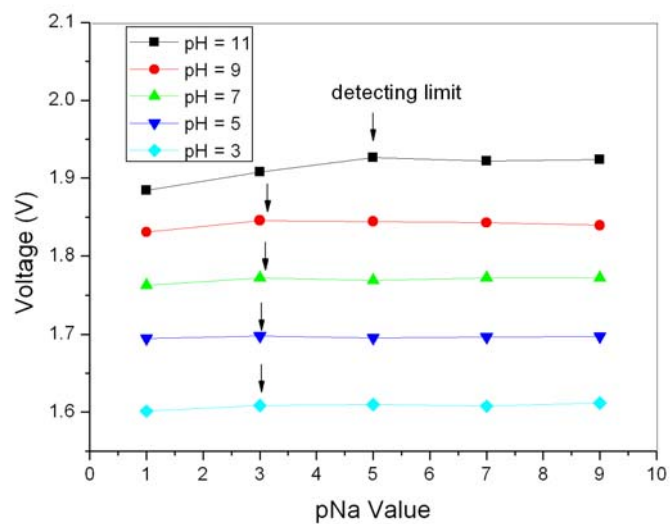
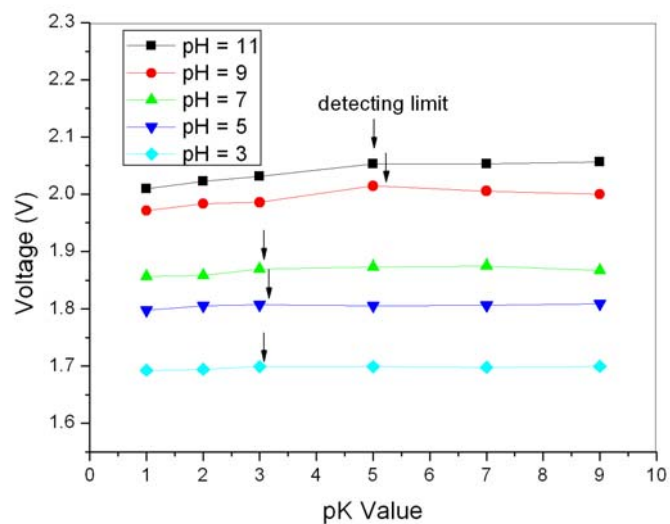


(a)



(b)

Figure 3-8 The (a) pK and (b) pNa responses of the ZrO_2 ISFET at pH=9



(b)

Figure 3-9 Detection limits and sensitivities of (a) K^+ and (b) Na^+ at the buffers of pH=3 to pH=11.

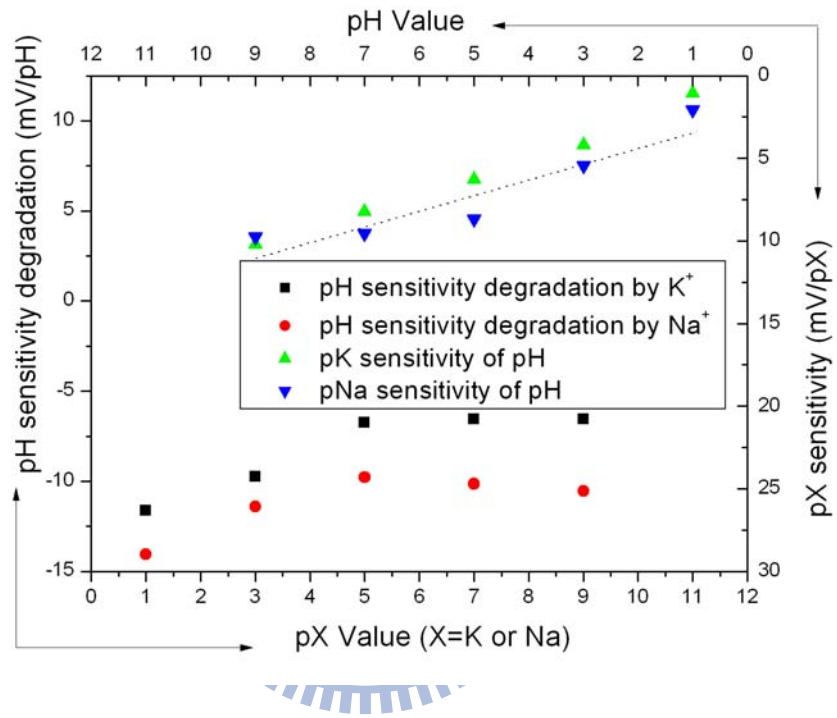



Figure 3-10 The multi-ion detecting characteristics of ZrO₂ gated ISFET. The pX (X=K or Na) sensitivities were measured at various pH buffer solutions. The pH sensitivities were degraded due to the K⁺ or Na⁺ interferences.

Table 3-1 The overall performances for samples with different post annealing temperature



	Sensitivity (mV/pH)	Linearity (%)	Drift (mV/h)	Hysteresis (mV) at different pH loop	
				7→3 →7 →11 →7	7→11 →7 →3 →7
Not annealed	39.54	95.83	2.4	-6.36	5.7
600°C	54.5	99.96	0.54	1.43	5.45
700°C	42.0	99.12	1.9	-12.52	22.27
800°C	45.65	99.07	1.76	4.46	8.23
900°C	48.17	98.27	1.0	53	11.67

Chapter 4

A Novel pH-dependent drift improvement method for ZrO₂ gated pH-ISFETs

4.1 Introduction

Since the first work for the Ion Sensitive Field Effect Transistor (ISFET) published by P. Bergveld in 1970 [4.1], numerous chemical and biomedical applications based on ISFET were developed. ISFET has the advantages of rapid response, small size, high input-impedance and low output-impedance, as well as the applicability of semiconductor and integrated-circuit technologies. However, the device instability phenomenon, commonly known as drift, associated with hydrogen ion concentration and time for the ISFET is still one of the critical challenges in developing commercial ISFET-based biomedical sensors. In particular, the high accuracy desired for continuous monitoring in food [4.2] or biomedical applications requires a tolerable drift rate in pH-ISFETs. The phenomenon and algorithms have been widely discussed by many research groups [4.3-4.9]. The summarized factors for drift behaviors are: electric field enhanced ion migration within the gate insulator; electrochemical non-equilibrium conditions at the insulator solution interface; injection of electrons from the electrolyte at strong anodic polarizations to create negative space charge inside the insulator films; and the slow surface effects.

According to the studies of Chou et al. [4.10-4.14], the pH-independent and pH-dependent drift behaviors were observed on the ISFETs fabricated with different sensing materials and processes, such as hydrogenated amorphous silicon, tin oxide, amorphous tungsten oxide and AlN, etc. The pH-independent drift was defined as that the

measured potential difference over a period of time in which the ISFET was immersed in the buffer solution of fixed pH value. Proposed solutions to improve pH-independent drift includes the specially designed compensative readout circuits [4.15], the new device structure with metal oxide as gate contact [4.16] and the choices of proper sensing films to suppress the influence of the pH-independent drift [4.17-4.19]. However, a promising method to deal with the pH-dependent drift has not been available up to date. The pH-dependent drift is obtained by measuring sensors under different pH values buffer solutions and its behavior is quite different from pH-independent drift because of its non-constant characteristics in different pH value electrolytes.

The pH-dependent potential drift is the function of hydrogen ion concentration; as a result, the overall drift - which consists of pH-independent and pH-dependent potential differences - is difficult to be compensated.

Drift behavior of membrane based ISFETs, such as SiO_2 , Si_3N_4 , Al_2O_3 and Ta_2O_5 were reported [4.20-4.23]. The voltage shift of devices immersed in electrolyte before 103 mins were 3–30 mV for Ta_2O_5 [4.21, 4.22, 4.24], ~40 mV for Si_3N_4 [4.4, 4.21] and around 50 mV for Al_2O_3 [4.20]. On the other hand, the drift measured after 103 mins were in the range of 0.01-1 mV/ pH. This behavior of hyperbolic-like change with time restricts the measurement accuracy of ISFETs for the first 103 mins.

Eisenman's theory of ion selectivity has shown that the selectivity is determined by the electrostatic field strength at the ion exchange sites [4.5]. Surface sites of ZrO_2 are considered to have strong field strength and therefore should have pH sensitivity. Meanwhile, due to the intrinsic mechanical stability of metal oxide, easy miniaturization and compatibility with CMOS processing, ZrO_2 is a good candidate for ISFET development. Experimental results show that the ZrO_2 ISFETs have high pH sensitivity of 57.5 mV/pH, wide linear detecting range of pH 1–13 and low drift of 0.1–0.2 mV/hr after

103 mins operation [4.25]. It is comparable with other high performance ISFETs, such as Ta₂O₅ ISFET [4.21].

For many applications, the pH-ISFETs are stored in dry environment and always begin each measuring session with a two-point calibration at different pH buffer solutions, such as pH = 7.0 and pH = 4.01. Those calibrations are always executed in the first hours, which endure the severe potential drift. Meanwhile, the amount of pH-dependent drift is also different, which means that the overall drift cannot be compensated with a simple constant amount. As a result, the accuracy of measurement is restricted or some more complicated compensation circuits are required.

In this study, a novel compensation method by means of sequential measurement of both n-channel and p-channel co-fabricated ZrO₂ gate ISFETs to improve the pH-dependent drift effect was developed and illustrated.

4.2 Experiment



4.2.1 Device fabrication

The detailed fabrication procedures and fundamental characteristics of ZrO₂ gate ISFETs has been reported [4.18]. Figure 4-1 shows a schematic diagram of the ZrO₂ gate ISFET, which was fabricated by the Metal Oxide Semiconductor Field Effect Transistor (MOSFET) technique. The SiO₂ dielectric FETs were fabricated on both p-type and n-type silicon wafers with (100) orientation accordingly, and their source/drain areas were fabricated with phosphorus/boron ion implantation respectively. A 30-nm-thickness sensing layer of the ZrO₂ membrane was deposited onto the SiO₂ gate FET by DC sputtering with 4-inch diameter and 99.99% purity of Zirconium target in oxygen atmosphere The total sputtering pressure was 20 mTorr in the mixed gases Ar and O₂ for

200 mins while the base pressure was 3×10^{-6} Torr, and the RF power was 200 W and the operating frequency 13.56 MHz. Detailed fabrication processes please refer to Chapter 3.2.

4.2.2 Packaging and measurement

Figure 4-2 shows the measurement setup and a HP4156A semiconductor parameter analyzer, which was used for measuring the $I_{DS}-V_{GS}$ characteristics for the ZrO₂ gate ISFETs soaked in pH buffer solutions (purchased from R.D.H., Seelze, Germany), where source-drain voltage $V_{DS} = 2$ V was kept constant. A container was bonded to the gate region of ISFET by using epoxy resin. All the measurements were performed based on a commercial Ag/AgCl glass reference electrode, which was connected to the gate voltage supplier to provide stable bias potential for device operation. The measurements were performed at room temperature of 25 °C, which was kept constant by a temperature control system, and all the setup was placed in a dark box. The measurement of drift was performed and calculated according to the time frame of the first to seventh hours.

4.3 Results and discussions

4.3.1 pH sensitivity of n-channel and p-channel ZrO₂ gate ISFETs

Figure 4-3 shows the similar sensitivities for both n-channel and p-channel ZrO₂ gated ISFETs. The measurements were conducted with constant source-drain current and the changes of gate voltage were observed with soaking in various pH buffer solutions. The values were 58.7 and 57.1 mV/pH, respectively. According to the site-biding theory [4.1], the surface potential established by buffer solution will dominate the change of threshold voltage. The sensitivity has been extensively described in terms of the intrinsic buffer capacity and the differential capacitance. General expression for the sensitivity of

pH-ISFET [4.26]:

$$\frac{\Delta\Psi_0}{\Delta pH_B} = -2.3 \frac{q}{kT} \alpha \quad (4-1)$$

with

$$\alpha = \frac{1}{\frac{2.3kTC_{dif}}{q^2\beta_{int}} + 1} \quad (4-2)$$

Note that α is a dimensionless sensitivity parameter with value depending on the intrinsic buffer capacity β_{int} and the differential capacitance C_{dif} . These two factors are determined by the sensing material, processes and electrolyte tested. In this experiment, ZrO₂ sensing films fabricated for both n-channel and p-channel ISFETs were with the same processes. Consequently, their pH sensitivities should be the same.

4.3.2. Drift rate of n-type and p-type ZrO₂ gate ISFETs

Figures 4-4 and 4-5 show the drift of the n-channel and p-channel ZrO₂ ISFET, respectively: the results revealed that the drift is pH-dependent. The potential drifts for pH = 3, 5, 7, 9 and 11 during the time frame of the first seven hours are -58.55, -51.54, -41.61, -34.66 and -32.52 mV, respectively. On the other hand, the values are 13.33, 6.04, -4.91, -25.92 and -30.82 mV for the p-channel ZrO₂ ISFET. The drift rate for each type of pH-ISFET between hours one to seven was defined as drift voltage divided by time, and the results are shown in Figure 4-6. The drift rate *versus* different hydrogen concentrations shows the opposite trends for both n-channel and p-channel ISFETs, respectively. According to the model proposed by Jamasb *et al.* [4], the gate voltage drift can be expressed as below:

$$\Delta V_G(t) = -(Q_D + Q_I + Q_{inv}) \cdot \left(\frac{\varepsilon_n - \varepsilon_{HL}}{\varepsilon_n \varepsilon_{HL}} \right) x_{HL}(\infty) \left\{ 1 - \exp \left[- \left(\frac{t}{\tau} \right)^\beta \right] \right\} \quad (4-3)$$

Where Q_D and Q_{inv} represent the charges stored in the semiconductor depletion layer

and the inversion charge, respectively. The signs of Q_D and Q_{inv} are determined based on the device polarity. Q_I is the effective charge per unit area induced in the semiconductor by the various types of charges that may be present in the insulator, and the magnitude and distribution of the charge entering can be attributed. ε_n and ε_{HL} represent the dielectric constant of the original sensing layer and the hydrated layer, and x_{HL} the final thickness of the modified layer. β is the dispersion parameter satisfying $0 \leq \beta \leq 1$. The term $x_{HL}(\infty) \left\{ 1 - \exp \left[- \left(\frac{t}{\tau} \right)^\beta \right] \right\}$ represents the chemical hydration dispersive transport, which is an effect that alters the capacitance of dielectrics.

In general, a drift behavior is regarded as a superposition effect of a chemical and an electrical change at the surface of the gate insulator [4.15]. The chemical change represents the hydration dispersive transport whose degree was determined by both of the hydration species and the material properties of the sensing films. According to the result of previous study [4.18], the drift rate of the ZrO_2 film is similar to the result of the Al_2O_3 [4.20], whose extracted value of x_{HL} was 13.39 Å. It implies that the ZrO_2 is also highly effective as transport barrier and the x_{HL} of ZrO_2 should be the same level. Comparing with the thickness of the deposited ZrO_2 layer (300 Å), it is relatively small. Hence, the hydration transport should be the weak function of $\Delta V_G(t)$ in this work. On the other hand, when the device is immersed in solutions of different ionic strength, ε_n and ε_{HL} could be slightly different because of different hydration species. However, since the x_{HL} of the ZrO_2 film is small, the capacitance of hydrated layer is also small and therefore the overall capacitance of the combination of the hydrated and un-hydrated sensing layer was close to the capacitance of the original layer. As a result, $\left(\frac{\varepsilon_n - \varepsilon_{HL}}{\varepsilon_n \varepsilon_{HL}} \right)$ is a weak function of pH and was regarded identical for both n-channel and p-channel ISFETs.

In this work, the trends of the pH-dependent threshold voltage differences were

mainly attributed to the overall charge of $(Q_D + Q_I + Q_{inv})$. Both Q_D and Q_{inv} are determined by the nature of the device and are nearly a constant amount under fixed operating conditions. Hence, the pH-dependent drift will be primarily governed by the amount of Q_I in this work. The electrical biasing voltage is a direct effect, which drives in or pulls out the surface and beneath charges of sensing layer, with the result that the effective electrolyte-insulator surface charges density alters and therefore the threshold voltage changes. Accordingly, the pH-dependent drift can be described as follows:

$$\Delta V_{G,pH}(t) = -Q_I \left(\frac{\varepsilon_n - \varepsilon_{HL}}{\varepsilon_n \varepsilon_{HL}} \right) x_{HL}(\infty) \left\{ 1 - \exp \left[- \left(\frac{t}{\tau} \right)^\beta \right] \right\} \quad (4-4)$$

The dependency of the hydrogen ion concentration was observed. The electrolyte/solid interface charges induced by the higher concentration of the majority species (H^+ for positive biasing and OH^- for negative biasing) were easily influenced by biasing forces and caused the larger potential differences.

4.3.3. Drift rate and pH sensitivity of combined n-channel and p-channel ZrO₂ gate ISFETs

Figure 4-7 shows the schematic diagram of the proposed system and measurement method. The n-channel and p-channel ISFETs can be easily co-fabricated on the same wafer by the standard CMOS processes. While the applied biasing voltage was positive, the n-channel ISFET operated in the linear mode as sensing component and the p-channel ISFET was in cut-off mode. The sensing performances were mainly determined by n-channel ZrO₂ gate ISFET and the altered threshold voltages should be read out. Similarly, the altered threshold voltages for p-channel ISFETs also should be read out while applying negative biasing voltage. Post signal processing would take the average for both outputs.

Figure 4-8 shows the results of the drift and the pH sensitivity of ZrO₂ gate ISFET

measured by the proposed method. The drift from pH 3 to pH 7 was greatly suppressed from 20mV to nearly zero, and drift from pH 7 to pH 11 was also significantly suppressed to less than ± 5 mV. According to Equation (4-4), the pH-dependent drift could be the same but opposite sign for n-channel and p-channel ISFETs; therefore, by measuring both n-channel and p-channel ISFETs sequentially and taking their average values, the elimination of the pH-dependent drift is obtained as Equation (4-5).

$$\Delta V_{G,pH}(t) = -Q_I \left(\frac{\varepsilon_n - \varepsilon_{HL}}{\varepsilon_n \varepsilon_{HL}} \right) x_{HL}(\infty) \left\{ 1 - \exp \left[- \left(\frac{t}{\tau} \right)^\beta \right] \right\} \approx 0 \quad (4-5)$$

Figure 4-9 shows the variations of the drift measured at different pH values from the second hour to seventh hour for n-channel, p-channel ISFETs and the proposed compensation method. The box charts show the range, standard deviation and mean values of drift measured at pH 3–pH 11. The mean values represent the overall drift and the ranges represent the pH-dependent drift for devices. As observed, the mean values measured at different times for p-channel ISFETs have less potential difference than those of n-channel ISFETs as shown in Figure 4-9 (a) and (b). It seems that p-channel ISFETs have better drift performance. However, their ranges become larger over time while the device is immersed in electrolyte. It revealed that no matter what time the measurements were executed, the exact pH value can not be determined due to the wide range of the potential differences which are pH-dependent. On the contrary, as shown in Figure 4-9 (c), the measurement results performed with the proposed compensation method suppressed the ranges significantly. It represents that the pH value for test solutions with proposed method can be determined at any time, and only simple compensation skills are needed. As a result, the pH-dependent drift is significantly improved and the measurement accuracy is increased.

4.4 Summary

A proposed scheme and compensation method to improve the pH-dependent drift for ZrO_2 pHISFETs was successfully demonstrated. By the sequential measurement and the post processing of the signals for both n-channel and p-channel ISFETs, the results show that the 75–100% pH-dependent drifts are significantly improved and the nearly constant drift rate *versus* pH value is obtained. Meanwhile, the pH measurement sensitivities are maintained and a practical integrated scheme adopting this method is also illustrated. With the integrated scheme, the calibration accuracy will be greatly improved and no complicated compensation circuit design is required.



References

- [4.1] Bergveld, P. Development of an ion-sensitive solid-state device for neuro-physiological measurements. *IEEE Trans. Biomed Eng. BME* **1970**, 17, 70-71.
- [4.2] Bousse, L.; Bergveld, P. The role of buried OH sites in the response mechanism of inorganic-gate pH-sensitive ISFETs. *Sens. Actuat.* **1984**, 6, 65-78.
- [4.3] Jamasb, S.; Collins, S. D.; Smith, R.L. A physical model for threshold voltage instability in Si₃N₄-gate H⁺-sensitive FET's (pH-ISFET's). *IEEE Trans. Electron Devices* **1998**, 45, 1239-1245.
- [4.4] Abe, H.; Esashi, M.; Matsuo, T. ISFET's using inorganic gate thin films. *IEEE Trans. Electron Devices* **1979**, 26, 1939-1944.
- [4.5] Topkar, A.; Lal, R. Effect of electrolyte exposure on silicon dioxide in electrolyte-oxide-semiconductor structures. *Thin Solid Films* **1993**, 232, 265-270.
- [4.6] Buck, R. P. Kinetics and drift of gate voltages for electrolyte-bathed chemically sensitive semiconductor devices. *IEEE Trans. Electron Devices* **1982**, 29, 108-115.
- [4.7] Dun, Y.; Wei, Y. D.; Wang, G. H. Time-dependent response characteristics of pH-sensitive ISFET. *Sens. Actuat. B* **1991**, 3, 279-285.
- [4.8] Esashi, M.; Matsuo, T. Integrated micro multi ion sensor using field effect of semiconductor. *IEEE Trans. Biomed Eng. BME* **1978**, 25, 84-92.
- [4.9] Tsai, C. N.; Chou, J. C.; Sun, T. P.; Hsiung, S. K. Study on the time-dependent slow response of the tin oxide pH electrode. *IEEE sensors journal* **2006**, 6, 1243-1249.
- [4.10] Chou, J. C.; Wang, Y. F. Preparation and study on the drift and hysteresis properties of the tin oxide gate ISFET by the sol-gel method. *Sens. Actuat. B* **2002**, 86, 58-62.

- [4.11] Chou, J. C.; Hsiao, C N. The hysteresis and drift effect of hydrogenated amorphous silicon for ISFET. *Sens. Actuat. B* **2000**, 66, 181-183.
- [4.12] Chiang, J. L.; Jan, S. S.; Chou, J. C.; Chen, Y. C. Study on the temperature effect, hysteresis and drift of pH-ISFET devices based on amorphous tungsten oxide. *Sens. Actuat. B* **2001**, 76, 624-628.
- [4.13] Chiang, J. L.; Chou, J. C., Chen, Y.C.; Liao, G. S.; Cheng, C. C. Drift and hysteresis effects on AlN/SiO₂ gate pH ion-sensitive field-effect transistor. *Jpn. J. Appl. Phys.* **2003**, 42, 4973–4977.
- [4.14] Bousse, L.; Van Den Vlekkert, H.H.; De Rooij, N. F. Hysteresis in Al₂O₃-gate ISFETs. *Sens. Actuat. B* **1990**, 2, 103-110.
- [4.15] Hendrikse, J.; Olthuis, W.; Bergveld, P. A drift free nernstian iridium oxide pH sensor. *Proceedings Transducers* **1997**, 2, 1367-1370.
- [4.16] Hein, P.; Egger, P. Drift behaviour of ISFETs with Si₃N₄-SiO₂ gate insulator. *Sens. Actuat. B* **1993**, 13, 655-656.
- [4.17] Bousse, L.; De Rooji, N. F.; Bergveld, P. Operation of chemically sensitive field-effect sensors as a function of the insulator-electrolyte interfac. *IEEE Trans. Electron Devices* **1983**, 30, 1263-1270
- [4.18] Chang, K. M.; Chao, K. Y.; Chou, T. W.; Chang, C. T. Characteristics of zirconium oxide gate ion-sensitive field-effect transistors. *Jpn. J. Appl. Phys.* **2007**, 46, 4333-4337

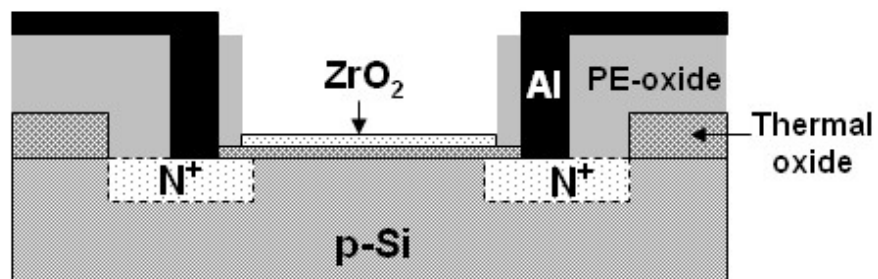


Figure 4-1 Schematic diagram of ZrO₂ gate ISFET, which was fabricated by the Metal Oxide Semiconductor Field Effect Transistor (MOSFET) technique.

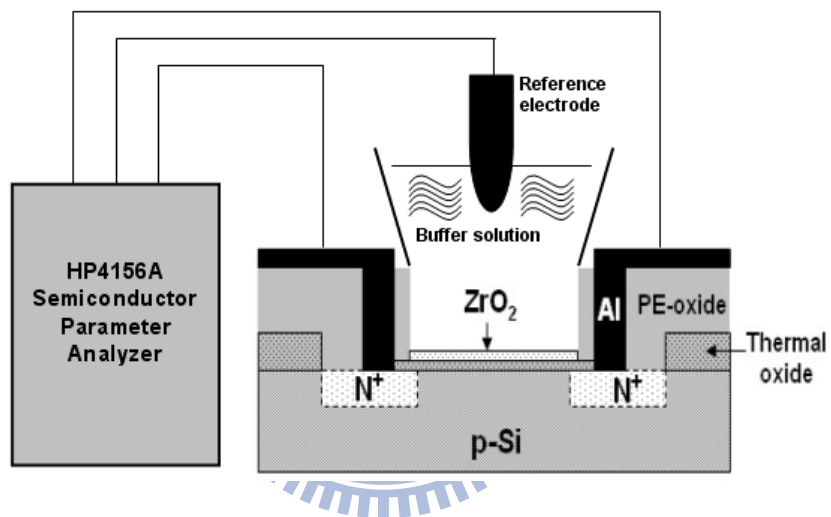


Figure 4-2 The measurement setup and a HP4156A semiconductor parameter analyzer, which was used for measuring the $I_{DS}-V_{GS}$ characteristics for the ZrO₂ gate ISFETs.

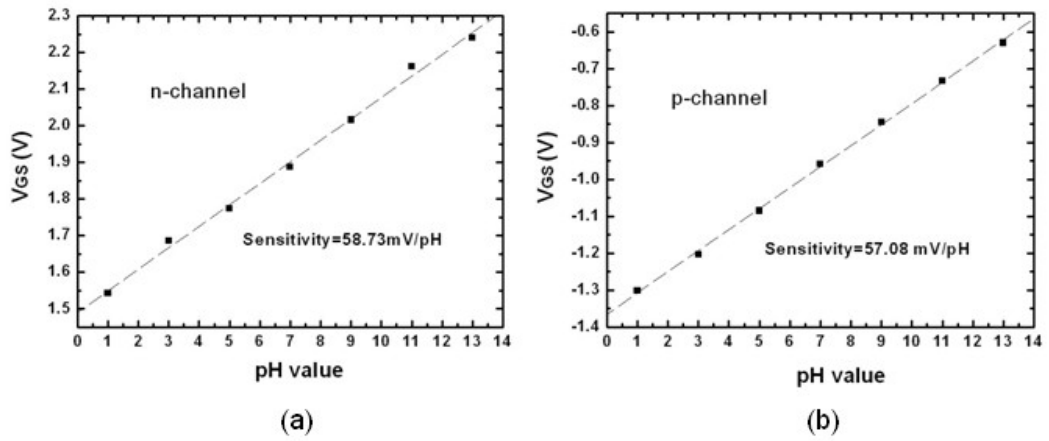


Figure 4-3 The sensitivity of (a) n-channel and (b) p-channel ZrO₂ gate ISFETs.

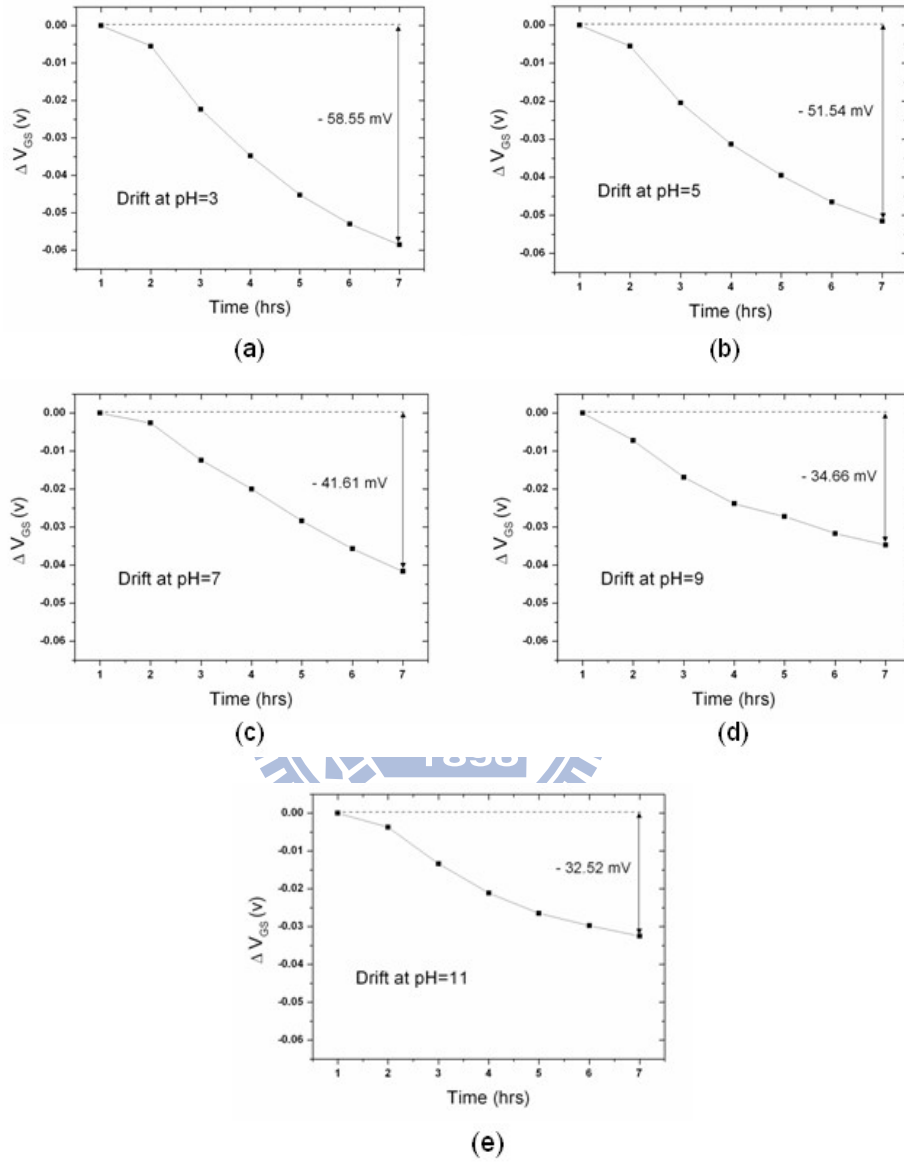


Figure 4-4 The drift of the n-channel ISFET over the first seven hours at (a) pH3 (b) pH5 (c) pH7 (d) pH9 (e) pH11. The drift over the first seven hours was (a) -58.55mV (b) -51.54mV (c) -41.61mV (d) -34.64mV and (e) -32.52mV, respectively.

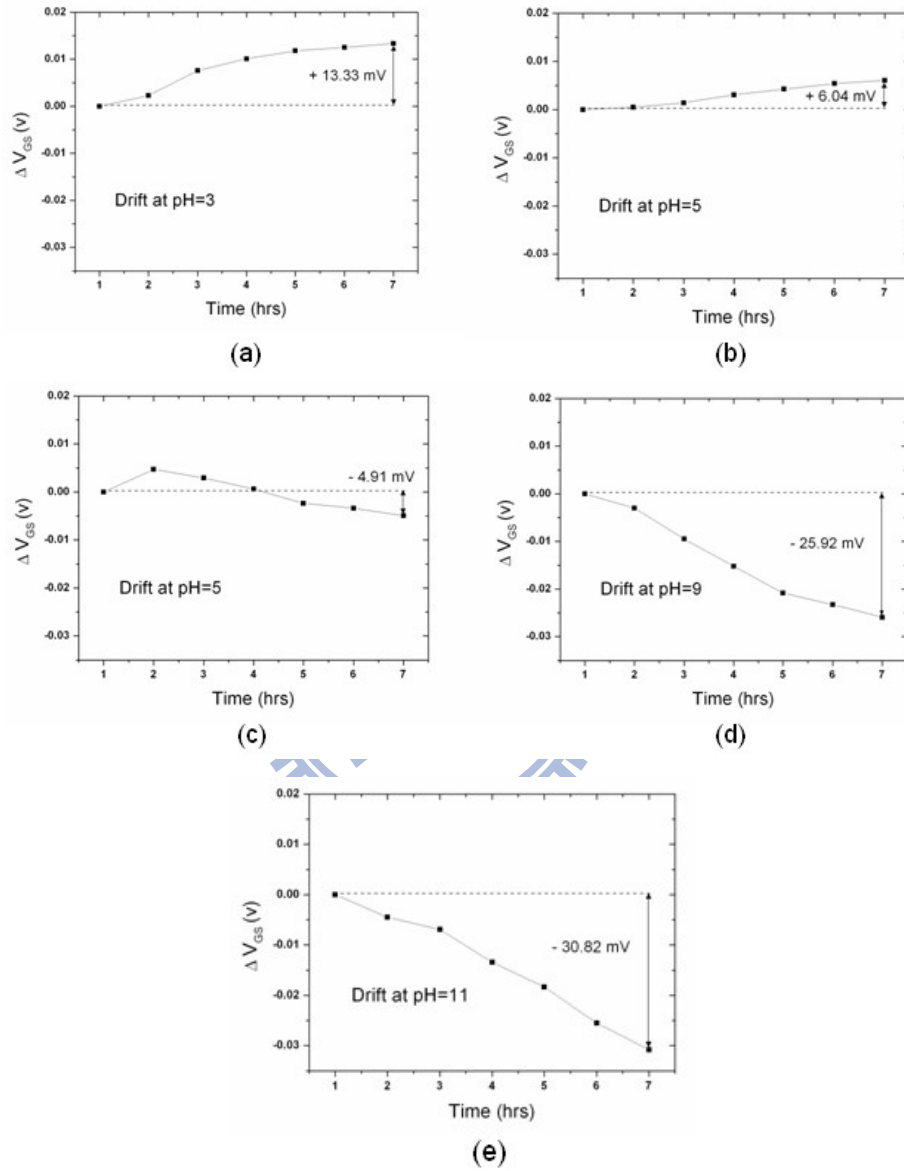


Figure 4-5 The drift of the p-channel ISFET over the first seven hours at (a) pH3 (b) pH5 (c) pH7 (d) pH9 (e) pH11. The drift over the first seven hours were (a) 13.33mV (b) 6.04mV (c) -4.91mV (d) -25.92mV and (e) -30.82mV, respectively.

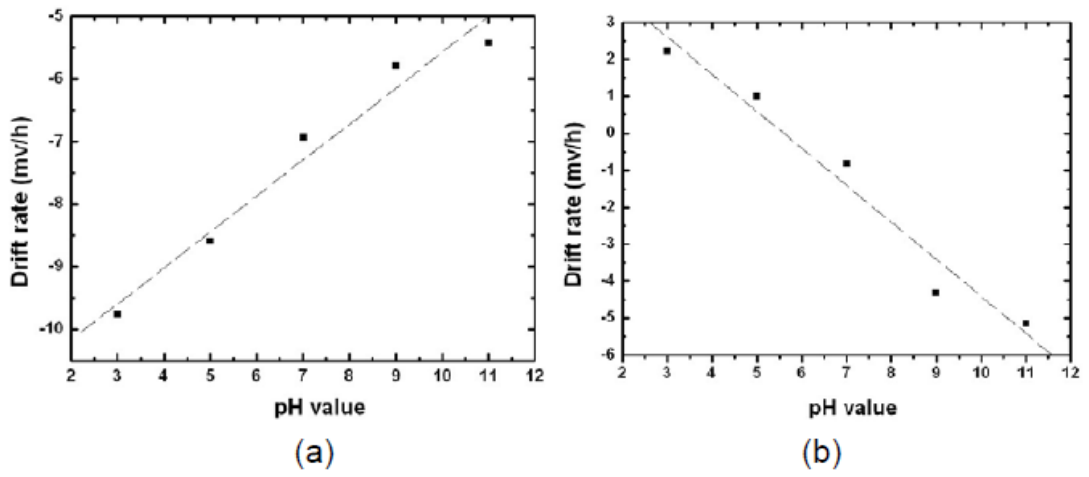


Figure 4-6 The drift rate of (a) n-channel ISFET and (b) p-channel ISFET for the first seven hours.

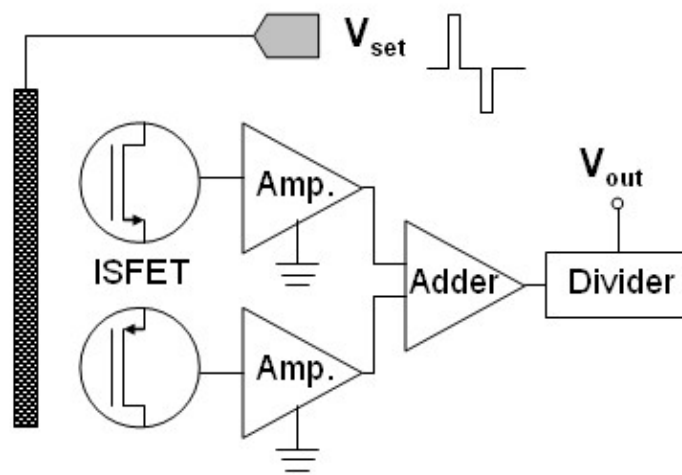


Figure 4-7 The schematic diagram of the proposed system and measurement method.

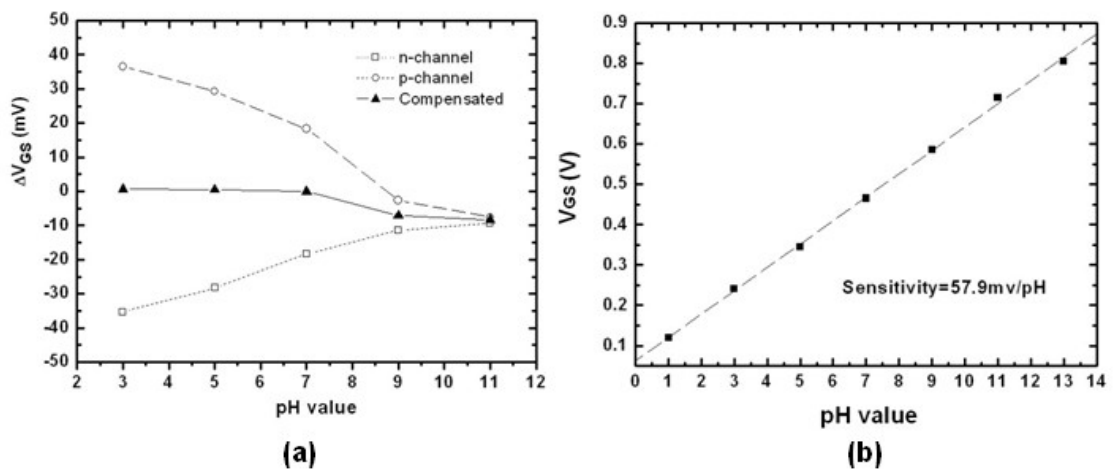


Figure 4-8 (a) The pH-dependent drift of n-channel, p-channel and corrective ISFETs measured at the seventh hour. (b) The pH sensitivities with the proposed compensation method.

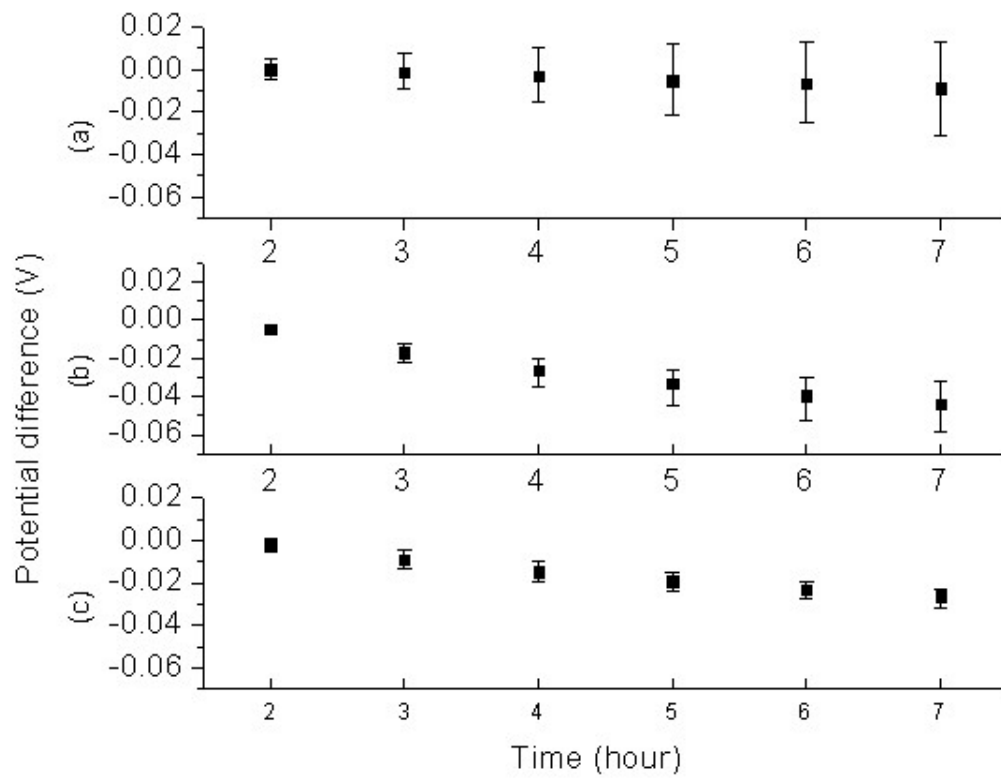


Figure 4-9 The variations of the drift measured at different pH values from the second hour to seventh hour for n-channel, p-channel ISFETs and the proposed compensation method.

Chapter 5

Development of FET-type reference electrodes for pH-ISFET applications

5.1 Introduction

Because the ion-sensitive field-effect transistors (ISFETs) were introduced by Bergveld [5.1] in 1970, they appear to be one of the potential sensors to be used for biological applications due to the advantages of fast response, high maturity, economical scale of semiconductor process, and feasibility of miniaturization, which is attractive for in situ measurements. However, a micro-ISFET requires a miniaturized on-chip reference system, which is challenging for fabrication processes. There are two categories of on-chip reference systems under development: The first type includes miniaturized Ag/AgCl reference electrodes with encapsulated liquid reference solutions [5.2-5.4]; however, the leakage of the reference solutions limits the device lifetime and affects the measurement accuracy. The other type is reference field effect transistor (REFET), which was first proposed by Matsuo [5.5] and Janata [5.6]. Matsuo first introduced the concept of a REFET, which is an identical ISFET whose sensing layer is modified to be chemically insensitive.

Janata incorporated the REFET into a system that consisted of an ISFET/REFET pair, a quasi-reference electrode (QRE), and differential measurement circuits. QRE is simply a noble metal that replaces a complicated reference electrode; however, the potential in the metal/liquid interface is unstable because the interface is polarized. Therefore, the interfacial potential is thermodynamically undefined, which becomes the common noise of the ISFET/REFET differential system. To eliminate this common noise and maintain

measuring sensitivity, the development of REFETs should match with ISFETs to satisfy the requirements of differential measurements.

Several approaches to fabricate REFETs have been proposed. Matsuo and Nakajima [5.7] used an ion-blocking parylene as a chemically inert membrane. However, quasi-instability problems made parylene-gated REFET not practical in a differential ISFET/REFET measurement setup [5.8]. Another method to produce REFET was through a grafted membrane with a long alkyl chain silane [5.9]; nevertheless, the result shows that the gate surface sites cannot be captured sufficiently to obtain a low pH sensitivity. Van den Berg et al. reported that the total elimination of the pH-sensitive groups by chemical monolayer modification cannot be achieved [5.10]. A poly(vinyl chloride) membrane has also been used to form an ioninsensitive layer [5.11-5.17], and normally their operating range is in between pH 2 and 9. Through kinds of modification, such as silylating pretreatment [5.13], modifying a membrane by adding lipophilic cations [5.14], and using a buffered poly(2-hydroxyethyl methacrylate) [5.15] or negative photoresist (PR) [5.16] layers, polymer-based low sensitivity ion-unblocking REFETs could be produced.

Nafion is a perfluorosulfonated material and is resistant to chemical attack. It has been widely used for ion exchange or immobilization applications. Nafion was used as an outer layer to immobilize the chloride ion or nanoparticles while developing electrodes of pH sensors [5.18]. It was also used for pH measurement with a decrease in oxidation–reduction potential error [5.19]. Anh et al. utilized the Nafion membrane to reduce ion interferences from the electrolyte [5.20]. Nafion is also popular at biosensor fields [5.21, 5.22], where enzymes were immobilized with Nafion. In this work, Nafion was introduced to combine with ioninsensitive polymers for REFET system fabrication. The sensitivity, electrical properties, and drift behavior were investigated.

5.2 Experiment

The Nafion solution (5 wt %) was obtained from DuPont, and pH buffer solutions were purchased from RDH (Frankfurt, Germany). Hexamethyldissilazene (HMDS) and PR (FH6400) were obtained from the Nano Facility Center, National Chiao Tung University. The preparation of the NaCl solution was for the Na⁺ ion measurement. The NaCl salt was electronic grade, and solutions were prepared in deionized water with different mole concentrations, 10⁻³, 10⁻², 10⁻¹, and 1 M.

The fabrication of ZrO₂-gated ISFETs was reported [5.23]. The ZrO₂-gated ISFET fabricated by the metal-oxide-semiconductor field-effect transistor (MOSFET) technique was described in last chapters. To test the performance of REFETs, a QRE was also fabricated with Ti/Pt deposition by sputtering with a thickness of 150/350 Å.

Ion-insensitive polymer materials, PR (FH6400), and conductive polymer, poly(3-hexylthiophene) (P₃HT), were incorporated to modify the ZrO₂ film. Two types of membranes were prepared and tested: One type was a double-layer structure, as shown in Figure 5-1 (a); the Nafion and polymer-based materials, PR (FH6400) or P₃HT, were deposited on the top of the original sensing layer (ZrO₂) step by step. The other type was a single layer, as shown in Figure 5-1 (b), with polymers entrapped in the Nafion solution and then casting on the top of the ZrO₂ film. To improve the adhesion of PR and P₃HT with ZrO₂, thin HMDS was pretreated on the ZrO₂ surface in advance. All of the above membranes were heated at 70°C for 1 min and then dried in air for over 12 hour. The epoxy resin film, which is an excellent electrical insulator, was deposited by casting on the top of

the ZrO₂ layer to form the ion-blocking membrane for the electrical property comparison test.

The measurement setup for the REFET system evaluation is as described in last chapters. For the drift performance test, the same device was soaked in the buffer solution for the first and second tests, which lasted for 4 hour, respectively. The device was dried in air in between the two tests. To prevent from light influence, the measurements were entirely executed in a dark box.

5.3 Results and discussions

Figures 5-2 (a) and (b) show the pH and pNa sensitivities of the sole ZrO₂ membrane and with Nafion coating, respectively. The pH and pNa sensitivities of the ZrO₂ membrane with and without Nafion coating are the same. According to the study of Gorchkov [5.24], the pH response of an ISFET would be influenced by the natures of the polymeric membranes, as the consequence of the “equivalent membrane charge.” Therefore, the slightly higher sensitivity of the ZrO₂ membrane with the Nafion coating could be explained as extra cations stored in the Nafion membrane that leads to a surface potential increase. However, the effect is limited. Meanwhile, Nafion is a perfluorinated polymer that can be divided into three parts: a hydrophobic fluorocarbon backbone C–F, an interfacial region of relatively large fractional void volume, and clustered regions where the majority of the ionic exchange sites, counter ions, and absorbed water exist [5.25, 5.26]. Accordingly, the Nafion membrane was a low impedance film, which unblocks the hydrogen and sodium ions; those ions from the electrolyte can pass through the Nafion membrane with a low resist and an established potential on the ZrO₂ surface. The pNa

sensitivity was much lower than the pH sensitivity. The result reveals that it was mainly dominated by the selectivity property of the ZrO₂ film, though the fact that the mobility of H⁺ was about 5 times that of Na⁺ in the Nafion membrane [5.27]. The selectivity coefficient can be determined by the methods based on the Nicolsky–Eisenman equation [5.28]. Meanwhile, the linearity of the pNa response was not as good as the pH response. The difference might be that the Nafion membrane has a slightly higher affinity for Na⁺ than for H⁺ [5.27], which affects the interface potential between the Nafion membrane and the ZrO₂ film. As shown in Figure 5-2 (c), the I_{DS}-V_{GS} curves were similar for both membranes except the threshold voltage shift; it revealed that ZrO₂ films with or without Nafion coating have identical electrical characteristics. The REFETs produced by additional membrane coating on the top of the ISFETs should maintain the original electrical properties, such as transconductance, for differential measurements.

Table 5-1 and Figure 5-3 show the measurement results of pH and pNa sensitivities for the tested conditions. Sensitivities to the hydrogen ions for all tested polymer-based REFETs were below 10 mV/pH except P₃HT without HMDS pretreatment. However, pH sensitivities of all the REFETs were reduced. The reasons for the dramatic pH sensitivity decrease can be explained by employing a site-binding model [5.29, 5.30]. The pH sensitivity of an ISFET is expressed in Equations 4-1 and 4-2. According to the equations, large values of C_{dif} / β_{int} would result in a lower pH sensitivity. This means that surfaces with small buffer capacity (small value of surface reactive sites and of surface charges) show low pH sensitivity. For the double-layer polymer/Nafion as shown in Figure 5-1 (a), the sensing layers were PR and P₃HT, whose surface site densities are smaller than ZrO₂; therefore, the pH sensitivities were low. For the single-layer PR/Nafion composite, as shown in Figure 5-1 (b), it was long chain hydrocarbon molecules which have the characteristic of a small buffer capacity and result in a dramatic decrease in the pH

sensitivities. For the single-layer P₃HT/Nafion composite, because P₃HT is the conductive polymer that provides extra paths for electrons to pass through the membrane, the pH sensitivity was higher than that of the PR/Nafion composite.

HMDS is an adhesion promoter for hydrophobic polymers that attempt to attach on hydrophilic inorganic films. By comparing the pH sensitivity of the tested composite films 2 and 3, 4 and 5, and 6 and 7, all films with the HMDS layer have less sensitivity variation than those without the HMDS layer. It shows that the additional deposition of HMDS improved the stability of test films. Polymerbased HMDS also reduced the pH sensitivity. Figure 5-6 shows the I_{ds} - V_{gs} curves of the HMDS coated ZrO₂ membrane. The sensitivity was decreased from 57.89 to 37.22 mV/pH, and the coating of HMDS caused more than a 35% reduction in sensitivity. Accordingly, the insensitivity character of REFET was not only dominated by the entrapped hydrophobic polymers but also contributed by HMDS. It was evident by comparing films 2 and 3, 4 and 5, and 6 and 7 that the films with the HMDS layer obtained lower pH sensitivity than those without the HMDS layer.

Among all the test films, the combination of Nafion-PR composite/HMDS has the lowest pH sensitivity, and the similar pNa response as the ZrO₂ film, as shown in Figure 5-5, demonstrated the capability to serve as a REFET. Comparing with Figure 5-2 (b), the linearity became worse for the pH response but became better for pNa. The reasons for both cases are different. For pH, it is because the measured potential range was highly reduced that the measurement error becomes more significant. For pNa, a possible reason is that the property of the Nafion film was altered by the mixed composition, which restricted the transport of Na⁺ and the potential variation and, therefore, became more stable.

Figure 5-6 shows the differential result of the pH and pNa measurements for the ISFET/REFET arrangement; responses with more than 50 mV/pH sensitivity and less than 5 mV/pNa interference can be obtained in the range of pH 1–13. Polymers entrapped in

Nafion play the role of blocking the most paths of ion exchange to achieve a low ion sensitivity requirement for REFET. Nevertheless, the induced impedance change by the alteration of the overall membrane composition should be considered. Figure 5-7 describes the transconductance (g_m) curves of the ISFET, the proposed REFET, and the REFET with epoxy coating membranes. The g_m curve with epoxy-REFET shows different behaviors from the other two. On the other hand, the curves of the proposed REFET and ISFET show similar curvatures in the linear region ($V_{gs}-V_{th}$: 0 – 1.2 V). The g_m curves represent the signal transformation characteristics of the device. An effective differential measurement requires similar g_m curvatures for ISFET and REFET in pair. Otherwise, mismatch issues would occur. Because the epoxy is an ion-blocking membrane that causes a polarizable interface whose potential difference changes as a consequence of the potential difference across the whole system, it would alter the original electrical properties of an ISFET. Consequently, the electrical mismatch of the ISFET/REFET differential pair would result in the common mode noises, which cannot be entirely eliminated. On the contrary, an ion-unblocking REFET as proposed causes a nonpolarizable interface, whose potential difference across it is virtually fixed. Meanwhile, it maintains the electrical properties of the original film and makes the ISFET/REFET differential pair match, which can easily eliminate the common mode noises with simple readout circuits. The g_m of the ZrO_2 membrane was slightly altered due to the addition of PR; however, the electrical characteristic in most linear regions was not altered accordingly, which provided an operating region for the ISFET/REFET pair in wide dynamic pH measurements.

In this experiment, it was found that the measurement could not be conducted without the Nafion protection because P3HT and PR alone would dissolve in the buffer solution within a very short time period. The drift performances of the Nafion-PR composite/HMDS film were 3.5 mV/h and less than 1 mV/h for the first and second 4 h tests, as shown in

Figure 5-8. It demonstrated that the incorporation of the Nafion enhanced the stability of the proposed REFET.

5.4 Summary

In this study, a method of fabricating reference ISFETs by combining Nafion and ion-insensitive polymers was proposed. With a differential arrangement, sensitivities of 52.1 mV/pH and 4.61 mV/pNa based on the ZrO₂ sensing film were obtained in the range of pH 1–13; it demonstrated good performance for ISFET applications. Meanwhile, the drift performances were 3.5 mV/h and less than 1 mV/h for the first and second 4 h tests. With the high pH sensitivity and the low interference of pNa performed by the proposed functional polymer combination, a chemically protective ion-unblocking membrane associated with the ion insensitivity polymers provides a promising way for REFET fabrications. Meanwhile, the transconductance match of the proposed REFET/ISFET pair would simplify the differential readout circuits.

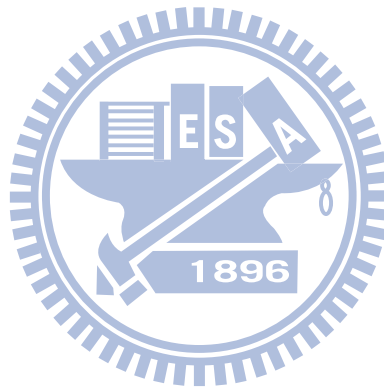
References

- [5.1] Bergveld, P. Development of an ion-sensitive solid-state device for neuro-physiological measurements. *IEEE Trans. Biomed. Eng. BME* **1970**, 17, 70-71.
- [5.2] Shimada, K.; Yano, M.; Shibatani, K.; Komoto, Y.; Esashi, M.; Matsuo, T. Application of catheter-tip isfet for continuous in-vivo measurement. *Med. Biol. Eng. Comput.* **1980**, 18, 741-745.
- [5.3] Smith, R. L.; Scott, D. C. A solid state miniature reference electrode. *Proceedings of the IEEE/VSF Symposium on Biosensors*, Los Angeles, CA, September **1984**, 15-17, 61-62.
- [5.4] Hiroaki, S.; Taishi, H.; Satoshi, S.; Isao, K. Micromachined liquid-junction Ag/AgCl reference electrode. *Sens. Actuat. B* **1998**, 46, 146-154.
- [5.5] Matsuo, T.; Esashi, M. *153rd Meet. Electrochem. Soc. Ext. Abstr.* **1978**, 78-1, 202-203.
- [5.6] Janata, J.; Huber, R. J. Ion-sensitive field effect transistors. *Ion-Sel. Electrode Rev.* **1979**, 1, 31-79.
- [5.7] Matsuo, T.; Nakajima, H. Characteristics of reference electrodes using a polymer gate ISFET. *Sens. Actuat. B* **1984**, 5, 293-305.
- [5.8] Bergveld, P.; van den Berg, A.; van der Wal, P. D.; Skowronsk, P. M.; Sudhölter, E.J.R.; Reinhoudt, D.N. How electrical and chemical requirements for REFETs may coincide. *Sens. Actuat. B* **1989**, 18, 309-327.
- [5.9] Rocher, V.; Chovelon, J. M.; Jaffrezic-Renault, N.; Cros, Y.; Birot, D. An oxynitride ISFET modified for working in a differential mode for pH detection. *J. Electrochem. Soc.* **1994**, 141, 535-539.

- [5.10] van den Berg, A.; Bergveld, P.; Reinhoudt, D. N. Sudhölter, E. J. R. Sensitivity control of ISFETs by chemical surface modification. *Sens. Actuat. B* **1985**, 8, 129-148.
- [5.11] van den Berg, A. Ion sensors based on ISFET's with synthetic ionophores. PhD Thesis, Univ. of Twente, the Netherlands, 1988.
- [5.12] van den Berg, A.; van der Wal, P. D.; Skowronsk, P. M.; Sudhölter, E. J. R.; Reinhoudt, D. N.; Bergveld, P. Nature of anionic sites in plasticized poly(vinyl chloride) membranes. *Anal. Chem.* **1987**, 59, 2827-2829.
- [5.13] Errachid, A.; Baussells, J.; Jaffrezic-Renault, N. A simple REFET for pH detection in differential mode. *Sens. Actuat. B* **1999**, 60, 43-48.
- [5.14] Chudy, M.; Wróblewski, W.; Brzózka, Z. Towards REFET. *Sens. Actuat. B* **1999**, 57, 47-50.
- [5.15] Dawgul, M.; Pijanowska, D. G.; Krzyskow, A.; Kruk, J.; Torbicz, W. An influence of polyHEMA gate layer on properties of ChemFETs. *Sensors* **2003**, 3, 146-159.
- [5.16] Lee, Y. C.; Sohn, B. K. Development of an FET-type reference electrode for pH detection. *J. Kor. Phys. Soc.* **2002**, 40, 601-604.
- [5.17] Lai, C. S.; Lue, C. E.; Yang, C. M.; Dawgul, M.; Pijanowska, D. G. Optimization of a PVC membrane for reference field effect transistors. *Sensors* **2009**, 9, 2076-2087.
- [5.18] Kinlen, P. J.; Heider, J. E.; Hubbard, D. E. A solid-state pH sensor based on a Nafion-coated iridium oxide indicator electrode and a polymer-based silver chloride reference electrode. *Sens. Actuat. B* **1994**, 22, 13-25.
- [5.19] Luo, X. L.; Xu, J. J.; Zhao, W.; Chen, H. Y. Ascorbic acid sensor based on ion-sensitive field-effect transistor modified with MnO₂ nanoparticles. *Anal. Chi. Acta.* **2004**, 512, 57-61.

- [5.20] Anh, D. T. V.; Olthuis, W.; Bergveld, P. Hydrogen peroxide detection with improved selectivity and sensitivity using constant current potentiometry. *Sens. Actuat. B* **2003**, 91, 1-4.
- [5.21] Soldatkin, A. P.; Volotovskiy, V.; El'skaya, A. V.; Jaffrezic-Renault, N.; Martelet, C. Improvement of urease based biosensor characteristics using additional layers of charged polymers. *Anal. Chi. Acta.* **2000**, 403, 25-29.
- [5.22] Volotovskiy, V.; Young, J. N.; Kim, N. Urease-based biosensor for mercuric ions determination. *Sens. Actuat. B* **1997**, 42, 233-237.
- [5.23] Chang, K. M.; Chao, K. Y.; Chou, T. W.; Chang, C. T. Characteristics of zirconium oxide gate ion-sensitive field-effect transistors. *Jpn. J. Appl. Phys.* **2007**, 46, 4333-4337.
- [5.24] Gorchkov, D. V.; Soldatkin, A. P.; Maupas, H.; Martelet, C.; Jaffrezic-Renault, N. Correlation between the electrical charge properties of polymeric membranes and the characteristics of ion field effect transistors or penicillinase based enzymatic field effect transistors. *Anal. Chi. Acta.* **1996**, 331, 217-223.
- [5.25] John Payne, Nafion[®] - Perfluorosulfonate Ionomer, April, 2005 from <http://www.psrc.usm.edu/mauritz/nafion.html>
- [5.26] Tsao, J. P.; Lin, C. W. Preparations and characterizations of the Nafion/SiO₂ proton exchange composite membrane. *J. Mater. Sci. Eng.* **2002**, 34, 17-26.
- [5.27] Okada, T.; Moller-Holst, S.; Gorseth, O.; Kjelstrup, S. Transport and equilibrium properties of Nafion membranes with H⁺ and Na⁺ ions. *J. Electroanal. Chem.* **1998**, 442, 137-145.

- [5.28] Pechhold, W.; Liska, E.; Grossmann, H. P.; Hagele, P. C. On present theories of the condensed polymer state. *Pure Appl. Chem.* **1976**, 46, 127-134.
- [5.29] Van Hal, R. E. G. A general model to describe the electrostatic potential at electrolyte oxide interface. *Adv. Colloid Interface Sci.* **1996**, 69, 31-62.
- [5.30] Bergveld, P. ISFET, Theory and practice. *IEEE Sensor Conference*, Toronto, Oct. **2003**.



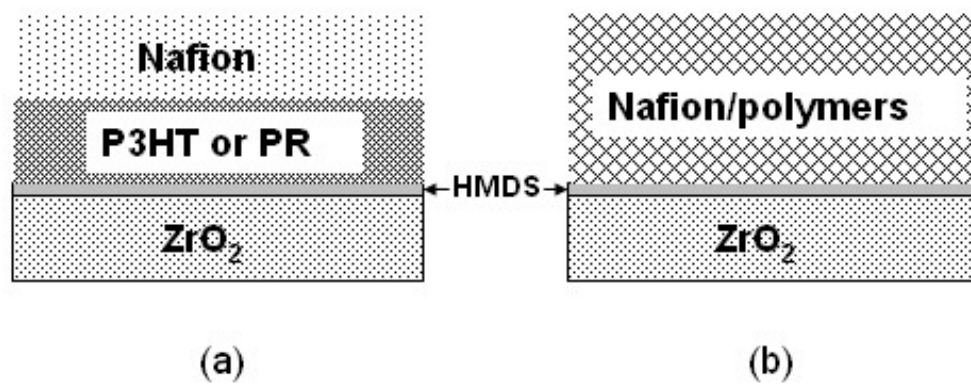
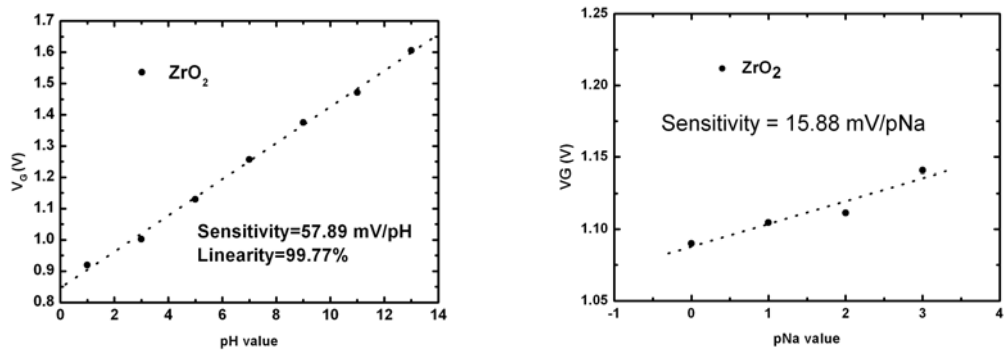
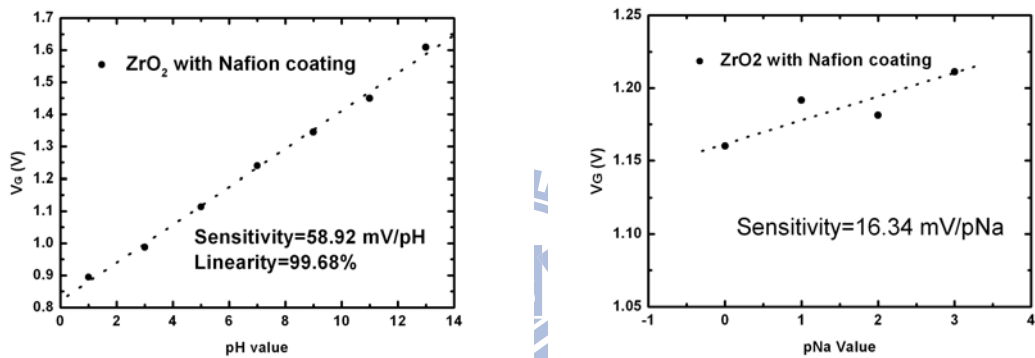


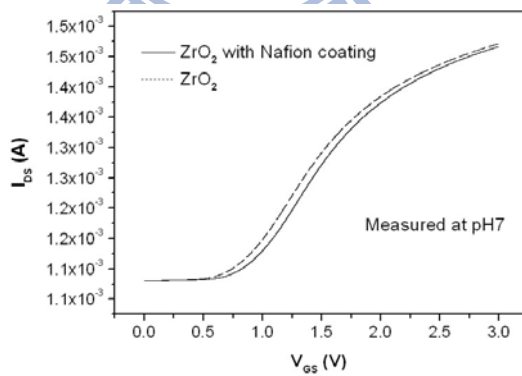
Figure 5-1 Tested membranes prepared with two methods: (a) Encapsulation and (b) entrapment.



(a)



(b)



(c)

Figure 5-2 Hydrogen and sodium sensitivities of (a) ZrO₂ and (b) ZrO₂ with Nafion coating gated ISFETs. The pH and pNa sensitivities are (a) 57.89 and (b) 58.92 mV/pH and (a) 15.88 and (b) 16.34 mV/pNa, respectively. (c) The I_{DS}-V_{GS} curves of ZrO₂ with and without Nafion coating.

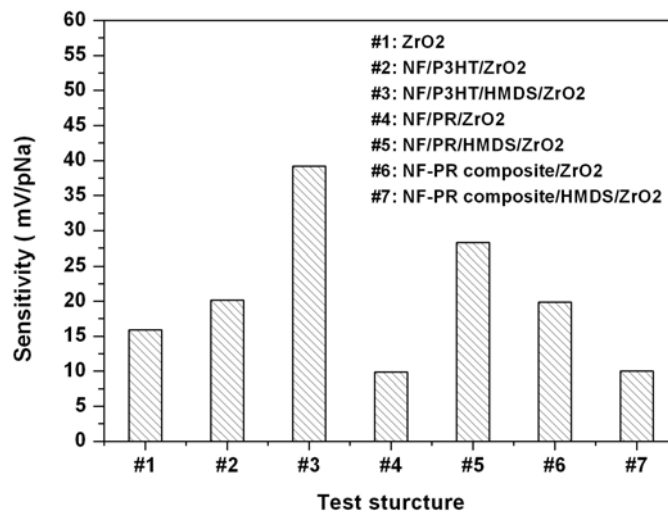
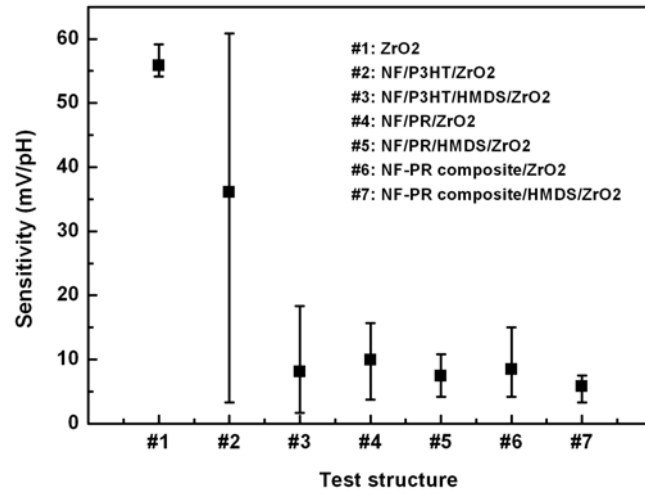


Figure 5-3 Measurement results of pH and pNa sensitivity for tested structures.

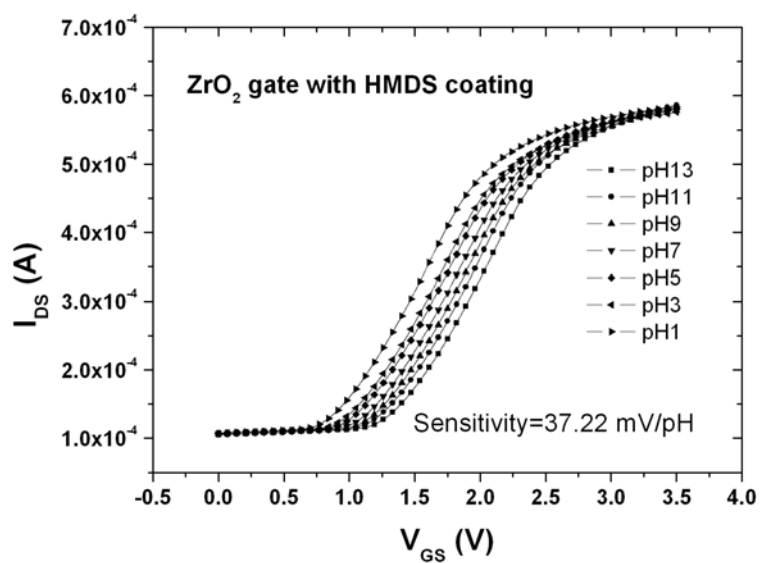


Figure 5-4 I_{DS} - V_{GS} curves of HMDS coated ZrO_2 membrane.

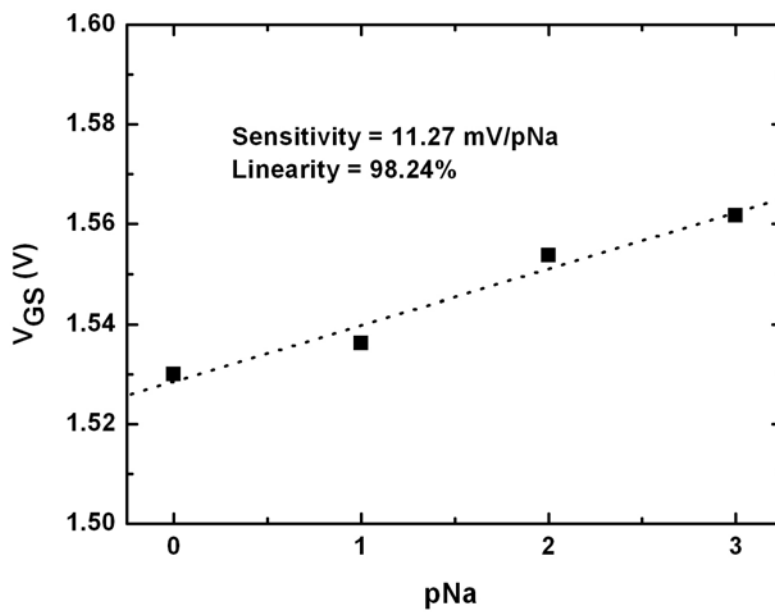
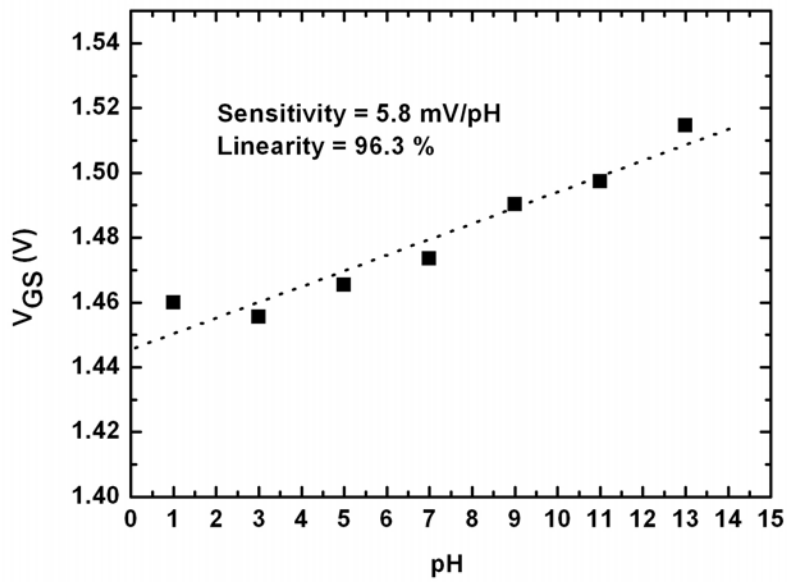
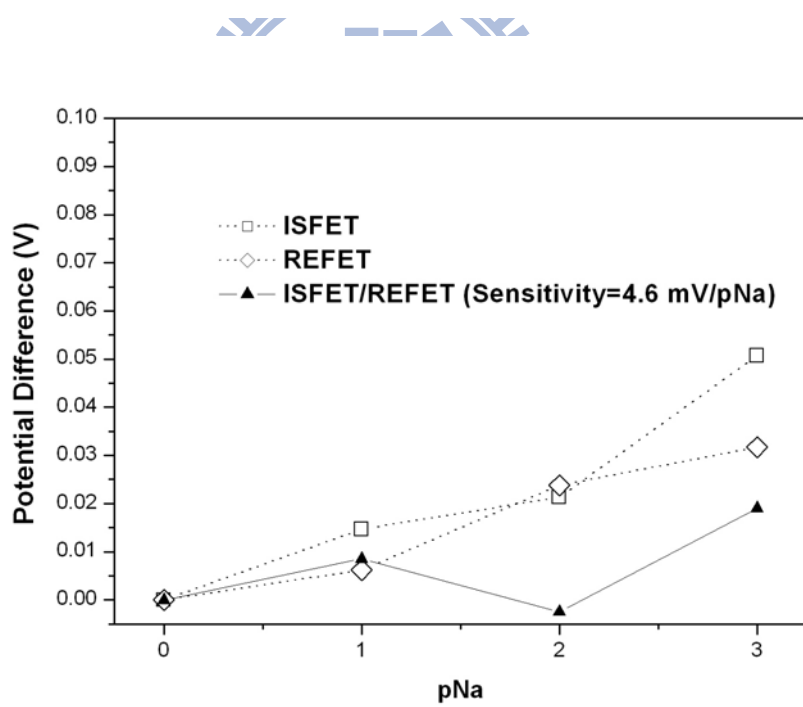
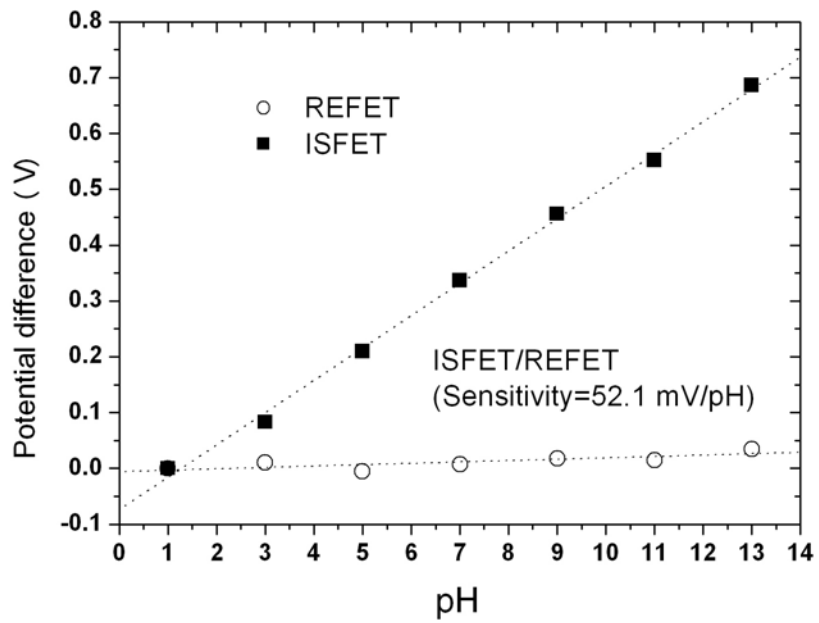


Figure 5-5 The pH and pNa response of Nafion-PR composite/HMDS/ZrO₂ ISFET.



Figurer 5-6 Measurement results of pH and pNa response with ISFET/REFET differential arrangement.

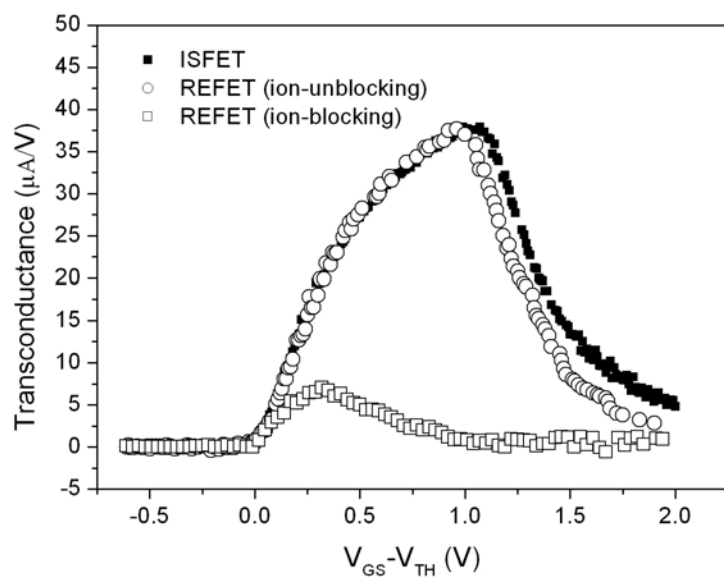


Figure 5-7 Transconductance ($g_m = dI_{DS}/dV_{GS}$) of the ZrO_2 gated ISFET, the proposed REFET (ion-unblocking) and REFET with epoxy coating on ZrO_2 gate (ion-blocking)

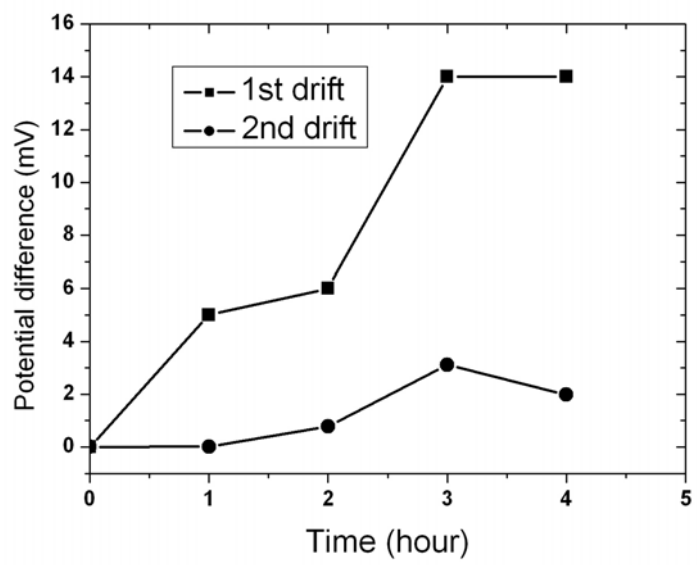
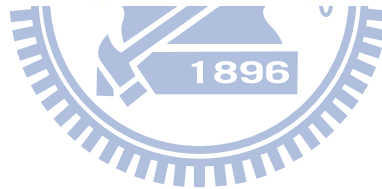


Figure 5-8 Drift performance of the proposed REFET.

Table 5-1 Responses of hydrogen ions and sodium ions for tested structures.

Test structure	H ⁺ sensitivity (mV/pH)	H ⁺ linearity (%)	Na ⁺ sensitivity (mV/pH)	Na ⁺ linearity (%)
1 ZrO ₂	57.89	99.8	15.88	96.2
2 NF/P3HT/ZrO ₂	36.11	99.6	20.17	81.8
3 NF/P3HT/HMDS/ZrO ₂	8.07	96.5	39.21	99.1
4 NF/PR/ZrO ₂	9.92	99.5	9.9	97.9
5 NF/PR/HMDS/ZrO ₂	7.43	94.3	28.27	96.9
6 NF-PR composite/ZrO ₂	8.47	98.5	19.89	97.9
7 NF-PR composite/HMDS/ZrO ₂	5.8	96.3	11.27	98.2
8 epoxy resin/ZrO ₂	4.7	93.9	—	—



Chapter 6

Development of an ion sensitive field effect transistor based urea biosensor with solid state reference systems

6.1 Introduction

Field-effect transistor (FET) based solid state biosensors are a promising tool in biological applications due to the maturity of semiconductor technology. In particular, the feasibility of miniaturization enables advanced applications, such as the surgical operations [6.1]. Enzyme field-effect transistors (EnFETs) are miniaturized biosensors which are typical ion-sensitive FET (ISFET) based biosensors, with an additional immobilized enzyme layer coating on the surface of gate dielectrics of a FET [6.2-6.6]. Those additional layers were fabricated on the supporting materials with entrapped enzyme coatings. The immobilization of the biological component to protect it from the environmental conditions results in decreased enzyme activity [6.7]. The activity of immobilized molecules depends upon surface area, porosity, hydrophilic character of the immobilizing matrix, reaction conditions and the methodology chosen for immobilization. Recently, conducting polymers were regarded as suitable candidates as supporting matrix for biological immobilization applications due to their numerous advantages [6.8].

NafionTM is one of the popular materials selected as supporting matrix for chemical or biological sensors [6.9-6.11]. It is a perfluorosulfonated material, with high conductivity in the range of $10^{-1} \sim 10^{-2}$ S/cm [6.12], which has three parts: a hydrophobic fluorocarbon backbone C-F, an interfacial region of relatively large fractional void volume and the clustered regions where the majority of the ionic exchange sites, counter ions, and absorbed

water exist. The rigid backbone is resistant to chemical attack, which protects the entrapped materials, such as polymers and enzymes, to prevent from demixing. Meanwhile, the large fractional void volume and conducting property avoid severe degradation of the activity of immobilized molecules.

According to the ISFET sensors with single structure [6.13] and ISFET/REFET differential pair structure [6.14], they show that the readout circuits and stable reference systems are essential for miniaturizing purpose. In general, there are two combinations to achieve the purpose: one is the solid-state reference electrode (SRE) with an ISFET (SRE/ISFET) associated with a single ended readout circuit [6.15, 6.16]; the other one is the noble metal electrode, which called quasi-reference electrode (QRE), integrated with an ISFET and a REFET (QRE/ISFET/REFET) associated with two ended differential readout circuits [6.17-6.19].

For the first single-ended combination, the design of the readout circuits is simple if SRE provides a stable potential. Extensive developments for the miniaturized solid state reference electrode were proposed [6.20-6.24]. However, in order to achieve a thermodynamically defined potential difference at the reference electrode/liquid interface, the complications of the structures are enormous and there are many drawbacks, such as the leakage of the reference solutions that limits the device lifetime and measurement accuracy [6.25, 6.26].

For the second two-ended combination, the reference electrodes were substituted with the QRE. The QRE is a noble metal which is deposited with sputtering or evaporation method. Since the simplicity of the fabrication processes of QRE, the miniaturized sensors can therefore be achieved easily. However, the designs of the differential readout circuits are more complicated due to the concern of the common mode noise and the device match of ISFET/REFET. The common mode noise, which were induced from the polarized

thermodynamically undefined metal/liquid interface, are usually eliminated with the differential methods. Figure 6-1 shows the schematic diagram of the typical common-mode differential circuit. The purpose of a differential amplifier is to sense the change in its differential input while rejecting changes in its common-mode input. The desired output is differential, and its variation should be proportional to the variation in the differential input. Variation in the common-mode output is undesired. The common-mode rejection ratio (CMRR) of a differential circuit measures the tendency of the device to reject the common signals for both input leads, and it indicates that the amount of the common-mode signal will appear in the measurement. The CMRR was defined as

$$CMRR = \left| \frac{A_{DM}}{A_{CM-DM}} \right| \quad (6-1)$$

where A_{DM} denotes the circuit gain in the differential-mode, and A_{CM-DM} denotes the common-mode to differential-mode conversion. An important device parameter regarding the CMRR is the transconductance (g_m) which represents the sensitivity of the device. For a high g_m , a small change in V_{GS} results in a large change in I_{DS} at fixed V_{DS} , which provide higher sensitivity for measurement. The transconductance was defined as Equation (6-2):

$$g_m = \left. \frac{\partial I_{DS}}{\partial V_{GS}} \right|_{V_{DS}=\text{const}} \quad (6-2)$$

Assume that the g_{m1} and g_{m2} are the transconductances of M1 and M2, respectively. We have

$$A_{CM-DM} = -\frac{\Delta g_m R_D}{(g_{m1} + g_{m2})R_{SS} + 1} \quad (6-3)$$

where $\Delta g_m = g_{m1} - g_{m2}$.

According to Equations (6-1) to (6-3), the transconductance mismatch of ISFET/REFET pair will significantly degrade the CMRR, which represents the noise coming from reference electrode metal/liquid interface will influence the measurement

accuracy. An alternative method to increase the CMRR is to design high A_{DM} circuits; however, it requires a large number of additional components and increases the complexity of the circuit. Therefore, a transconductance matched ISFET/REFET pair will prevent the cost from degraded CMRR and increase the measurement accuracy.

In this work, three steps of the sensor design was performed: firstly, the fabrication and characterization of the sole SRE, REFET and urease-EnFET. Then the modifications of transconductance match for devices, and the last step was to evaluate the performances of sensors with single-ended and two-ended differential combinations based on both the glass Ag/AgCl reference electrode (GRE) and QRE. The NafionTM was used as common supporting matrix to immobilize functional materials, urease and photoresist, to fabricate the EnFETs, SREs and REFETs. The urea response, response time, storage time and the electrical properties of sensors were also investigated.



6.2 Experiment

6.2.1. Reagents Preparation

5 wt% NafionTM solutions were obtained from DuPont, and pH buffer solutions were purchased from RDH (Frankfurt, Germany). Photoresist (FH6400) was obtained from Nano Facility Center, National Chiao Tung University. The urease (EC 3.5.1.5, 5 U/mg, lyophilized) was purchased from Merck corp. Urea [$\text{CO}(\text{NH}_2)_2$, Merck corp.] and all the other reagents were of analytical grade. The phosphate buffer solution (PBS) was prepared in deionized water. The tested urea solutions are prepared with urea power mix with PBS, and their concentrations are 1.25 mg/dl, 10 mg/dl, 40 mg/dl, 80 mg/dl, 120 mg/dl and 240 mg/dl, respectively.

6.2.2. ISFET fabrication and membranes preparation

The ZrO₂ gated ISFETs were fabricated by the MOSFET technique. A 30-nm-thickness ZrO₂ film was deposited onto the SiO₂ gate ISFET by DC sputtering. The total sputtering pressure was 20 mTorr in a gas mixture of Ar and O₂ for 200 minutes, while the base pressure was 3×10^{-6} Torr, and the RF power was 200 W. The quasi-reference electrode (QRE) was fabricated with Ti/Pd deposition by sputtering with a thickness of 150 Å/350 Å. The detailed process flows and characteristics of sensitivity, linearity and drift of the ZrO₂ ISFET were reported in [6.27]. The ZrO₂ gate ISFET exhibited the high pH sensitivity of 57.5mV/pH. The membranes of solid-state reference electrodes (SREs), and EnFETs were fabricated with the photoresist and urease entrapped in a Nafion™ supporting matrix. Figure 6-2 shows the schematic diagrams of ISFET, EnFET and REFET.

In the case of SRE fabrication, the photoresist was mixed with Nafion™ in a 1:1 ratio, and then drop coated on the top of the QRE and dried in air for 24 hours. A similar process was used to fabricate the REFET by drop coating the mixture on the top of the ISFETs; three photoresist/Nafion™ ratios of 1:1, 3:1 and 5:1 were prepared for the REFETs' test. For the EnFET, the enzymatic layers were prepared by mixing urease solution (10 mg of the urease in 100 µL of 5 mM PBS) with Nafion™ solution (100 µL Nafion™ in 100 µL of 5 mM PBS) in the ratios of 1:1, 5:1 and 20:1, then depositing them on the top of the gate region of the ISFETs by the drop coating method and drying in air for 24 hours. To obtain a consistent membrane thickness, care was taken to control the droplet volume.

6.2.3. Packaging and measurements

Figure 6-3 shows the combinations of EnFET measuring systems. A container is bonded to enclose the gate region of ENFET by using epoxy resin. HP4156A semiconductor parameter analyzer was used to investigate and collect the electrical data. The I_{DS} - V_{GS} curves of EnFETs were obtained with constant drain-source voltage $V_{DS} = 2$ V while the devices were soaked in the buffer solution of 10 mM PBS with pH = 6. Since the products of the urea hydrolysis may alkalize maximally up to pH 9, the set of initial pH value should cover the range of optimal urease activity (pH 7.0~7.5). Meanwhile, according to the report in [6.3], the higher initial pH value of the buffer results in reduction of amplitude of the analytical signal. Accordingly, the initial pH in this experiment was set at pH 6.0. As standard reference electrode, the commercial Ag/AgCl glass reference electrode was connected to the gate voltage supplier to provide the stable bias potential for device operation. In order to prevent from the light influence, the measurements were conducted in a dark box. The devices were stored dry at 4°C in darkness during the measurements.

6.3 Results and discussions

Figure 6-4 shows the I_{DS} - V_{GS} and the transconductance curves of the ZrO_2 gate ISFETs with and without NafionTM coating. The result reveals that their curvatures are identical, which described the electrical property of the NafionTM. The I-V and g_m relationships of the ISFETs operating in linear region can be described as follows:

$$I_{DS} = \frac{1}{2} C_{ov} \mu \left(\frac{W}{L} \right) \left[(V_{GS} - V_{th}) V_{DS} - \frac{1}{2} V_{DS}^2 \right] \quad (6-4)$$

$$g_m = \left. \frac{\partial I_{DS}}{\partial V_{GS}} \right|_{V_{DS}=\text{constant}} = \frac{1}{2} C_{ov} \mu \left(\frac{W}{L} \right) V_{DS} \quad (6-5)$$

where C_{ov} represents the overall capacitance of subsequent layers on sensing area, the μ represents the electron mobility of device and $\left(\frac{W}{L} \right)$ represents the geometric ratio of gate. According to Equations (6-4) and (6-5), since the devices were fabricated with the same size, material and process, the similar curvatures represented that the additional Nafion™ membrane did not alter the overall capacitance of the gate layers.

A way to visualize the electrical properties of a membrane is to make use of the simple equivalent circuit representation as shown in Figure 6-5 [6.28]. The R_{CT} denotes the charge-transfer resistor and C_D denotes the double-layer and membrane capacitor. If the resistor is very high, the capacitor charges up to the value of the potential difference set by the source.

This is the behavior of a polarizable (ion blocking) interface. To polarize an interface means to alter the potential difference across it. On the contrary, if the resistance in parallel with the capacitor is low, then any attempt to change the potential difference across the capacitor is compensated by charge leaking through the low-resistance path. This is the behavior of a nonpolarizable (ion unblocking) interface. With high conductivity and low impact on overall capacitance, the Nafion™ membrane is ion-unblocking and suitable as a supporting material.

Figure 6-6 and Table 6-1 show the responses and performance of the fabricated urease-EnFET measured with standard Ag/AgCl GRE. The concentration of the phosphate buffer solution was 10 mM and the tested urea concentrations were from 1.25 mg/dL to 240 mg/dL. The response performance depends not only on the amount of entrapped urease, but also on the initial pH, ambient buffer capacity and ionic strength of solutions as well as on the surface area, porosity and the physical characteristics of both the enzyme and the

supporting material.

The results showed that the urea sensitivity was proportional to the amount of urease entrapped in the membrane. Less urease entrapped in the membrane will degrade the ability of urea detection. On the other hand, though the sensitivity and detection limits were enhanced with high enzyme loading, the device lifetime was limited due to the enzyme leakage. The entrapment process or membrane confinement of enzyme may be a purely physical caging or involve covalent binding. To enhance the chemical binding capability may increase the enzyme loading and achieve higher sensitivity. Except the consideration of the volumetric surface area available to the enzyme, which determines the maximum binding capacity, another consideration was that the nature of supporting material should have a considerable affect on an enzyme's expressed activity and apparent kinetics. In this experiment, the sensor with the urease/Nafion ratio of 5:1 successfully performed the detection, and the urea responses were from 12.9 mV to 198.1 mV for the urea concentrations from 8 mg/dl to 240 mg/dl. It demonstrated acceptable detection ability, response time and life time.

The urease biosensor based on the pH-ISFET detects pH change around the gate surface as a result of the urease catalyses the hydrolysis of urea is according to the following reaction:



According to [6.29], the mechanisms involved in the response of pH-based enzyme sensors include the reaction kinetics of the biological-recognition processes and the mass transport theory. In the steady state, a balance between the rates of mass transport of the urea from bulk solution to the urease membrane, production or consumption of the hydrogen ions by

the urease membrane and their transportation will be achieved, leading to a stable local pH change in the region of the membrane. We can then expect a change in the surface concentration of H^+ as a consequence of the change in the potential of the ISFET, and the concentration of urea therefore is indirectly measured. On the other hand, biosensors with indirect measurement are also impacted by the ambient buffer capacity and ionic strength, which are governed by many factors such as the concentration, dissociation constant and the ionic charge of electrolyte. For example, the increase of the phosphate buffer solution concentration will result in reduction of the EnFET sensitivity and change the linear part of the calibration curve as reported in [6.3, 6.30].

Figure 6-7 (a) shows that the response times of all tests were within 25 seconds. The response time of EnFETs depends on the diffusion of hydrogen ions, the buffer capacity of system and the membrane properties and thickness. In this experiment, the membranes were fabricated with drop coating method, the thickness of membranes were estimated to be $15\mu\text{m}$ but not standardized. The membranes were thick; however, the response times were short for all tests, which represented the porosity and ion unblocking property of the membranes with NafionTM as supporting matrix. Comparing with typical response time of 0.5~3 min. [6.30], this result demonstrated the quick response characteristics of the proposed EnFET. The storage and repeatability performances of the proposed EnFETs were shown in Figure 6-7 (b) and Table 2.

The results show that the urease entrapped membranes have good repeatability and long storage time. Figure 6-8 shows the electrical curves measured with GRE. The maximal g_m of the ISFET and EnFET were 38 and 27.9mA/V, respectively. For REFETs, they were 27.7, 19.2 and 10.7mA/V for the different photoresist/NafionTM ratios of 1:1, 3:1 and 5:1. Among the devices, the curves of EnFET and REFET with the photoresist/NafionTM ratio of 1:1 were matched. In principle, the transconductance is

mainly governed by the electron mobility, gate geometry and effective dielectric capacitance of the sensing layer. In this experiment, all devices were constructed on identical ISFETs, therefore their electron mobility and gate geometry were identical. Accordingly, the different g_m curves changed due to the capacitances change caused by the additional membrane. Since both types of membrane were composed of similar concept of combining conductive and insulated materials to achieve nonpolarizable interfaces, hence it is possible to modify the overall conductance and capacitance to make FETs electrically match by adjusting their compositions and thickness, etc. The result is particularly important for biosensors in differential readout design. Most biosensors immobilized biomaterials with chemical, physical or mixed approaches, and the sensing membranes fabricated in each way certainly alter the original electrical properties. The fabrication of REFETs was the similar case. Transconductance mismatched input pairs would induce many issues, such as the CMRR degradation, DC offsets restrict linear dynamic ranges, low voltage gain and nonlinear problems, etc. To solve those issues, extra components and complicated designs of circuits and device geometries are essential, therefore increases the difficulties of readout electronics. Even though, not all the problems induced by mismatch can be overcome. In many novel differential readout circuit designs proposed, the identical electrical properties of bio-FETs/REFETs pair were assumed [6.18, 6.31]; in other words, the previous device design of electrical match can reduce the loadings for circuit designs. Consequently, the g_m match for devices design must be considered. The curves in Figures 8 shows the results of designed REFETs with photoresist/NafionTM ratio of 1:1, 3:1 and 5:1, respectively. It shows that curve of REFETs with photoresist/NafionTM ratio of 1:1 can match with the curve of EnFET within the range of $V_{GS}-V_{TH} = 0\sim 1.3V$, which provides the wide ranges and larger g_m choices for readout circuits design consideration. In contrast, the other EnFET/REFET differential pairs only

matched at $V_{GS}-V_{TH} = 0\sim 0.2V$, where is so-called weak inversion region. As a result, the device sensitivity was relatively low and the dynamic operating range was restricted.

Figure 6-9 shows the urea responses of GRE/EnFET, SRE/EnFET, GRE/EnFET/REFET, QRE/EnFET/REFET and SRE/REFET combinations in this experiment. The zero urea response of SRE/REFET demonstrated the capability of being reference system for biosensor. Since the REFETs covered with nonpolarized membrane still possesses limited urea sensitivity of around 0.01 mV/mg/dl, the GRE/EnFET/REFET and GRE/EnFET have similar performance except that the urea sensitivity was slightly lower for the two-ended pair. However, it demonstrated that the fabricated REFETs were practical to be a reference system. On the other hand, the SRE/EnFET has the simplest on-chip structure with simple one-ended readout circuits. In this work, an alternative method was proposed to fabricate reference electrodes with coating ion-insensitive but ion-unblocking layers on the top of contact metal. This method suppressed the solid/liquid potential differences and provided relatively stable reference potential. Nevertheless, the result reveals one main disadvantage of that the sensitivity was severely degraded. Comparing the combinations, the on-chip QRE/EnFET/REFET transconductance-match pair with two-ended differential readout circuits demonstrated the comparable performance with GRE/EnFET and GRE/EnFET/REFET. Meanwhile, their storage time was more than 1 week. The results indicate the miniaturization of practical ISFET based biosensors can be realized.

6.4 Summary

The designed transconductance-match biosensors with solid state reference systems

for the differential readout electronics were investigated. Utilizing Nafion™ as supporting matrix provided the advantage of low initial charge-transfer resistance. The entrapment of the ion-blocking materials, such as urease and photoresist, can therefore be performed without altering the unpolarizable property of sensing membrane for EnFETs and REFETs. Meanwhile, through the modification of the membranes of REFETs and EnFETs, the optimal transconductance match for biosensor and REFET pairs can be determined. Such pairs can be easily integrated on-chip due to the simple readout electronics required, and are capable of performing comparable biological response with conventional large sized discrete sensors.



References

- [6.1] Covington, A. K.; Valdes-Perezgasga, F.; Weeks, P. A.; Brown, A. H. pH ISFETs for intramyocardial pH monitoring in man. *Analisis* **1993**, 21, 43-46.
- [6.2] Osaka, T.; Komaba, S.; Seyama, M.; Tanabe, K. High-sensitivity urea sensor based on the composite film of electroinactive polypyrrole with polyion complex. *Sens. Actuat. B* **1996**, 35-36, 463-469.
- [6.3] Pijanowska, D. G.; Torbicz, W. pH-ISFET based urea biosensor. *Sens. Actuat. B* **1997**, 44, 370-376.
- [6.4] Puig-Lleixa, C.; Jimenez, C.; Alonso, J.; Bartroli, J. Polyurethane-acrylate photocurable polymeric membrane for ion-sensitive field-effect transistor based urea biosensors. *Anal. Chimica Acta*. **1999**, 389, 179-188.
- [6.5] Soldatkin, A.P.; Montoriol, J.; Sant, W.; Martelet, C.; Jaffrezic-Renault, N. A novel urea sensitive biosensor with extended dynamic range based on recombinant urease and ISFETs. *Biosens. Bioelectron.* **2003**, 19, 131-135.
- [6.6] Jaffrezic-Renault, N.; Wan, K.; Senillou, A.; Chovelon, J. M.; Martelet, C. Development of new polymeric membranes for ENFETs for biomedical and environmental applications. *Analisis* **1999**, 27, 578-586.
- [6.7] Evtugyn, G. A.; Budnikov, H. C.; Nikolskava, E. B. Sensitivity and selectivity of electrochemical enzyme sensors for inhibitor determination. *Talanta* **1998**, 46, 465-484.
- [6.8] Gerard, M.; Chaubey, A.; Malhotra, B. D. Application of conducting polymers to biosensors. *Biosens. Bioelectron.* **2002**, 17, 345-359.
- [6.9] Kinlen, P. J.; Heider, J. E.; Hubbard, D. E. A solid-state pH sensor based on a Nafion-coated iridium oxide indicator electrode and a polymer-based silver

- chloride reference electrode. *Sens. Actuat. B* **1994**, 22, 13-25
- [6.10] Volotovskiy, V.; Nam, Y. J.; Kim, N. Urease-based biosensor for mercuric ions determination. *Sens. Actuat. B* **1997**, 42, 233-237
- [6.11] Chang, K. M.; Chang, C. T.; Chao, K. Y.; Chen, J. L. Development of FET-type reference electrodes for pH-ISFET applications. *J. Electrochem. Soc.* **2010**, 157, J143-J148.
- [6.12] Sone, Y.; Ekdunge, P.; Simonsson, D. Proton conductivity of Nafion 117 as measured by a four-electrode AC impedance method. *J. Electrochem. Soc.* **1996**, 143, 1254-1259.
- [6.13] Bergveld, P. Development of an ion-sensitive solid-state device for neuro-physiological measurements. *IEEE Trans. Biomed. BME* **1970**, 17, 70-71.
- [6.14] Janata, J.; Huber, R. J. Ion-sensitive field effect transistors. *Ion-Sel. Electrode Rev.* **1979**, 1, 31-79.
- [6.15] Ravezzi, L.; Conci, P. ISFET sensor coupled with CMOS read-out circuit microsystem. *Electron. Lett.* **1998**, 34, 2234-2235.
- [6.16] Khanna, V. K.; Kumar, A.; Jain, Y. K.; Ahmad, S. Design and development of a novel high-transconductance pH-ISFET (ion-sensitive field-effect transistor)-based glucose biosensor. *Int. J. Electron.* **2006**, 93, 81-96.
- [6.17] Rocher, V.; Chovelon, J. M.; Jaffrezic-Renault, N.; Cros, Y.; Birot, D. An oxynitride ISFET modified for working in a differential mode for pH detection. *J. Electrochem. Soc.* **1994**, 141, 535-539.
- [6.18] Ravezzi, L.; Stoppa, D.; Corra, M.; Soncini, G.; Dalla Betta, F.; Lorenzelli, L. A CMOS ASIC for differential read-out of ISFET sensors. *Proc. Int. Conf. Electronics, Circuits Syst.* **2001**, 3, 1513-1516.
- [6.19] Hammond, P. A.; Ali, D.; Cumming, D. R. S. Design of a single-chip pH sensor

- using a conventional 0.6- μm CMOS process. *IEEE Sensors Journal* **2004**, 4, 706-712.
- [6.20] Suzuki, H.; Hirakawa, T.; Sasaki, S.; Karube, I. Micromachined liquid-junction Ag/AgCl reference electrode. *Sens. Actuat. B* **1998**, 46, 146-154.
- [6.21] Shimada, K.; Yano, M.; Shibatani, K.; Komoto, Y.; Esashi, M.; Matsuo, T. Application of catheter-tip isfet for continuous in-vivo measurement. *Med. Biol. Eng. Comput.* **1980**, 18, 741-745.
- [6.22] Smith, R. L.; Scott, D. C. A solid state miniature reference electrode. *Proc. IEEE/VSF Biosensors*, Los Angeles, CA **1984**, 15-17, 61-62.
- [6.23] Huang, I. Y.; Huang, R. S. Fabrication and characterization of a new planar solid-state reference electrode for ISFET sensors. *Thin Solid Films* **2002**, 406, 255-261.
- [6.24] Maminska, R.; Dybko, A.; Wróblewski, W. All-solid-state miniaturised planar reference electrodes based on ionic liquids. *Sens. Actuat. B* **2006**, 115, 552-557.
- [6.25] Suzuki, H.; Hiratsuka, A.; Sasaki, S.; Karube, I. Problems associated with the thin-film Ag/AgCl reference electrode and a novel structure with improved durability. *Sens. Actuat. B* **1998**, 46, 104-113.
- [6.26] Suzuki, H.; Ozawa, H.; Sasaki, S.; Karube, I. A novel thin-film Ag/AgCl anode structure for microfabricated Clark-type oxygen electrodes. *Sens. Actuat. B* **1998**, 53, 140-146.
- [6.27] Chang, K. M.; Chao, K. Y.; Chou, T. W.; Chang, C. T. Characteristics of zirconium oxide gate ion-sensitive field-effect transistors. *Jpn. J. Appl. Phys.* **2007**, 46, 4333-4337.
- [6.28] Grattarola, M. ; Massobrio, G. Bioelectronics handbook: MOSFETs, Biosensors, and Neurons, McGRAW-HILL: New York, NY, USA, 1998

- [6.29] Van der Schoot, B.H.; Bergveld, P. ISFET based enzyme sensors. *Biosensors* **1988**, 3, 161-186.
- [6.30] Boubriak, O. A.; Soldatkin, A. P.; Starodub, N. F.; Sandrovsky, A. K.; El'skaya, A. K. Determination of urea in blood serum by a urease biosensor based on an ion-sensitive field-effect transistor. *Sens. Actuat. B* **1995**, 26-27, 429-431.
- [6.31] Morgenshtein, A.; Sudakov, B. L.; Dinnar, U.; Jakoson, C. G.; Nemirovsky, Y. CMOS readout circuitry for ISFET microsystems. *Sens. Actuat. B* **2004**, 97, 122-131.



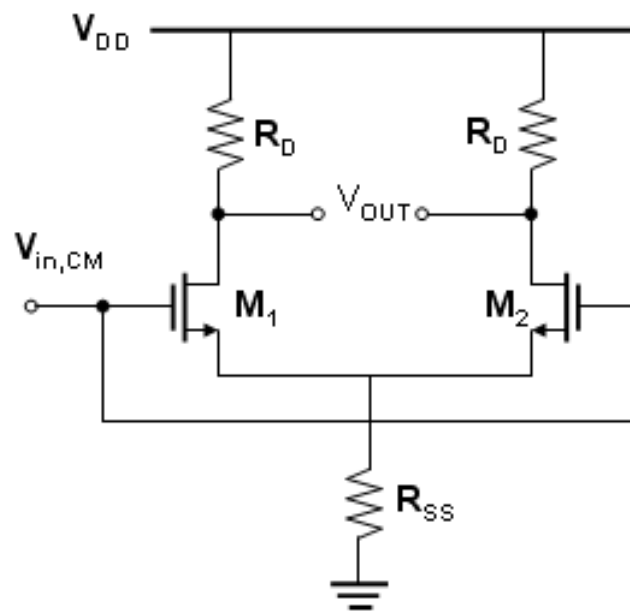


Figure 6-1 The schematic diagram of the typical common-mode differential circuit.

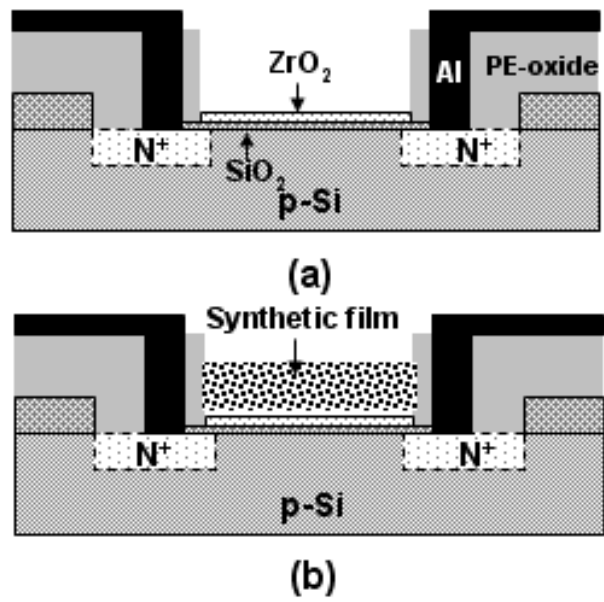


Figure 6-2 Schematic diagrams of (a) ISFET (b) EnFET and REFET

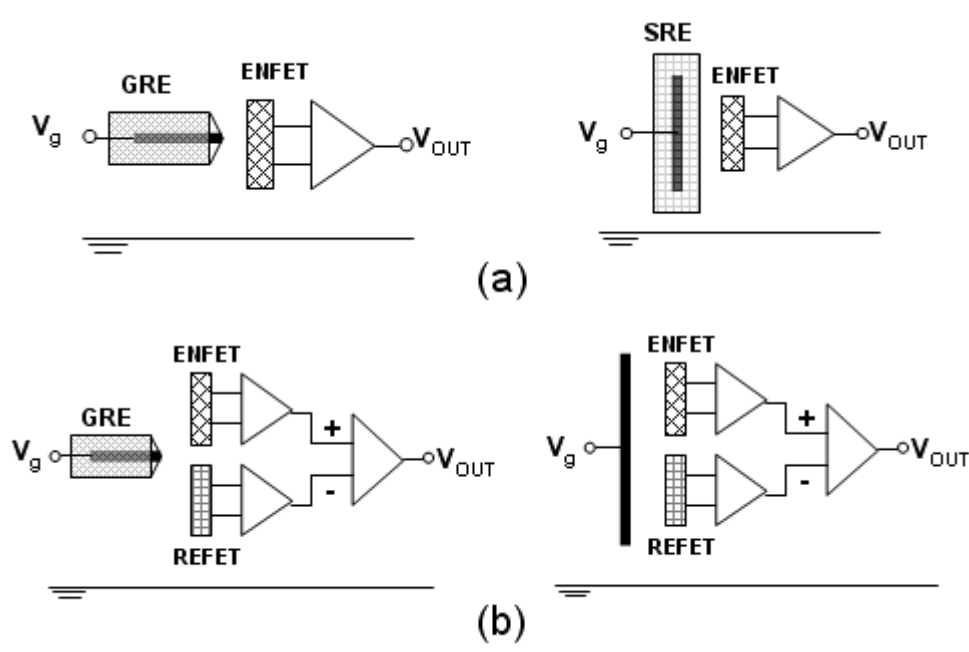


Figure 6-3 Test structures: (a) single-ended (b) two-ended differential pairs

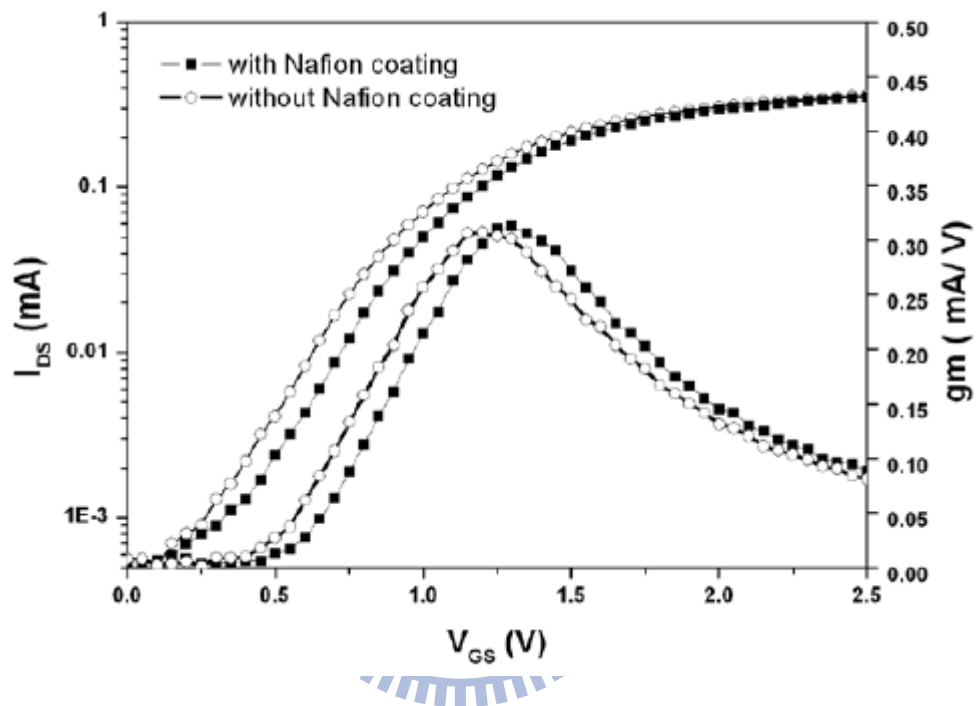


Figure 6-4 The I_{DS} - V_{GS} and transconductance (gm) curves of ZrO_2 gate ISFETs with and without NafionTM coating.

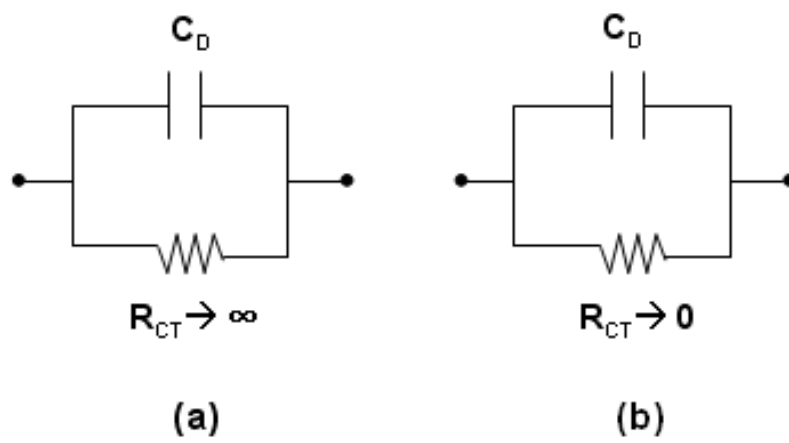


Figure 6-5 Equivalent circuit of (a) ideally polarizable interface and (b) ideally nonpolarizable interface.

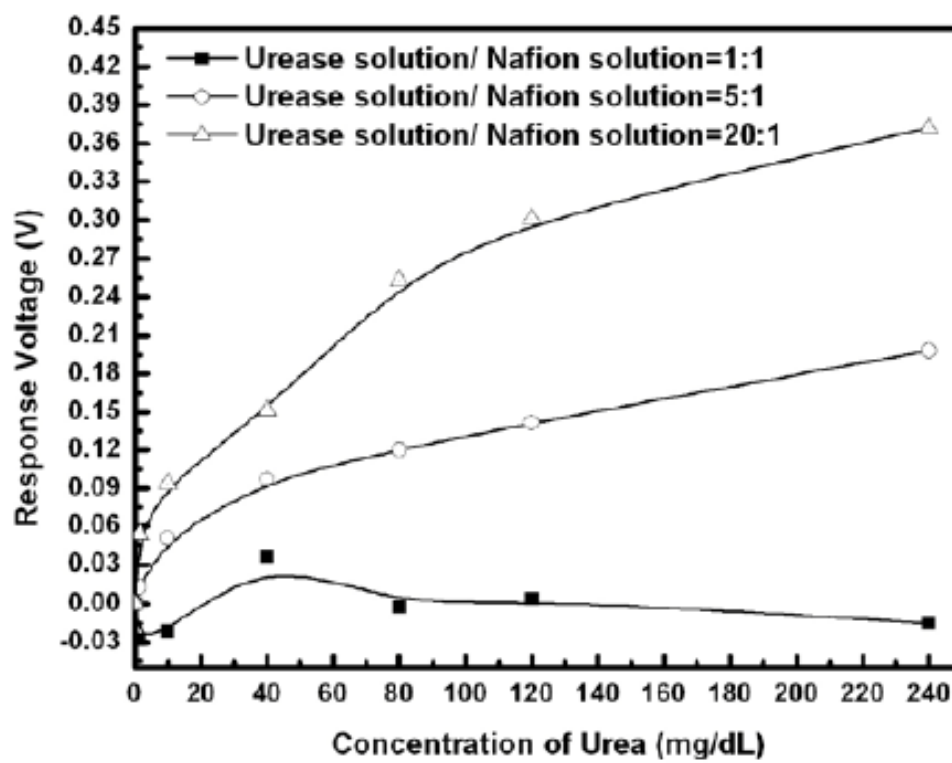
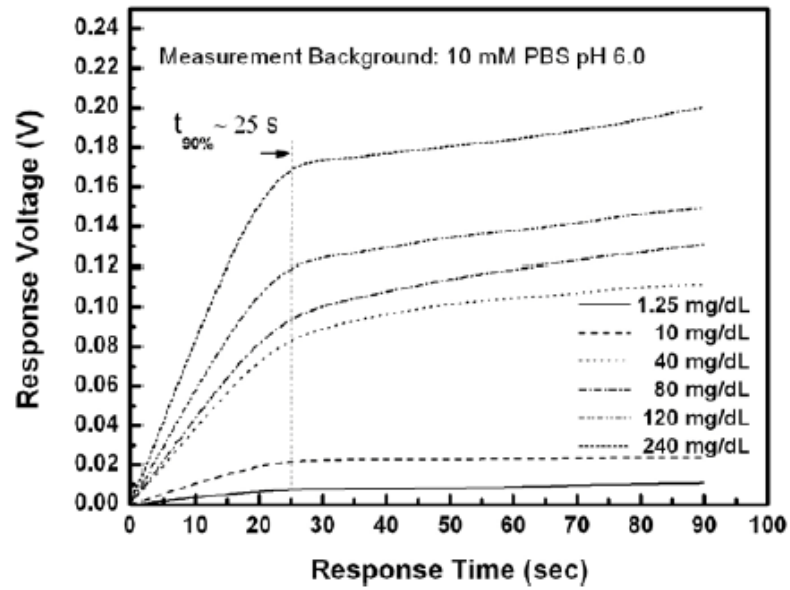
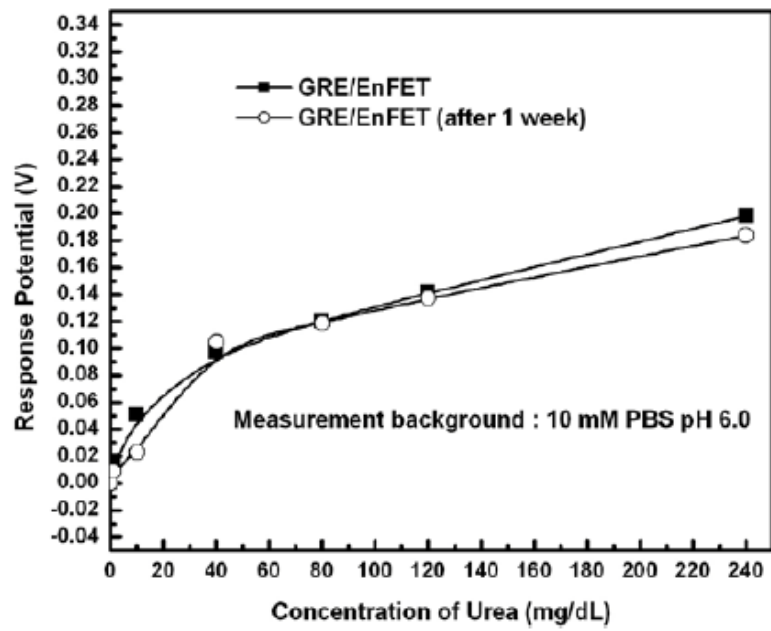


Figure 6-6 The urea responses of urease biosensors with different ratio of urease entrapped.



(a)



(b)

Figure 6-7 (a) Urea response of the GRE/EnFET (b) Storage and repeatability

performances of the GRE/EnFET dL in axis label.

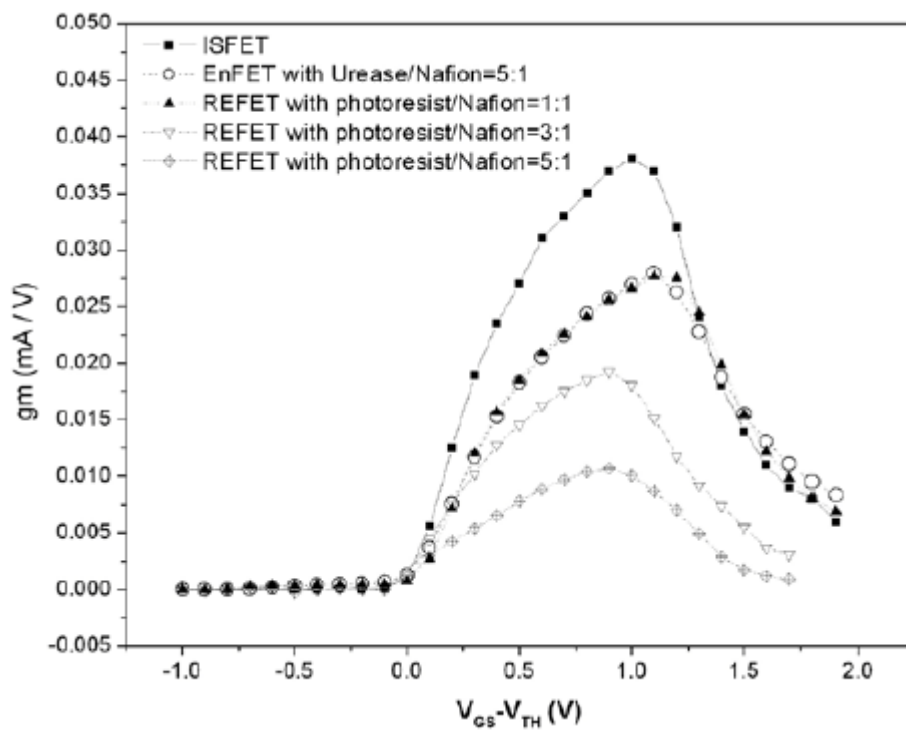


Figure 6-8 The I_{DS} - V_{GS} and g_m curves of ISFET, EnFET and REFETs

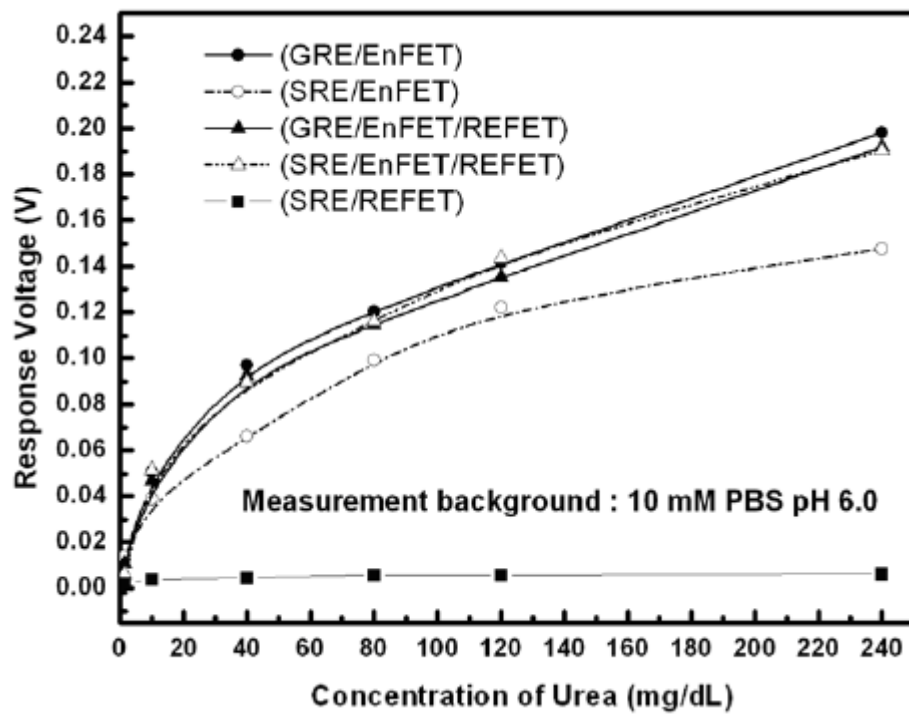


Figure 6-9 Urea response of test structures of the GRE/EnFET, SRE/EnFET, GRE/EnFET/REFET, QRE/EnFET/REFET and SRE/REFET dL in axis label.

Table 6-1 The urea responses and performance of sole urease biosensors with different ratio of urease entrapped.



Operation Temperature: 25 °C					
Urease solution : Nafion solution	Detection Limit (mg/dL)	Sensing Range (mg/dL)	Sensitivity (mV/per mg/dL)	Lifetime	Response Time (sec)
1:1	Not available	Not available	Not available	Not available	Not available
5:1	8	8~240	0.64	>7 days	25~60
20:1	1.25	1.25~240	1.33	<30 min	Not available

Table 6-2 The storage and repeatability performances of GRE/EnFET



Stored at 4 °C in darkness			
Urea Concentration (mg/dL)	Sensor Response (mV)	Sensor Response (after 1 week) (mV)	Storage Stability (% of sensor response)
1.25	12.9	8.8	68%
10	50.7	23	45%
40	97.1	104.6	92%
80	120.3	118.7	99%
120	141.4	137.6	97%
240	1988.1	183.6	93%

Chapter 7

Conclusions and future prospects

7.1 Conclusions

A miniaturized biological sensor platform based on the ion sensitive field effect transistor technology was developed and investigated. With optimal post deposition annealing process steps, the dense surface of ZrO_2 sensing film was obtained. Based on the high quality film, the ISFET demonstrates high pH sensitivity, linearity and low drift and hysteresis, which are suitable for chemical and biological detecting applications. Meanwhile, the ion selectivity and interference characteristics were also investigated. The results define the testing criteria, such as ionic strength, buffer capacity and ion species, of ZrO_2 -gate ISFETs. Since the pH-dependent drift is a fundamental error of ISFET measurement which can not be solved with post compensation electrical circuits, a novel method eliminating the pH-dependent drift was proposed. Through the simultaneous measurement with both n-channel and p-channel, the pH-dependent drift can be improved significantly.

To extend the applications of ISFET, the miniaturization is extremely important. A method of fabricating reference ISFETs by combining Nafion and ion-insensitive polymers was proposed. With a differential arrangement, high sensitivities of 52.1 mV/pH and low ion interference of 4.61 mV/pNa based on the ZrO_2 sensing film were obtained in the wide range of pH 1–13. The similar concept was adopted to immobilize the biorecognition materials. Utilizing NafionTM as supporting matrix provides the advantage of low initial charge-transfer resistance. The entrapment of the ion-blocking materials, such as urease and photoresist, can therefore be performed without altering the unpolarizable property of

sensing membrane for EnFETs and REFETs. Meanwhile, for future readout circuits design, the consideration of transconductance-match by modifying the composition of sensing films of devices is also presented.

7.2 Future works

Further enhancements on pH sensitivity are possible. Since the pH sensitivity are strongly correlated to the film quality and property, new materials, such as nanoparticles or magnetic particles, could be incorporated to the fabrication of sensing films. SEM, XRD and AFM metrology skills should be performed for further understanding of the relationships between the physical properties of sensing material and sensing mechanisms.

The platform is utilized to develop biosensors such as EnFETs. The results reveal that the developed urea biosensor has the performances of fast response, high sensitivity and acceptable lifetime. To prolong the lifetime, attempts to entrap other ion insensitive polymers and to improve the synthesis skills are necessary. Since the feasibility of immobilizing biorecognition materials with the ion-unblocking polymer based supporting matrix was demonstrated, it is predictable that some proteins with short chain length, e.g. glucose or DNA, can be immobilized with the proposed method.

To accommodate the requirements of industrial production, the post processes should be integrated with existing processes. Some state-of-the-art technologies, such as ink-jet deposition, screen printing and micro-fluidic channel etc., could be incorporated. Attempts to immobilize many biological materials with proposed platform and to design the readout circuits are practical future works.